Induced Pluripotent Stem cells disease modeling: approaching Gaucher and Tay Sachs

Erica Lorenzo Vivas

Aquesta tesi doctoral està subjecta a la llicència ***Reconeixement 3.0. Espanya de Creative Commons***.

Esta tesis doctoral está sujeta a la licencia ***Reconocimiento 3.0. España de Creative Commons***.

This doctoral thesis is licensed under the ***Creative Commons Attribution 3.0. Spain License***.

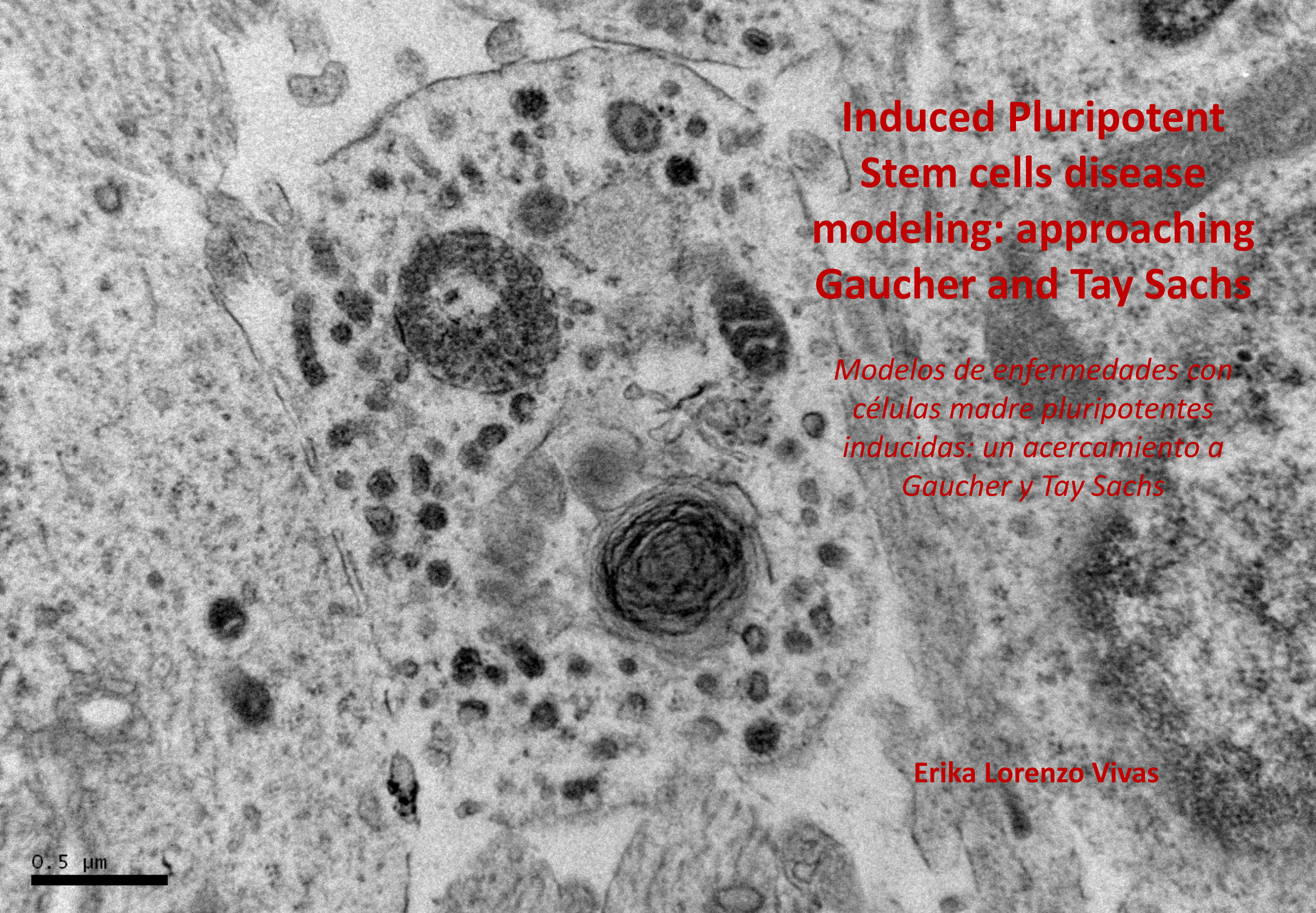

Induced Pluripotent Stem cells disease modeling: approaching Gaucher and Tay Sachs

Modelos de enfermedades con células madre pluripotentes inducidas: un acercamiento a Gaucher y Tay Sachs

Erika Lorenzo Vivas

INDUCED PLURIPOTENT STEM CELLS DISEASE MODELING: APPROACHING GAUCHER AND TAY SACHS

MODELOS DE ENFERMEDADES CON CÉLULAS MADRE PLURIPOTENTES INDUCIDAS: UN ACERCAMIENTO A GAUCHER Y TAY SACHS

Memoria presentada por **Erika Lorenzo Vivas** para optar al título de doctora por la Universitat de Barcelona. Programa de doctorado en Genética.

Tesis doctoral realizada en el Centro de Medicina Regenerativa de Barcelona (CMRB) bajo la dirección del Dr. **Gustavo Tiscornia** y la tutoría del Dr. **Emili Saló Boix**.

La interesada

Erika Lorenzo Vivas

Director

Gustavo Tiscornia

Tutor

Emili Saló Boix

A mi familia y amigos

“Be the change you wish to see in the world”

(Anonymous interpretation of Gandhi’s words)

INDEX

Abbreviations

Abbreviations

AFP	Alfa Fetoprotein
ASA	Alfa-Sarcomeric Actin
ASMA	Alfa-Smooth Muscle Actin
BBB	Blood-brain barrier
bFGF	Basic Fibroblast Growth Factor
DMEM	Dulbecco's Modified Eagle Medium
DNA	Deoxyribonucleic Acid
EB	Embryoid Bodies
EGC	Embryonic Germ Cells
ER	Endoplasmic Reticulum
ERT	Enzyme Replacement Therapy
ESC	Embryonic Stem Cells
FACS	Fluorescence-Activated Cell Sorting
FBS	Fetal Bovine Serum
FGF	Fibroblast Growth Factor
FGF8	Fibroblast Growth Factor 8
GBA	acid-β-glucosidase
GBA1	gene encoding acid-β-glucosidase (Glucocerebrosidase)
GD	Gaucher Disease
GFAP	Glial Fibrillary Acidic Protein
GFP	Green Fluorescent Protein
hESC	Human Embryonic Stem Cell
HexA	Hexosaminidase A
HFFs	Human Foreskin Fibroblasts
HIV	Human Immunodeficiency Virus
HSC	Haematopoietic Stem Cells
IMDM	Iscove's Modified Dulbecco's Medium
irHFFs	Irradiated Human Foreskin Fibroblasts
irMEFs	Irradiated Mouse Embryonic Fibroblasts
iPSC	Induced Pluripotent Stem Cells
KO	Knock Out
MCBs	Multillamelar cytoplasmic bodies (or multillamelar membranous bodies)
MEFs	Mouse Embryonic Fibroblasts
MEM	Minimum Essential Media
MET	Mesenchymal to Epithelial transition
miRNA	micro RNA
MMLV	Moloney Murine Leukaemia Virus
mRNA	Messenger RNA
MUG	4-methylumbelliferyl-2-acetamido-2-deoxy-β-D-glucopyranoside
MUGS	4-methylumbelliferyl-2-acetamido-2-deoxy-6-sulfo-β-D-glucopyranoside
NDM	Neural Differentiation Media
NEAA	Non-Essential Aminoacids
NPEM	Neural Precursor Expansion Media
NPSM	Neural Precursor Selection Media
ORF	Open Reading Frame
OSK	Oct4, Sox2, Klf4
OSKM	Oct4, Sox2, Klf4, c-Myc

OSN	Oct4, Sox2, Nanog
PAS	Periodic Acid Shiff
PCR	Polymerase Chain Reaction
PEI	Polyethylenimine
PFA	Paraformaldehyde
P/S	Penicillin/Streptomycin
RNA	Ribonucleic Acid
SHH	Sonic Hedgehog
SNMs	Spherical Neural Masses
SRT	Substrate Reduction Therapy
TBS	Tris Buffered Saline
TEM	Transmission Electron Microscopy
TH	Tyrosine hydroxylase
TS	Tay Sachs
WT	Wild Type

INTRODUCTION

I. Human diseases models

Model organisms such as the fruit fly, nematodes, bacteria, yeast, zebra fish or rodents and other large animal models have been the focus of much of the biological research of the last 150 years. The construction of theoretical and empirical systems is a fundamental method of scientific research. These systems, or models, are simplified representations of the phenomenon under study, which are particularly useful when the manipulations that can be done on the 'real' phenomenon are limited for technical or ethical reasons. In few areas of science this is more obvious than in research on human biological phenomena.

It is generally accepted that primitive medicine arose by trial and error of treatments for different diseases or conditions directly on human patients, in the context of belief systems rooted in particular cultural traditions. Our modern medical knowledge has arisen in the last 200 years as the collective output of countless physicians, scientists and researchers. Disease modeling in the modern sense is a relatively recent development that has arisen as a consequence of the explosion of biological knowledge and technology of the last 60 years, particularly in the fields of molecular genetics, molecular and cellular biology and physiology. For the better part of the 20th century, the mouse has been the most widely used animal model in biomedical research. The advantages of the mouse as a model system compared to other alternatives are many. The mouse is phylogenetically closer to humans than, say, *Drosophila*, *C. elegans* or *Danio rerio*; it is small, prolific and relatively cheap and easy to maintain, especially compared to larger models such as pigs, sheep or primates. Importantly, it allows in vivo analysis at the organism level. Since the 1980's, the development of techniques for genetic manipulation of the mouse have made this animal one of the best available options for modeling human genetic disease. Gene targeting and trans-

genic technology have led to the development of many mouse models for a wide range of both loss and gain of function disorders.

Studies *in vivo* allow for experimental approaches in the physiological environment of a whole organism: interacting cell types and organ systems can be studied *in situ* or isolated and evaluated *in vitro*. Inbred strains provide a constant genetic background, reducing environmental noise and enhancing reproducibility across laboratories. This is important in polygenic and low penetrance genetic diseases, allowing the identification of single components of the phenotype (Williams et al. 2004).

While its advantages are well recognized, the mouse system is not without drawbacks. While the mouse is relatively phylogenetically close to humans, there exist species-specific differences at multiple levels which limit the fidelity of the mouse system to faithfully reproduce many clinical human phenotypes; furthermore, drugs with significant impact on mouse models failing in human clinical trials is relatively common. (Wilson 1996; Odom et al. 2007; Perel et al. 2007). The genetic strategies and manipulations required to reproduce the disease phenotype may be complex and introduce unexpected secondary effects (Liu et al. 1998) thus, sometimes, further complex genetic manipulation is needed (Enquist et al. 2007).

In humans, cellular *in vitro* models derived from patient biopsies have the advantage of offering convenient access to the basic biochemical environment in which the disease takes place but the disadvantage that the context and influence of the higher levels of organization are lost. Primary culture cells are used for basic studies, drug screening or toxicity tests, but their limited proliferation potential and the difficulty to obtain biopsies of affected tissues limit their use. On the other hand, patient multipotent stem cells have higher proliferation potential and can be differentiated to a limited number of cell types, but are difficult to procure.

Introduction

In recent years, disease models have been established by deriving hESC from genetically diagnosed preimplantational embryos (Pickering et al. 2005; Mateizel et al. 2006) and with the derivation of induced pluripotent stem cells from patient's biopsied primary cells. Given their central characteristic of self-renewal and pluripotency, they offer both large amount of biological material and the possibility of differentiation to the disease relevant cell types.

There is no perfect model; all have their advantages and disadvantages. The main advantage of animal disease models is that they allow *in vivo* observations and hypothesis testing all the way up to the organismal level. The main disadvantage is that by their very nature of not being human, species specific differences can have a profound effect on the phenotype. Efforts have been made in humanizing animal models, being able to engraft human cells in nude mice to perform *in vivo* experiments, but still, the physiological environment is not human and some differences may persist (Watanabe et al. 2009). In human pluripotent stem cell based disease models, the main disadvantage is that they do not provide the physiological environment of a whole organism and their principal advantage is being human. Taking this into account, disease models can be complemented: human based cell models can be used for studying the molecular mechanisms of the disease and as a high through-put system for drug testing and development; meanwhile, animal models, which resemble the human disease phenotype, can be used for studying systemic aspects of the disease as well as pharmacokinetics of the drugs previously validated on the human cell-based system.

This PhD dissertation describes the development of induced pluripotent stem cell based models for two lysosomal storage diseases: Gaucher's Disease and Tay Sachs Disease.

II. iPSC

Embryonic pluripotent stem cells are defined by two characteristics: self-renewal and pluripotency. Self-renewal means that they can divide indefinitely without losing their pluripotency, which is the ability to differentiate to all the three germ layers of the developing embryo (ectoderm, mesoderm and endoderm) *in vivo* and *in vitro*. Embryonic pluripotent stem cells are derived from the inner cell mass of the blastocyst and are considered an *in vitro* equivalent of the inner cell mass population. Pluripotent stem cells can also be derived from differentiated cells by reprogramming.

The 2012 Nobel Prize was awarded to John B. Gurdon and Shinya Yamanaka for their work on reprogramming mature cells to a pluripotent state. In 1962 John B Gurdon was the first scientist to use the technique of somatic cell nuclear transfer to successfully reprogram a somatic cell nucleus by transferring it to an enucleated and unfertilized recipient egg cell, which led to development of a viable organism. (Gurdon 1962). Cellular reprogramming was later achieved with a number of techniques such as somatic cell fusion with ESC (Tada et al. 2001; Cowan et al. 2005) or EGC (Tada et al. 1997) or even the exposure of a somatic cell to ESC extracts (Taranger et al. 2005). In these techniques the somatic cell or nucleus is exposed to reprogramming factors present on the cytoplasm of the pluripotent cells. This led Yamanaka to screen 24 pluripotency-associated genes in order to identify the minimum combination of factors required to reprogram mouse fibroblasts to the pluripotent state. In 2006 Yamanaka's group published that reprogramming of a somatic cell could be achieved by ectopic expression of four known factors: Oct4, Sox2, Klf4 and c-Myc (OSKM) (Takahashi et al. 2006). The resulting pluripotent cells were called induced pluripotent stem cells (iPSC). This remarkable result offered new approaches for research and therapeutic applications, circumventing the ethical and immunological caveats of working with hESC (Fig1).

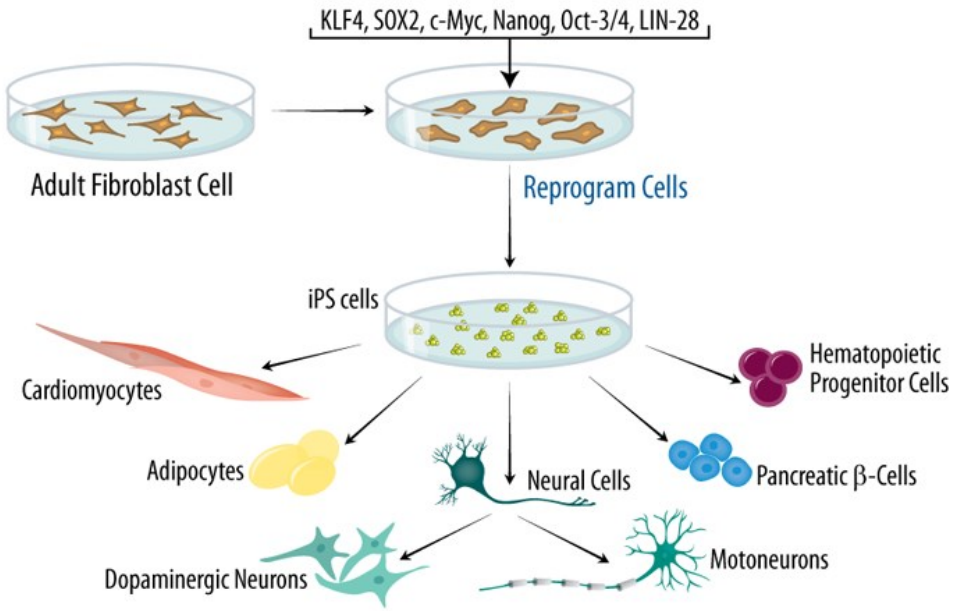

Fig 1. Induced pluripotent stem cells. Modified from http://www.rndsystems.com/

Since the first iPSC were derived, a number of reprogramming protocols and systems have been devised. Reprogramming to iPSC has been achieved with different cell types (fibroblasts, keratinocytes, lymphocytes, cord blood cells and neuronal progenitors, among others) and from different species reviewed in (Masip et al. 2010); different pluripotency factors combinations have been used (Yu et al. 2007; Feng et al. 2009; Heng et al. 2010) and in some cases, the number of factors used has been decreased (Huangfu et al. 2008; Nakagawa et al. 2008; Kim et al. 2009). There is also a wide variety of methods for delivery of the reprogramming factors summarized in Table 1 (Gonzalez et al. 2011)

The mechanism by which the ectopic expression of pluripotency factors in a somatic cell results in reprogramming to the pluripotent state is an active area of research. It has been proposed that during reprogramming, cells undergo three distinct phases (Samavarchi-Tehrani et al. 2010). The first one involves the establishment of a pre-

Integrative methods	Viral	Retrovirus Lentivirus
	DNA Based	Linearized DNA PiggiBac transposon
Non integrative methods	Viral	Adenovirus Sendai virus
	DNA Based	Episomal Minicircles
	RNA Based	Messenger RNA microRNAs
	Others	Protein Small molecules

Table 1. Different methods for reprogramming. Reprogramming factors can be delivered into the cells by integrative or non-integrative methods which can use viral vectors or DNA based vectors. Non integrative methods also deliver the reprogramming factors as mRNA or proteins. MicroRNAs and small molecules have demonstrated to help in the process, rising the efficiency and the speed (reviewed in Gonzalez et al. 2011)

pluripotent state through the increase of cell cycle rate and completion of a mesenchymal to epithelial transition (MET). The second phase is the maturation phase in which some embryonic stem cell factors (Nanog, Sall4, Esrrb, Rex1, Tcl1, Cripto and Nodal) start to be expressed. And the third phase in reprogramming is the consolidation of the pluripotent state, in which the endogenous pluripotency network becomes independent from the ectopic transcription factor expression by epigenetic remodeling of chromatin. The resulting iPSC have proven to be similar to the ESC derived from the inner cell mass of the blastocyst, with similar differentiation capabilities (Boulting et al. 2011), gene expression and epigenetic patterns (Maherali et al. 2007; Okita et al. 2007; Wernig et al. 2007; Mikkelsen et al. 2008; Guenther et al. 2010).

As models, IPSC present a number of advantages: 1) they are relatively straightforward to derive, 2) there is a wide range of cell types as starting populations which can be obtained from patient biopsies or cell repositories, 3) potentially, they can be differentiated into the disease specific relevant cell type populations, 4) they offer a virtually unlimited source of biological material for study or drug screening , 5) if derived from patients bearing genetic mutations, no genetic engineering is required to create the model and 6) panels of iPSC with different genotypes of the same disease can be created to study mutation specific aspects of the disease.

III. Characteristics of a modelable disease

Although any disorder with a genetic basis is amenable for iPSC modeling, not all diseases present the same challenges. Monogenic diseases are easier to model because usually the genetic basis is known and phenotypes may be confirmed clearly by rescue with the WT gene. Diseases with high penetrance and a cell autonomous phenotype are considered more tractable. Polygenic and complex diseases are more difficult to model with iPSC due to their strong environmental component. Similarly, early onset diseases are more straightforward to model than disorders that take decades to develop. Another important feature to have into account is the cellular types affected by the disease and the existence of robust differentiation protocols to derive them from iPSC. Such a protocol must be available or needs to be established. Most differentiation protocols usually generate heterogeneous populations in which the required cell type is more or less enriched, so purification schemes may be required.. Ideally, the cell phenotype must be strong, easily measured and ideally cell-autonomous, not relying on the interactions with other cell types, although in some cases co-culturing the implicated cell type can be attempted (Dimos et al. 2008).

Some diseases may impair reprogramming and correcting the genetic defect prior the generation of iPSC might be required (Raya et al. 2009). Reprogramming process requires cell division and during the process the epigenetic landscape of the cell is remodeled, so disorders which affect DNA repair, senescence pathways and cell proliferation, or that involve epigenetic mechanisms, may make the generation of IPSC difficult or impossible. On the other hand, given the epigenetic base of the reprogramming process, even if an epigenetic based disease can be reprogrammed to iPSC, it is possible that the disease phenotype cannot be recapitulated (Urbach et al. 2010).

Finally, another factor to consider is the availability and fidelity of alternative disease models, particularly in mouse. Lack of good models for a disease will add value to an iPSC model of the disorder, a situation encountered in many orphan diseases. This PhD dissertation focuses on the development and characterization of iPSC models of Gaucher and Tay Sachs diseases, both lysosomal storage disorders that fulfill many of the previous characteristics.

IV. Gaucher disease

Gaucher's disease (GD) is an autosomal recessive lysosomal storage disorder which affects 1 in 40,000-60,000 live births in the general population and 1 in 400-600 live births in Ashkenazi Jews (Grabowski 1993). GD is caused by mutations in the GBA1 gene, which encodes for the acid-β-glucosidase (GBA) enzyme (also known as glucocerebrosidase, ceramide β-glucosidase or glucosilceramidase) that catalyzes glucosylceramide (also known as ceramide β-glucoside or glucocerebroside) into ceramide and glucose (Brady et al. 1965). Mutations in the GBA1 gene can cause decreased enzyme stability, retention and degradation of the enzyme in the endoplasmic reticulum and impaired trafficking to the lysosome (Jmoudiak et al. 2005; Ron et al. 2005). Glucocerebrosidase dysfunction leads to the accumulation of glucosylceramide and glucosyl-

sphingosine in the lysosome of macrophages, Kupffer cells, neurons, osteoclasts, T-cells and dendritic cells causing a multisystemic clinical presentation in patients.

Clinical presentacion

GD clinical features cannot be predicted from the genotype, which are very variable and differ from one patient to another, being the most characteristic the hepatosplenomegaly due to the presence of gaucher cells. The patients also present hematopoietic abnormalities, neuropathy, bone and pulmonary manifestations and dermal problems. GD has been classified in three different clinical groups attending to the onset age of the first symptoms and the presence and progression of the neurological damage (Knudson et al. 1962).

Type I. Non neuronopathic (OMIM #230800). The most important feature for its classification is that there are no neurological symptoms. 90% of the GD diagnosed patients belong to this clinical group. Also, it is the less severe clinical presentation of the disease. It is a systemic presentation, with great variability in onset, clinical features and its progression. Symptoms can appear at any age, ranging from the newborn to the elderly patients, but the most frequent age of onset is adulthood. Symptoms include hepatosplenomegaly, skeletal defects, hematopoietic abnormalities and in some patients, dermal pigmentation, fatigue, late puberty, renal, pulmonary and cardiac complications.

Type II. Acute neuronopathic (OMIM #230900). It is the least frequent presentation of the disease (1 in 150,000 live births), but also the most severe. It is characterized by the early onset of the symptoms and its quick progression. GD type II patients present CNS damage in multiple brain structures with gliosis, microglial proliferation and neuronal degeneration. Patients start developing the symptoms before the 6th month of age and usually die before the 3th year of age.

Type III. Chronic neuronopathic (OMIM #2310000). It is an intermediate phenotype between type I and II presenting both systemic and neurological symptoms. The symptoms appear during childhood or puberty with identical visceral affectation as in the type I form and a neurological phenotype with a slower progression and less severe presentation than the type II form.

Diagnosis

Histologicaly, lipid laden macrophages take on a typical morphology (Gaucher cells) and can be detected with PAS staining on biopsies from bone marrow, liver or spleen. This procedure was the first diagnostic test. Nowadays enzymatic diagnosis is less invasive and more specific, using easy-access primary cells as leukocytes or fibroblasts for assaying the decrease on the activity of the GBA (Beutler et al. 1970a; Beutler et al. 1970b; Beutler et al. 1971). The test is based on the use of 4-methylumbelliferyl-P-D-glucopiranoside, a synthetic substrate of GBA that generates fluorescent 4-MU (4-methylumberlliferone), that can be detected on a spectrofluorometer or by FACS, an alternative which is more sensitive than the traditional enzymatic assay allowing discerning between healthy, carriers and patients (Rudensky et al. 2003).

DNA analysis is used for detecting mutations on the GBA1 gene and in some cases predicts the progression of the disease as some genotypes are associated with particular progression rates. This genetic test is useful for carrier detection or in prenatal individuals which are possibly affected and also for performing statistics on the population. In order to facilitate the diagnosis, some methods, enzymatic and genetic, have been developed that use dry blood as starting material (Devost et al. 2000; Chamoles et al. 2002).

Treatment

There is a supportive care treatment for Gaucher patients directed to alleviate its symptoms. It includes spleen surgery for the treatment of the cytopenias, blood transfusion in case of anemia, analgesics and the use of prosthesis and/or drugs that inhibit the osteoclasts action as a treatment for the bone injury (Bembi et al. 1994).

Systemic aspects of the disease can also be treated by enzyme replacement therapy (ERT), substrate reduction therapy (SRT) and pharmacological chaperone therapy (PCT) for the stabilization of the GBA.

ERT consists of regular intravenous infusion of the modified GBA so it can be recognized and incorporated into the macrophages. There are four drugs: alglucerase (commercialized as Ceredase®) is of placental origin and semisynthetic; imiglucerase (commercialized as Cerezyme®) which is a recombinant protein expressed in eukaryotic cells; α-velaglucerase (commercialized as VRIPV®) produced in fibrosarcoma cell lines, and α-taliglucerase (commercialized as Elelyso®) is produced in plant cells. Unfortunately as the recombinant enzyme cannot cross the blood-brain barrier (BBB), ERT as a therapeutical option is limited to the systemic aspects of the disease and is mainly used to treat GD types I and III. This treatment has significant clinical impact on patients, although not all aspects of the disease respond equally well: for example splenohepatomegaly can be reversed, but bone and lung symptoms are more resistant to treatment (Beutler 2004).

SRT is based on the reduction of the pathogenic accumulation of glucosylceramide by the inhibition of the glucoceramide synthase by imino sugars as N-butyldeoxynojirimycin (also known as NB-DNJ, Miglustat or Zavesca®). Another drug inhibiting the glucosylceramide synthesis is the eliglustat tartrate (Genz-112638) which is currently in clinical trial phase II. Despite their small size, imino sugars cannot cross

the BBB so SRT is only applicable in type I or III patients which cannot be treated by ERT or as a complement to other treatments (Aerts et al. 2006).

Pharmacological chaperones are non-protein compounds that stabilize misfolded proteins protecting them against degradation by the proteasome and promoting their trafficking to their correct subcellular compartment. For GD, a number of compounds have been or are in development, such as imino sugars-based scaffolds as N-(n-nonyl) deoxynojirimycin (NN-DNJ), the SRT compound NB-DNJ or Isofagomine (IFG) and its derivatives. Aminnocyclitols, another type of glycomimetic structure different from the imino sugars have also been studied for their chaperoning capabilities. The small size of the chaperone compounds could help in the BBB crossing, but only a few have been reported to reach the brain reviewed by (Benito et al. 2011).

A further option for treatment of the systemic presentation (mostly due to the presence of Gaucher cells) is bone marrow transplant, but the associated risks are high and finding a compatible donor is difficult (Ringden et al. 1995).

A related option is gene therapy by replacement of the mutated GBA1 gene in hematopoietic stem cells and is designed to permanently correct the defect. It implies the extraction of hematopoietic stem cells from the patient and its *ex-vivo* manipulation to introduce the corrected gene. DNA delivery in these cells is done by lentivirus (Enquist et al. 2006; Enquist et al. 2009). Also it has been achieved the expression of GBA in a mouse model by adenoviral delivery (McEachern et al. 2006) which can cause random insertions in the genome or problems in the autoimmune response.

Currently, the acute neuronal degeneration typical of GD type II has no treatment, although pharmacological chaperones offer hope in the development of therapies for GD able to cross the BBB.

Biochemistry

The GBA enzyme is a lysosomic glycoprotein composed by 497 aminoacids whose molecular weight depends on its glycosylation state. The function of the GBA is the catalysis of the glucosylceramide into ceramide and glucose in the lysosome (Fig 2). GBA recognizes glucosylesphingosine as a minor substrate resulting also in elevated levels of this molecule in GD patients brain (Nilsson et al. 1982) and plasma (Dekker et al. 2011). GBA can also recognize and catalyze artificial β-glucosydic substrates, which is useful in the activity tests.

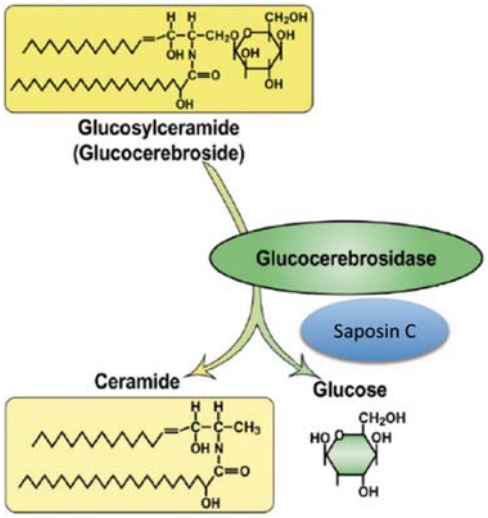

Fig2. GBA activity. Modified from Sidransky 2004

Glucosylceramide arrives to the lysosome by endocytosis (Furst et al. 1992; Sandhoff et al. 1994). In an acidic pH, saposin C (SAP C), an activator of the reaction, is hydrophobic, increasing its affinity to the membrane. SAP C joins and attracts GBA. SAP C interaction with the membrane destabilizes it, promoting the association of the GBA to the glucosylceramide, favoring the hydrolyzation of the substrate by GBA.

Genetics

Gaucher disease heredity is autosomal and recessive. It is caused by mutations in the GBA1 gene and, in a few cases, by mutations on the gene codifying the prosaposin (which will give rise to SAP A, B, C and D).

GBA1 gene is located at Chr1q21 (Barneveld et al. 1983; Ginns et al. 1985). At 16Kb from the 3' end of the GBA1 gene there is a pseudogene (Zimran et al. 1990) with a high nucleotide identity (Horowitz et al. 1989) which may complicate the identification of the mutations. Recombination between gene and pseudogene can occur, producing non-functional recombinant alleles. The pseudogene is not translated due to premature stop codons (Sorge et al. 1990). The GBA1 gene is 10,4Kb long and has 11 exons and its cDNA is of 2.5Kb. There are two functional start codons, separated by 20 amino-acids which are part of the signal peptide.

More than 200 mutations has been described on the GBA1 gene which include missense mutations (the majority), insertion or deletion mutations (some of which result in frame shifts), non-sense mutations, splice site mutations, recombination events between the gene and pseudogene and regulatory mutations. The most prevalent mutations are p.N370S, p.L444P, 84GG, p.D409H, IVS2+1g>a, and p.R463C which collectively account for the 90% and 75% of the total observed GD mutations in Jews and non-Jew populations respectively (Beutler et al. 1993; Horowitz et al. 1993).

In general there is a poor genotype-phenotype correlation in GD. Some relations have been established, but even in homozygotes the phenotype may vary between individuals. The presence of the mutation p.N370S in at least one of the alleles ensures a type I phenotype with no neurological affectation, with the second allele influencing the severity of the overall phenotype (Zimran et al. 1989; Cormand et al. 1997). On the other hand, the presence of the mutation p.L444P is associated to neuronopathic forms of the disease (type II and III) (Koprivica et al. 2000; Stone et al. 2000). In homozygosis, p.L444P usually leads to type III form and if associated with a null mutation in heterozygosis, the phenotype will be type II. Homozygote p.D409H patients present a rare form of the type III characterized by cardiac complications (Abrahamov et al. 1995; Chabas et al. 1995). The presence of Rec alleles (recombination between the GBA and the GBA

pseudogene) in homozygosis leads to the perinatal lethal form of the disease (Tayebi et al. 2003).

Models

Modeling Gaucher Disease in the mouse has been surprisingly difficult and most *in vitro* studies for the study of the mechanism of the disease and drug testing have been done in patient fibroblasts.

The analysis and characterization of different mutants of the GBA1 gene has been possible by using different expression systems as baculovirus and *Spodoptera frugiperda* (army worm) (Grabowski et al. 1989; Grace et al. 1990; Choy et al. 1996; Grace et al. 1999) or *vaccinia* expression system infecting BSC40 or HeLa cells (Hodanova et al. 2003), or by transfection in NIH3T3 (Ohashi et al. 1991) or COS cells (Grabowski et al. 1989; Alfonso et al. 2004). These systems were used to study the catalytic activity of the enzyme and its possible correlation with the genotype.

Expressing the GBA can give a lot of information of the enzyme, its activity and kinetics, but the used models can contribute little to the knowledge of the phenotype produced in the different cells and less to the disease phenotype observed in the patients. Several attempts have been done trying to model GD in mouse. The first one was a KO of the GBA1 gene, newborns had a GBA activity of 4% and died at 24 hours after birth (Tybulewicz et al. 1992).

Mice models resembling the human point mutations on the GBA1 gene appeared later creating by site-directed mutagenesis RecNciI and p.L444P which both correlate with types II and III forms of GD respectively. RecNciI homozygous mice presented low GBA activity and accumulation of glucosylceramide in brain and liver; meanwhile, p.L444P

homozygous mice had higher GBA activity than RecNcil and showed no detectable accumulation of glucosylceramide in neither brain nor liver. Both homozygous mutants died at 48 hours after birth due to problems in the epidermal permeability barrier caused by the lack of glucosylceramide in the epidermis (Liu et al. 1998). A p.L444P homozygous mouse model was possible when combined with a heterozygous KO of the glucosylceramide synthase. These mice were able to live more than a year showing a multisystemic inflammation; but no Gaucher cells were found nor a large accumulation of glucosylceramide (Mizukami et al. 2002). Mouse models for the point mutations p.N370S, p.V394L, p.D409H and p.D409V have also been developed. Human patients with p.N370S homozygosis present the type I form of the disease, the mildest form; in contrast, p.N370S homozygous was lethal in the newborn mice. The other mutants present a reduced GBA activity and a glucosylceramide accumulation in visceral organs but never in the brain (Xu et al. 2003).

The only murine models which show neuronopathic features as rapid motor neuron dysfunction, seizures, neurodegeneration and apoptotic neuronal cell death, are the developed by Enquist and colleagues (Enquist et al. 2007) which had low GBA expression in the skin in order to prevent the early lethality observed in other Gaucher disease GBA KO models. Using these models it was determined that microglial cells are not the primary cause, but influence in the progression of the neurological effects.

Although valuable for the study of the loss of function of GBA, the model developed by Enquist is not a reproduction of the mutants observed in the human population, so, even if some of the features of the disease are recapitulated and we can increase our knowledge on the metabolism of the different tissues in the disease, we cannot use Enquist model for drug testing because the system lacks the expression of the deficient GBA.

Gaucher disease features have been reproduced in iPSC derived from patient fibroblasts type I (p.N370S/ p.N370S), type II (p.L444P/RecNcil and p.L444P/p.G202R) and type III (L444P/L444P) (Park et al. 2008; Panicker et al. 2012; Tiscornia et al. 2013). Differentiation of the obtained iPSC into macrophages and neurons recapitulated the phenotypic hallmarks of the disease and demonstrated to be a good platform for drug screening.

V. Tay Sachs disease

Tay Sachs disease is an autosomal recessive lysosomal storage disorder included in the group of G_{M2} gangliosidoses which affects 1 in 360.000 newborns in the general population and 1 in 2500-3600 in Ashkenazi Jews. TS is caused by mutations on the HEXA gene, which encodes for the α-subunit of the β-hexosaminidase A enzyme (HexA) that is part of the complex that catalyzes ganglioside G_{M2} degradation. This leads to G_{M2} ganglioside accumulation on the lysosomes of neuronal cells, interfering with the normal cell activity and causing neuronal degeneration.

Clinical presentation

Several different variants of the Hex α-subunit deficiency have been found, correlating the enzymatic residual activity to the clinical phenotype: the higher the activity of the HexA, the later and milder the symptoms. Tay Sachs has three different clinical manifestations: infantile acute and two late onset forms subacute and chronic. Late onset forms cover manifestations from late infantile period to adult age. (Gravel et al. 2001)

In the infantile acute form the first symptoms appear at age 3-5 months with weakness, hampered growth, lack to response to external stimuli and loss of mental and motor skills. Observation with an ophthalmoscope reveals the classical cherry red spot

Fig 3. Cherry red spot observed in the infantile acute form of Tay Sachs disease

(Fig 3). Patients suffer of progressive weakness and hypotonia. Seizures start some months after the neurological manifestations and increase with the progression of the disease. Also progressive blindness and marked hyperacusis appear before the year. After 10 months of age, there is a rapid progression of the disease, increasing the severity of the symptoms; by the 18^{th} month macrocephaly can be observed. On the last stage of the disease, the children show decerebrate body posturing, difficulties for swallowing and are completely unresponsive to external stimuli. Death usually occurs between age 2 and 4.

Late onset subacute form: it starts with ataxia at age between 2 and 10 years. There is a progressive psychomotor deterioration and dystonia in parallel to developmental regression and dementia, involving speech impairment. Blindness occurs later than in the acute infantile as well as seizures. By the age of 10 to 15 years, patients are in a vegetative state and die few years later.

Late onset chronic: can appear at any point from childhood to adulthood, presenting great variability in the clinical manifestations and progression. Symptoms include psychomotor deterioration, dystonia, spinocerebellar degeneration, dysarthria and psychotic manifestations.

Diagnosis

Enzymatic activity assays are common for TS diagnoses and can be performed from serum, leukocytes (Suzuki et al. 1971), fibroblasts (Okada et al. 1971) and even dried blood samples (Lukacs et al. 2011). Detection of α subunit deficiency in HexA enzyme is achieved by synthetic chromogenic or fluorogenic substrates as 4-methylumbelliferyl-2

-acetamido-2-deoxy-β-D-glucopyranoside (MUG) and 4-methylumbelliferyl-2-acetamido-2-deoxy-6-sulfo-β-D-glucopyranoside (MUGS) which, upon hydrolysis, 4-methylumbelliferone is released and can be detected fluorometrically. HexA isoenzyme (αβ) can degrade both substrates meanwhile HexB (ββ) can only degrade MUG. For TS patient diagnosis enzymatic analysis of HexA activity (MUGS degradation) is expressed as a percentage of total Hex activity (MUG) (Hechtman et al. 1993). Also, differential heat stability of HexA respect HexB is used for patient diagnosis by measuring activity before and after inactivating HexA by heat; HexA activity is the difference between the two measured activities (Kaback et al. 1977). Prenatal diagnoses can be performed with amniotic fluid or chorionic villus samples (Grabowski et al. 1984; Callahan et al. 1990).

When enzymatic assays show HexA deficiency, DNA analysis is essential to confirm the phenotype and evaluate the possible progression of the disease regarding the genotype. DNA analysis is also useful for population screening as the carried out on Jewish in order to identify carriers and couples at risk of breeding affected children and receive proper genetic counseling

Treatment

Sadly, there is no treatment for Tay Sachs in which the progression of the disease is reversed not even halted. The therapy for these patients is focused on supportive care. Nevertheless different therapeutic approaches are being studied as enzyme replacement therapy (ERT), substrate reduction therapy (SRT), bone marrow transplantation, gene therapy, or the last one, the induction of exocytosis.

ERT in TS has been tried in humans with no success (Johnson et al. 1973; von Specht et al. 1979). TS pathophysiology is centralized in the nervous system which means that

the treatment enzyme must overcome two barriers to succeed. One is crossing the blood brain barrier, which was assessed by intrathecal infiltration of the enzyme with no successful results (von Specht et al. 1979). The other is efficiently targeting to the neurons for which mannose-6-phosphate must be on the surface of the enzyme for neuronal recognition and uptake. In this sense, recombinant phosphomannosylated HexA enzymes are being produced and initial results in mice and human fibroblast are promising (Akeboshi et al. 2007; Akeboshi et al. 2009; Tsuji et al. 2011).

SRT have been focused on the inhibition of glucosylceramide synthase by N-butyldeoxynojirimycin (NB-DNJ) also known by miglustat. Studies of miglustat administration to TS and Sandhoff model mice show a diminution of G_{M2} accumulation in the brain and in the severity of the neuropathology (Platt et al. 1997; Baek et al. 2008). Nevertheless, when these studies were carried with human patients no improvement of the symptoms was observed (Maegawa et al. 2009; Shapiro et al. 2009) maybe because in mice, the HEXA gene deficiency does not produce such an accumulation of G_{M2} as it does in humans.

Cell therapy has been tried by bone marrow transplant with no benefit for the patient (Hoogerbrugge et al. 1995). Also, correction of the enzymatic defect has been tried by viral delivery on neural progenitors which then were implanted on the mice brain or introduced directly into the brain (Lacorazza et al. 1996; Martino et al. 2005; Cachon-Gonzalez et al. 2006) with promising results but still need to be probed their efficacy in human patients.

Pharmacological chaperone pyrimethamine was found by screening of already approved compounds of the Food and Drug Administration (Tropak et al. 2007) and has already been tested in TS patients with an increase on HexA activity, but still with no clear signs of neurological improvement due to the short term study (Clarke et al. 2011; Osher et al. 2011). Other pharmacological chaperones are being designed and

tested in TS cell lines (Rountree et al. 2009) but further studies are needed to test their efficiency in patients.

A new drug target for treating lysosomal storage diseases is the lysosomal exocytosis. Promoting lysosomal exocytosis by increasing intracellular Ca^{2+} levels can restore normal lysosome size and content in lysosomal storage diseases, including TS (Klein et al. 2005; Medina et al. 2011; Xu et al. 2012).

Biochemistry

Gangliosides are glicosphingolipids formed by a ceramide (N-acylsphingosine) and an oligosaccharide chain which contains one or more molecules of sialic acid (N-acetylneuraminic acid, NANA or NeuAc) (Berg et al. 2007). They localize on the plasma membrane with the oligosaccharide chains on the extracellular matrix (Thompson et al. 1985). The highest ganglioside concentration is found on the gray matter of the brain (Ando 1983), particularly in the plasma membranes of nerve endings, dendrites and synapses (Hansson et al. 1977). Gangliosides are involved in cell-cell interaction, pathogen binding, co-receptors in hormone signaling and it has been hypothesize their importance in the synapse and neuronal transmission (Rahmann et al. 1976; Ando 1983).

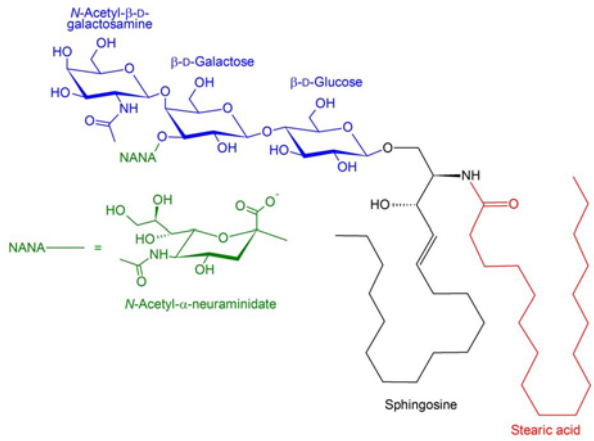

Fig 4. GM2 ganglioside structure

Ganglioside biosynthesis starts from ceramide at the cytosolic leaflet of the ER, going through Golgi where glycosyltransferases and sialyltransferases add in sequence the corresponding carbohydrate component.

Gangliosides reach the plasma membrane by vesicle flow. G_{M2} ganglioside is formed by a lactosylceramide with a NeuAc and an N-acetylgalactosamine residue (Fig 4). For G_{M2} degradation, plasma membrane is endocytosed passing through endosomal compartments to reach the lysosome. There, HexA enzyme starts G_{M2} degradation with the help of the G_{M2} activator which lifts and exposes the carbohydrate chain to the HexA enzyme, allowing the excision of the terminal N-acetylgalactosamine residue (Gravel et al. 2001).

HexA enzyme is composed by two subunits: an α-subunit of approximately 55KDa and a β-subunit of about 23KDa. Subunit α is encoded by HEXA and subunit β is encoded by HEXB gene. There are two other hexosaminidases isozymes, HexB which is composed by two β subunits (ββ) and HexS, composed by two α subunits (αα), but only HexA can degrade G_{M2}. G_{M2} gangliosidoses are caused by mutations in any of the the HexA subunits α (Tay Sachs), β (Sandhoff) or in the G_{M2} activator (AB variant).

Genetics

Tay Sachs disease is caused by mutations on the HEXA gene which encodes for the α-subunit of the HexA enzyme. HEXA gene is located in Chr15q23 and contains 14 exons, expanding 35kb length (Proia et al. 1987; Takeda et al. 1990).

More than 100 mutations have been found on HEXA gene (Kaback 2000) including large and small deletions, missense, nonsense, frame-shift and splice site alterations. The clinical presentation is closely related to the residual activity of the HexA enzyme. Mutations on the HEXA gene causing a full deficiency of the α-subunit are associated with the infantile acute form of the disease. This include small in-dels causing frame-shift and the majority of splicing mutations as the cases of the two most common mutations in infantile TS among Ashkenazi Jews, the 1278ins4 (Myerowitz et al. 1988) and

the IVS12+1 G>C (Arpaia et al. 1988; Myerowitz 1988; Ohno et al. 1988). Other mutations related to the infantile form are those affecting protein processing as E482K, R504C and G269S (d'Azzo et al. 1984; Nakano et al. 1988; Paw et al. 1991)

Late onset subacute form is associated with mutations that maintain some residual activity of the HexA and include aminoacid substitutions as G250D (Trop et al. 1992) and two mutations affecting α-subunit processing R499H and R504H (Paw et al. 1990), in which the histidine allows some phosphorylation so the α-subunit can associate with the β and become into HexA active enzyme on the lysosome. Late onset subacute is also related to B1 variant mutations in which the mutations do not alter the association of α and β subunits, but alters the activity of the HexA as are the mutations observed in R178 and D258 (Tanaka et al. 1990; Triggs-Raine et al. 1991; Fernandes et al. 1992).

In the case of the late onset chronic form, there is one major mutation associated which is G269S (Paw et al. 1989) which is common between Ashkenazi Jews.

Models

G_{M2} gangliosidoses are naturally occurring in animals as dogs, cats, pigs, sheep and even flamingos (Pierce et al. 1976; Neuwelt et al. 1985; Zeng et al. 2008; Torres et al. 2010; Sanders et al. 2013), but usually are sporadic exceptions, studies post-mortem and are not maintained as a lineage.

Different Tay Sachs murine models have been developed by interruption of exon 8 or exon 11 of the HEXA gene (Yamanaka et al. 1994; Boles et al. 1995; Cohen-Tannoudji et al. 1995; Phaneuf et al. 1996). Biochemically, HexA is inactive, but Tay Sachs mice do not develop the clinical features observed in human. Unlike humans, mice can degrade G_{M2} by HexA activity or by sialidase action, performing a bad model for studying TS mutations and testing drugs. For the study of the effect of G_{M2} accumulation it is used the

Sandhoff mice model, which lacks HexB activity and recapitulates hallmarks of the human G_{M2} gangliosidosis.

Recently, it has been proved that cultures of NPC can mimic the hallmarks of the brain disease, but again, the NPC used were derived from mice and are useless for biochemical studies on HexA function or drug discovery (Martino et al. 2009).

Objectives

Objectives

In the context of the CMRB, whose principal aim is to apply the knowledge on stem cell to the study of diseases and the seek of possible cellular therapies; the main objective of the thesis was to apply the technology of iPSC to genetic diseases for modeling.

The specific objectives of the study are:

1. Generation and characterization of iPSC lines from Gaucher and Tay Sachs patient fibroblasts.

2. Differentiation of the cell lines into appropriate tissues and corroboration of the disease phenotype.

3. Use of the developed models in drug testing and confirm phenotype reversion.

Material & Methods

Cell Culture

All the cell lines were cultured at 37°C, 5% CO_2, 90% humidity

HFF culture and irradiation

HFF-1 cell line was fed with *IMDM media* and media was changed every 2-3 days. When the culture reached 80-90% of confluence, cells were passaged by trypsinization with trypsin-EDTA 0,25% (Invitrogen #25300-056) and seeded at a density of 70.000 cells/cm^2.

For irradiation, cells were grown until 100% of confluence, trypsinized, resuspended in *IMDM media* and irradiated at 45Gy. IrHFF were frozen in *freezing media* ($4x10^6$ irHFF per vial). IrHFF were plated on gelatin-coated plates at a density of $3x10^6$ irHFF in a 10cm plate if freshly irradiated or at a density of $4x10^6$ irHFF in 10cm plate if thawed from a frozen vial.

MEF isolation and irradiation

MEFs were derived from E13,5-E14,5 day old CD1 strain embryos. The liver was excised from the embryos which were then decapitated and bled. Embryos were minced and trypsinizated with trypsin-EDTA 0.05% (Invitrogen #25300-054) for 20-30 minutes and filtered through a 40µm cell strainer. Resulting cells were seed in a ratio of 2 embryos per 15cm plate and fed with *DMEM complete media* containing 2% P/S (Gibco #15140-122). Upon reaching 100% of confluence, MEFs were passaged with trypsin-EDTA 0,05% in a ratio 1:3-1:5.

For irradiation MEFs were amplified 1:6 up to passage 4. When fibroblasts reach 100% confluence they are treated with 0,25% trypsin-EDTA, resuspended in *DMEM complete medium* and irradiated at 45Gy. IrMEFs were frozen in *freezing media* ($4x10^6$ irMEFs per vial). IrMEFs were plated on gelatin (Chemicon #ES-006-B) coated plates at a density of $3x10^6$ irMEF in a 10cm plate if freshly irradiated or at a density of $4x10^6$ irMEF in 10cm plate if thawed from a frozen vial.

PA6 culture

The mouse bone marrow–derived stromal cell line PA6 was maintained in *PA6 media* and passed by trypsinization with 0,05% trypsin-EDTA in a ratio 1:3-1:6

OP9 culture

The murine stromal cell line OP9 was maintained in *OP9 media.* When cells achieved 85-95% of confluence they were passaged 1:3 by trypsinization with 0,05% trypsin-EDTA.

Obtention and culture of GD and TS patient fibroblast

Gaucher disease fibroblasts were obtained from a patient diagnosed with GD type2 following the protocol approved by the Hospital Clinic de Barcelona. Briefly, the biopsy sample was cut and seed in a dish with *DMEM complete media*. When fibroblasts were confluent, cells were passaged with 0,05% trypsin-EDTA. Patient diagnosis was based on the clinical manifestations and a low acid-β-glucosidase activity. Analysis of the GBA1 gene sequence confirmed the presence of a p.[Leu444Pro];[Gly202Arg] compound heterozygote mutation.

Tay Sachs fibroblasts were obtained from the Coriell Cell Repository sample #GM00527 which contain a compound heterozygote mutation of p.[Trp420Cys](c.1260G>C) in one allele and IVS11+1G>A (c.1330+1G>A) in the other.

GD fibroblasts, TS fibroblasts and WT fibroblasts were cultured in *DMEM complete* media.

iPSC derivation

2µg of the reprogramming DNA were nucleofected into 10^6 low passage GD and TS fibroblasts with the NHDF nucleofection kit (Lonza #VPD-1001) following the manufacturer's protocol. The nucleofected fibroblasts were seed on irradiated HFF feeder layer, and fed every other day with *HES media* for one week, after which HES was replaced by *HES conditioned media.* After 4-6 weeks colonies appeared on the plate and were picked manually for expansion.

iPSC culture

GD, TS and WT iPSC were cultured on irHFF feeder layers and fed with *HES media.* Cells were passaged mechanically every 7-10 days. In order to obtain pure iPSC without feeder contamination, iPSC were seed on matrigel (Becton Dickinson #356231) coated plates with $6x10^5$ irHFF and fed with *HES conditioned media*. After 1-2 passages, iPSC were seed on matrigel coated plates, fed with *HES conditioned media* and passaged by trypsinization with Trypsin-EDTA 0.05%.

Reprogramming cassette elimination

iPSC lines cultured on matrigel were treated for 1 hour with a Rock inhibitor (Y27632) then were trypsinized and transduced in suspension with a non-integrative lentiviral vector expressing Cre recombinase and cherry fluorescent protein. They were plated on irHFF feeder layer and fed with *HES conditioned media*. 72 hours later cherry positive cells were sorted by FACS and plated for subclone isolation. Loss of the reprogramming cassette was confirmed by southern blot.

GBA1 and HexA rescue

GD and TS iPSC lines were genetically rescued by transduction with a lentiviral vector constitutively expressing GBA1 or HexA, respectively. iPSC lines cultured on matrigel were treated for 1 hour with a Rock inhibitor (Y27632) then were trypsinized and trans-

duced at low multiplicity of infection. Subclones were screened for lentiviral integration by PCR, followed by an acid-β-glucosidase activity assay.

iPSC characterization

IPSC lines were tested for alkaline phosphatase activity using the Blue Membrane Substrate solution kit (Sigma #AB0300) following the manufacturer's guidelines.

Pluripotency was tested on iPSC colonies growing on irHFF covered slide flasks by immunofluorescence with antibodies against Oct4 (Santa Cruz #sc-5279), Sox2 (ABR #PAI-16968), Nanog (R&D #AF1997), Tra1-60 (Chemicon #MAB4360), Tra1-81 (Chemicon #MAB4381), SSEA3 (Hybridoma Bank #MC-631) and SSEA4 (Hybridoma Bank #MC-813-70) pluripotency markers (Marti et al. 2013).

iPSC *in vitro* differentiation into endoderm

iPSC were detached and cultured as EBs on ultra-low attachment cell culture plates in *EB media* for 3 days in suspension. 6-10 EBs were plated per slide flask (pre-coated with gelatin 0.1%) and fed with *EB media* each 2-3 days until 15-20 days. Samples were then fixed with PFA 4% (Sigma #P6148-500G) and immunostained for endodermal markers as AFP (Dako #A0008) and FoxA2 (R&D #AF2400).

iPSC *in vitro* differentiation into mesoderm

iPSC were detached and cultured as EBs on ultra-low attachment cell culture plates in *EB media* supplemented with 0.5mM ascorbic acid (Sigma #A4544-25g) for 3 days in suspension. 6-10 EBs were plated per slide flask (pre-coated with gelatin 0.1%) and fed with *EB media* supplemented with 0.5mM ascorbic acid each 2-3 days until 15-20 days. Then, samples were fixed with PFA 4% and immunostained against mesodermal markers as ASMA (Sigma #A5228) and ASA (Sigma #A2172).

iPSC *in vitro* differentiation into ectoderm

iPSC were detached and cultured as EBs on ultra-low attachment cell culture plates in *N2/B27 media* for 4 days in suspension. 6-10 EBs were plated on a confluent PA6 cells slide flasks pre-coated with gelatin 0.1% and fed with *N2/B27 media* each 2-3 days until 14-16 days. Samples were then fixed with PFA 4% and immunostained against ectodermal markers Tuj1 (Covance #MMS-435P) and GFAP (Dako #Z0334).

iPSC *in vivo* differentiation

10^6 iPSC were injected into the testis of SCID beige mice and 8–12 weeks later teratomas were surgically removed, fixed in PFA 4% and immunostained against endoderm (AFP and Foxa2), ectoderm (Tuj1, GFAP) and mesoderm markers (ASMA and ASA). All animal experiments were conducted following experimental protocols previously approved by the Institutional Ethics Committee on Experimental Animals, in full compliance with Spanish and European laws and regulations

Lentiviral production

A third generation lentiviral system was used following previously published protocols (Tiscornia et al. 2006). 1,2x10^7 of 293T cells were plated in a 150mm plate coated with poly-L-Lysine in *DMEM complete media*. 24 hours later DNA (HIV based vector plasmid, pMDL, pRev and pVSV-G) transfection was performed with PEI (Polysciences #24765) in a 4:1 ratio (PEI:DNA). After 16 hours media was changed for 15ml of OptiMEM (Gibco #11058-021) per 150mm plate. Media with the viral particles was collected at 24 and 48 hours after OptiMEM was added for the first time, filtered through a 0.22µm filter and ultracentrifuged at 19.4k rpm (Beckman Coulter Optima™ L-90k Ultracentrifuge SW32 rotor) for 2hours and 20minutes. Pellet was resuspended in PBS (Cambrex #17-516F), aliquoted and stored at -80°C.

Differentiation to dopaminergic neurons

iPSC were differentiated to dopaminergic neurons using previously published protocols (Cho et al. 2008a; Cho et al. 2008b).

Step 1: iPSC were detached and cultured as EBs on ultra-low attachment cell culture plates in *Cho EB media* for 5-7 days changing media every other day. EBs were transferred to matrigel coated plates and maintained with *NPSM* for 5 days with media change every other day and cysts were removed. After 5 days on *NPSM*, media was changed to *NPEM* with media change every other day for 7 days more.

Step 2: neural structures were mechanically dissected and cultured on suspension on ultra-low attachment plates and were fed with NPEM every other day. Neural structures formed SNMs which were cultured with *NPEM* with media change every other day and mechanically passaged every 10 days.

Step 3: SNMs were dissected in very small pieces (1 SNM~ 10-20pieces) and seed on matrigel coated slide flasks with *NPEM*. After 24 hours, *NPEM* was replaced by *NDM* (day 1 of differentiation). On day 4 *NDM* was supplemented with 200ng/ml SHH (Peprotech #100-45) and 100ng/ml FGF8 (Peprotech #100-25). On day 8, ascorbic acid (Sigma #A4544-25g) at a final concentration of 200µM was added to the *NDM* supplemented with SHH and FGF8 and media was changed every other day until the end of the protocol (day 14 of differentiation).

Chaperone treatment

Chemical chaperones were synthesized and characterized by C. Ortiz Mellet and JM García Fernández as described (Luan et al. 2009; Aguilar-Moncayo et al. 2011). Fibroblasts were treated with chaperone compounds at 30µM final concentration for 4 days maintaining their culture conditions. The treatment in neurons was performed in the last 4 days of the dopaminergic differentiation, adding the chemical chaperones at 30µM final concentration to the supplemented NDM.

Organic compounds treatment

Organic compounds NCGC00160622-03 and NCGC00250218-01 were synthesized and characterized by Juan Marugán's group. Fibroblasts were treated with organic compounds at different concentrations for 5 days maintaining their culture conditions. The treatment in neurons was performed in the last 5 days of the dopaminergic differentiation, adding different concentrations to the supplemented NDM.

iPSC differentiation to macrophages

Step 1 (Raya et al. 2009): iPSC were detached and cultured as EBs on ultra-low attachment cell culture plates in *HES media* supplemented with 100 ng/ml mWNT3a (Peprotech #315-20) for 2 days. Then EBs were transferred onto OP9 feeders in a 1:1 mix of *HES media* and *hematopoietic differentiation media*. After 2 days media was changed to *hematopoietic differentiation media*. The following media change was performed by replacing of half volume of media for fresh media in 3-4 days. Further media changes were performed each 3-4 days by replacing 25% of media with fresh media for a total of 14 – 16 days.

Step 2 (Choi et al. 2011): cultures were trypsinized with 0.25% trypsin-EDTA, 0.1% collagenase type IV and DNAse I, washed with PBS and cultured in ultra-low attachment dishes in *Macrophage differentiation media A* for 2 days. Then cells were washed with PBS and cultured in *Macrophage differentiation media B* for additional 10 days. At this time, cells were collected, filtered through 100 µm cell strainer and used for further experiments.

Phagocytosis assay

For live cell imaging of phagocytosis, 50.000 cells were plated onto glass bottom dishes in 400µl of *Macrophage differentiation media B* and were allowed to attach overnight. Next day, media was replaced with 200µl of fresh *Macrophage differentiation media B* supplemented with opsonized FITC-Zymosan A particles (Life Technologies #Z2841) at a ratio of 20 particles per cell. After 100 minutes, non-internalized particles were washed away with PBS; cells were stained with Hoechst vital dye and analyzed with a confocal Leica SP5 AOBS microscope. For FACS analysis of phagocytic macrophages, cells were cultured in 12-well cell culture dishes at a density of 200.000 – 500.000 per well, treated with opsonized FITC-labeled Zymosan A particles, trypsinized and in some experiments stained with anti-CD14 antibody.

Media formulation

DMEM complete DMEM (Gibco #21969-035), 10% FBS (Gibco #10270-106), 1% GlutaMAX (Gibco #35050-038), 1% P/S (Gibco #15140-122)
IMDM media IMDM (Gibco # 21980-032), 10% FBS, 1% P/S
Freezing media 90% FBS, 10% DMSO (Sigma #D2650)

HES media KO DMEM (Gibco #10829-018), 20% KSR (Gibco #10828-028), 1% MEM NEAA (Cambrex #13-114), 1% GlutaMAX, 0.1% β-Mercaptoethanol (Gibco #31350-010), 0.5% P/S and 10ng/ml bFGF (Peprotech)

HES conditioned media Seed $4x10^6$ irMEFs in a 10cm plate. After 24 hours, *DMEM complete media was replaced by HES media*. HES conditioned media was harvested daily, filtered through a 0.22µm filter and supplemented with 10ng/ml bFGF

EB media KO DMEM, 10% FBS, 1% P/S, 1% GlutaMAX, 1% MEM NEAA, 0.1% β-Mercaptoethanol

PA6 media α-MEM with Ribonucleosides/Deoxyribonucleosides (Gibco #32571), 10% FBS, 1% P/S, 1% GlutaMAX

N2/B27 media 50% DMEM/F12 (Gibco #21331-046), 50% Neurobasal media (Gibco #21103-049), 1% P/S, 1% GlutaMAX, 0.5% N2 (Invitrogen #17502048), 1% B27 (Invitrogen #17502044)

Cho EB media DMEM/F12, 20% KSR, 1% GlutaMAX, 1% MEM NEAA, 1% P/S, 0.2% β-Mercaptoethanol

Neural Precursor Selection Media (NPSM) DMEM/F12, 1% GlutaMAX, 1% MEM NEAA, 1% P/S, 0.2% β-Mercaptoethanol, 0.5% N2 supplement

Neural Precursor Expansion Media (NPEM) DMEM/F12, 1% GlutaMAX, 1% MEM NEAA, 1% P/S, 0.2% β-Mercaptoethanol, 1% N2 supplement, 20ng/ml bFGF

Neuronal Differentiation Media (NDM) DMEM/F12, 1% GlutaMAX, 1% MEM NEAA, 1% P/S, 0.2% β-Mercaptoethanol, 1% N2 supplement, 2% B27 supplement

OP9 media α-MEM without Ribonucleosides/Deoxyribonucleosides (Gibco #32561), 20% FBS, 1% P/S, 1% GlutaMAX

Hematopoietic differentiation media IMDM, 10% FBS (Cultek #16SV30160-03), 1% P/S, 1% GlutaMAX, 10ng/ml bFGF, 10 ng/ml Flt3l (Peprotech #300-19), 10 ng/ml VEGF (Peprotech), 10 ng/ml BMP-4 (Peprotech), 20 ng/ml TPO (Peprotech #300-18), 25 ng/ml SCF (Peprotech #300-07)

Macrophage differentiation media A α-MEM without Ribonucleosides/ Deoxyribonucleosides, 10% FBS (Cultek), 1% P/S, 100µM MTG solution (Sigma) and 200ng/ml GM-CSF (Peprotech #300-03)

Macrophage differentiation media B IMDM, 10% FBS (Cultek), 1% P/S, 20ng/ml M-CSF (Peprotech #300-25) and 10ng/ml Il-1β (Peprotech #200-01B)

Imaging

Karyotyping

iPSC were treated with colcemid (Invitrogen #15212-046) for 40 minutes (fibroblasts for 2 hours). After colcemid incubation, cells were trypsinized in order to obtain a single cell dilution and pelleted. Cell pellet was resuspended in 0,075M KCl (Invitrogen #10575) and cold Carnoy fixative (methanol and acetic acid in a 3:1 ratio) was added. Cells were resuspended in Carnoy fixative, then were disrupted by falling to a slide from a height of 50cm. Samples were dried for 24 hours incubated at 120°C for 1,5 hours. Samples were stained with Wright dye and analyzed with Leica CytoVision platform.

Pluripotency and differentiation immuno-analysis

Slide flasks containing iPSC for analyzing pluripotency or differentiating EBs were fixed with 4% PFA for 30 minutes. Samples were incubated in blocking solution (1x TBS, 0,5% Triton, 6% Donkey serum) for 30 minutes and then the different primary antibodies combinations were incubated ON (48 hours for differentiating EBs) at 4°C diluted in TBS++ (1x TBS, 0,1% Triton, 6% Donkey serum). Secondary antibody was incubated for 2 hours at 37°C diluted in TBS++. Samples were analyzed on a confocal Leica SP5 AOBS microscope with Las AF (Leica Application Suite Advanced Fluorescence) (Marti et al. 2013).

Teratoma immuno-characterization

Teratomas were fixed in 4% PFA for 4 hours and embedded in paraffin. 5µm sections were made using a microtome in a sequential way, using at least three different areas of each teratoma. Samples were incubated with citrate buffer pH9 for 1 hour at 103kPa for antigen retrieval. Then, samples were incubated in blocking solution for 30 minutes at RT and different primary antibodies combinations were incubated for 24 hours at 4°C. Secondary antibody was incubated for 2 hours at 37°C diluted in TBS++. Samples were analyzed on a confocal Leica SP5 AOBS microscope with Las AF (Leica Application Suite Advanced Fluorescence)(Marti et al. 2013).

SNMs immunocharacterization

SNMs were fixed with 4% PFA for 75 minutes at 4°C and embedded in paraffin. Samples were cut in 5µm sections using a microtome and then were incubated with blocking buffer for 30 minutes at RT. Immunodetection of MAP2 (Santa Cruz #sc-32791) and Tuj1 was performed by primary antibody incubation for 24 hours at 4°C followed by secondary antibody incubation for 2 hours at 37°C. For *in toto* protocol SNMs were fixed with 4% PFA for 75 minutes at 4°C. Samples were incubated with blocking buffer for 2 hours at RT followed by ON incubation at 4°C. Primary antibodies PAX6 (Covance

#PRB-278P), MAP2 and Tuj1, were incubated for 72 hours at 4°C and secondary antibodies were incubated 2 hours at RT, then ON at 4°C followed by 2 hours at RT.
Samples were analyzed on a confocal Leica SP5 AOBS microscope with Las AF (Leica Application Suite Advanced Fluorescence)

Neuronal immunostaining
iPSC derived neurons with dopaminergic differentiation protocol were characterized using primary antibodies anti MAP2, PAX6, NeuN (Chemicon #MAB377), Neurofilament (Sigma N4142), Synapsin, TH (Sigma T8700-1VL) and Tuj1. Samples were fixed with 4% PFA for 30 minutes and incubated in blocking solution for 30 minutes. Then different primary antibodies combinations were incubated ON at 4°C diluted in TBS++. Secondary antibody was incubated for 2h at 37°C diluted in TBS++. Samples were analyzed on a confocal Leica SP5 AOBS microscope with Las AF (Leica Application Suite Advanced Fluorescence).

Gaucher's Disease phenotype immuno-characterization
Slide flasks containing neurons derived from GD iPSC were fixed with 2% PFA for 20 minutes then, samples were incubated in blocking solution without triton (1x TBS, 6% Donkey serum) for 1 hour and then primary antibodies for neuronal and lysosomal detection were added such as GBA (Abcam #ab55080), Lamp2 (Abcam #ab37024), Tuj1, TH and incubated for 72 hours at 4°C. Secondary antibody was incubated for 2h at 37°C. An increment of the signal was needed for GBA primary antibody, so an extra incubation for 2 hours at 37°C with an antibody anti-FITC conjugated with Alexa 488 (Invitrogen #A11090) was performed. Samples were analyzed on a confocal Leica SP5 AOBS microscope with Las AF (Leica Application Suite Advanced Fluorescence).

Tay-Sachs phenotype immuno-characterization
Slide flasks containing neurons derived from TS iPSC were fixed with 4% PFA for 20 minutes. Samples were incubated in blocking solution (1x TBS, 0,02% saponin, 6% Donkey serum) for 1 hour. Phenotype characterization was performed by incubating the samples with primary antibodies against Tuj1, Lamp2 and G_{M2} (gift from Konstantin Dobrenis) ON at 4°C. Secondary antibody was incubated for 2h at 37°C diluted in TBS++. Samples were analyzed on a confocal Leica SP5 AOBS microscope with Las AF (Leica Application Suite Advanced Fluorescence).

Transmission Electron microscopy
TS differentiated neurons were lifted with AccuMax and pelleted. Samples were fixated with a solution of 2,5% Glutaraldehyde in cacodylate for 2 hours at 4°C. Post-fixation was made with 1% OsO_4 in cacodylate for another 2 hours. Dehydration of the samples was performed with increasing concentrations of ethanol, finishing with incubation in propylene oxide. Sample embedding was done increasing concentrations of epoxy resin in propylene oxide followed by encapsulation of the resin and polymerization at 60°C

for 48 hours. Samples were cut with an ultramicrotome in 80nm sections. Negative staining of the section was made using uranyl acetate and lead (II) nitrate. Samples were observed at the JEOL JEM 1011 electronic microscope.

Molecular Biology and Biochemistry

Western blot analysis

Cells from differentiated and undifferentiated cultures were incubated in the presence or the absence of compounds 6S-ADBI-NJ or NOI-NJ (Luan et al. 2009). After indicated times, the cells were harvested and equal amounts of cell lysate (30mg from Bradford-determined RIPA homogenates) were separated by 10% SDS-polyacrylamide gel electrophoresis and transferred onto Immobilon PVDF membranes (Millipore #IPVH00010). For immunochemical detection, blots were incubated with primary antibodies anti-GBA and anti-actin. Subsequently incubated with secondary anti-mouse IgG peroxidase-conjugated antibody and developed with the chemoluminescence ECL plus (Amersham #RPN2132) detection system.

Acid-β-glucosidase enzymatic activity assay

Acid-β-glucosidase activity in cell pellets was determined as previously described (Cormand et al. 1997) with the fluorogenic substrate 4-methylumbelliferyl-b-D-glucopyranoside. Cellular pellet was resuspended in H_2O followed by 3 freeze-thaw cycles of 10 minutes each. Then Lowry protein quantification was performed. Samples were incubated for 1 hour at 37^{o}C with the substrate at 5mM. Activities were measured in triplicate in a Polarstar Omega A micro plate reader at 465nm emission. The results were presented as mean+SD. Student's t-test was used to examine the significance of differences between group means, and the differences in P-values, 0.05 were considered significant.

Acid-β-glucosidase activity in macrophages was measured by FACS as previously described (van Es et al. 1997). Briefly, 100.000 cells were incubated with 1mM FDGlu at 25^{o}C for 45 minutes. Specificity of the assay was confirmed by the use of 1mM CBE, a GBA irreversible inhibitor.

β-Hexosaminidase A enzymatic activity assay

HexA enzymatic activity was determined by measuring 4-methyllumbelliferone hydrolysis from the substrate. Cellular pellet was resuspended in H_2O followed by 3 freeze-thaw cycles of 10 minutes each. Then Lowry protein quantification was performed. Samples were incubated for 1 hour at 37^{o}C with the substrate at 1mM. Activities were measured in triplicate in a Polarstar Omega A micro plate reader at 465nm emission. The results were presented as mean+SD. Student's t-test was used to examine the sig-

nificance of differences between group means, and the differences in P-values, 0.05 were considered significant.

CD profile analysis

Cells were stained with monoclonal antibodies against human CD11b (BD Biosciences), CD14 (BD Biosciences), CD33 (BD Biosciences), CD163 (R&D systems) conjugated with fluorescein, phycoerythrin or allophycocyanin according to the manufacturer's instructions and analyzed by using Moflo high-performance cell sorter and flow cytometry analyzer Gallios. PI-stained dead cells were gated out. Human cell population was identified upon staining with antibodies against the pan-human marker TRA-1-85 (BD Biosciences).

RT-qPCR

Total RNA was extracted with Trizol (Invitrogen #15596-026) following manufacturer's protocol. cDNA was performed with the Cloned AMV First-Strand cDNA Synthesis Kit (Invitrogen #12328-040), using random hexamers. SYBR Green (Sigma #S4438) detection system was used in the RT-qPCR. RT-qPCR reaction was run in a 7900HT fast real time PCR system from Applied Biosystems. Specific primers were designed with Primer express software.

hGAPDH FP	GCACCGTCAAGGCTGAGAAC	hEndo-C-MYC FP	CGGGCGGGCACTTTG
hGAPDH RP	AGGGATCTCGCTCCTGGAA	hEndo-C-MYC RP	GGAGAGTCGCGTCCTTGCT
hEndo-OCT4 FP	GGGTTTTTGGGATTAAGTTCTTCA	Nanog FP	ACCAGAACTGTGTTCTCTTCCACC
hEndo-OCT4 RP	GCCCCCACCCTTTGTGTT	Nanog RP	CCATTGCTATTCTTCGGCCAGTTG
hEndo-SOX2 FP	CAAAAATGGCCATGCAGGTT	Rex1 FP	GCGTACGCAAATTAAAGTCCAGA
hEndo-SOX2 RP	AGTTGGGATCGAACAAAAGCTATT	Rex1 RP	ATCCTAAACAGCTCGCAGAAT
hEndo-KLF4 FP	AGCCTAAATGATGGTGCTTGGT	DNMT3B FP	TGCTGCTCCAGGGCCCGATA-CTTC
hEndo-KLF4 RP	TTGAAAACTTTGGCTTCCTTGTT	DNMT3B RP	TCCTTTCGAGCTCAGTGCACCA-CAAAAC

Table 2. Primers used in the qPCR por detection of pluripotency markers

Mutation analysis

Genomic DNA was extracted using DNeasy Blood & Tissue kit (Qiagen #69504). Primers for mutation analysis were designed flanking the mutation site in the genome. Sequencing was performed using Big Dye Terminator v3.1 Cycle kit (Invitrogen #4337455)

and samples were analyzed in a capillary sequencer (Applied Biosystems 3730xl or 3130xl DNA analyzer). GDExon7FP ATTCACCGAGCCCTGCAGTT GDExon7RP TTCACAAAGTATCTGGCCC; GDExon11FP AAGTTCATTCCTGAGGGCT GDExon11RP GTTTAGCACGACCACAACAG; TSExon11FP GATTCAGCCAGACACAATCA TSExon11RP CTCACCCCAGCTAAGTTGTT

iPSC authentication

GD and TS fibroblasts and derived iPSC samples were sent to qgenomics (http://www.qgenomics.com) in order to genotype STR markers: TH01, D21S11, D5S828, D13S317, D7S820, D16S539, CSF1PO, vWa y TPOX. The combination of these nine markers produces an allele profile with a 1 in $2.9x10^9$ probability of coincidence. Briefly, genomic DNA was extracted, a multiplex PCR with specific primers for the above STR markers followed by an electrophoresis and allele analysis.

Microarray processing and analysis

RNA was extracted using the miRNeasy Mini kit (Qiagen) following manufacturer's indications. RNA integrity was assessed using an Agilent 2100 bioanalyzer. All samples had high integrity (RNA integrity number (RIN) ≥8.7) and were subsequently used in microarray experiments. Amplification, labeling and hybridizations were performed according to the protocols from Ambion and Affymetrix. Briefly, 200ng of total RNA were amplified using the Ambion WT Expression Kit, labeled using the WT Terminal Labeling Lit of Affymetrix, and then hybridized to Human Gene 1.0 ST Array of Affymetrix, in a GeneChip Hybridization Oven 640. Washing and scanning were performed using the hybridization Wash and Stain Kit and the GeneChip System of Affymetrix (GeneChip Fluidics Station 450 and Gene-Chip Scanner 3000 7G).

Microarray data analysis was performed as follows: after quality control of raw data, it was background corrected, quantile-normalized and summarized to a gene level using the robust multi-chip average (RMA) (Irizarry et al. 2003) obtaining a total of 28 832 transcript clusters, excluding controls, which roughly correspond to genes. NetAffx annotations (version 32, human genome 19) were used to annotate analyzed data.

Hierarchical cluster analysis was performed to see how data aggregate and a heat map was generated with pluripotency genes. All data analysis was performed in R (version 2.15) with packages aroma.affymetrix (Bengtsson et al. 2008), Biobase, Affy, biomaRt and gplots. Ingenuity Pathway Analysis v9.0 was used to perform functional analysis of the results.

Reprogramming vector

The reprogramming vector consisted of a linear 10kb DNA fragment containing a polycistronic reprogramming cassette flanked by LoxP sites in order to allow removal of the cassette once the reprogramming is complete. Oct4, Sox2, Klf4, c-Myc and GFP

were linked through 2A self-cleaving peptides conforming the polycistron which expression is driven by a CAG promoter (Fig 5)

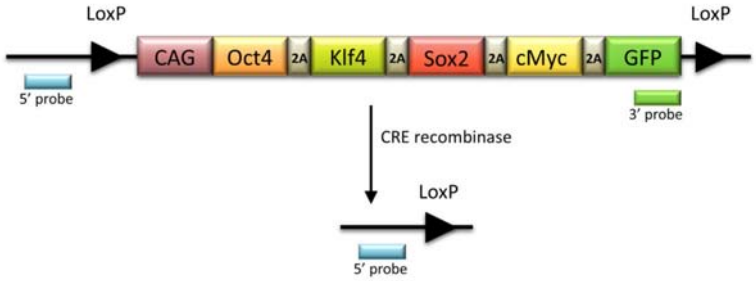

Fig 5. Reprogramming cassette

Southern blot

5µg of genomic DNA was digested with PstII and EcoRI (New England Biolabs), runned in a 1% agarose gel at low voltage and transferred to a positively charged nylon membrane by capillarity. Probes were designed both internal and external to the LoxP-flanked segment of the construct and were labeled with the PCR DIG probe synthesis kit following manufacturer's protocol. Hybridization of the probes was made ON at 65°C. Membranes were incubated with antibodies anti-DIG and development was made using CDP-Star chemoluminescent substrate.

Lentivirus expressing GBA1 or HEXA

GBA1 and HEXA genes were introduced separately in a typical VIH derived lentiviral backbone vector containing *cis*-acting sequences required for the retro-transcription and packaging of the vector. The 3'LTR has a deletion on the promoter-enhancer region making it a self-inactivating vector. The transgene is controlled by human β actin/ RU5 promoter and is followed by a WPRE sequence in order to confer stability to the RNA (Fig6)

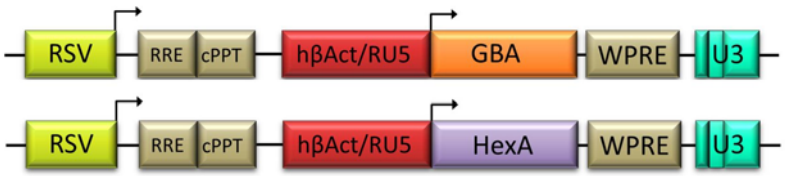

Fig6. Lentivirus expressing HEXA or GBA schema

Lentivirus expressing Cre recombinase

Cre recombinase was introduced in a typical VIH derived lentiviral backbone vector containing *cis*-acting sequences required for the retro-transcription and packaging of the vector. On the 3'LTR there is a LoxP site, so when Cre is expressed, the cassette is removed from the genome.

The 3'LTR has a deletion on the promoter-enhancer region making it a self-inactivating vector. Cre is controlled by CMV promoter and is followed by a WPRE sequence in order to confer stability to the RNA (Fig7)

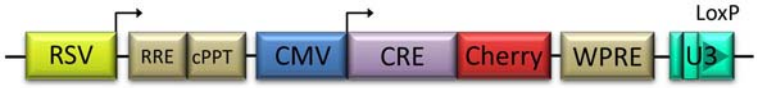

Fig7. Lentivirus expressing Cre schema

Packaging vectors

Third generation lentiviral vector systems consists of 4 plasmids. One is the lentiviral backbone with the transgenes and the other 3 plasmids supply the *trans* elements needed for the retro-transcription and packaging of the vector.

Vector pVSV-G carries the VSV-G gene, which encodes for a protein in the viral envelope responsible for the viral tropism. VSV-G is under the control of a CMV promoter.

Vector pRev carries the Rev protein which recognizes RRE in the viral mRNA and exports it to the cytoplasm.

Vector pMDL carries Gag-Pol precursor which is processed into an integrase, the reverse transcriptase and structural proteins. Non integrative lentiviral vectors were made with a pMDL vector which encodes for a Gag-Pol precursor which has an Asp64Val mutation on the integrase gene (Fig8).

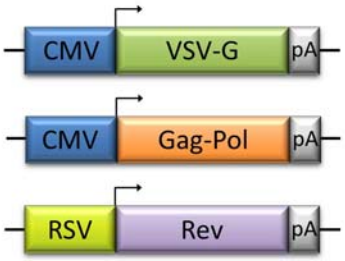

Fig8. Packaging vectors schema

Results

I. iPSC derivation and characterization

iPSC derivation can be performed from a number of different cell types by delivery of a combination of reprogramming factors to the cells through several alternative methods. In this work, the cells of choice were primary fibroblasts obtained from a biopsy of a patient diagnosed with GD type II carrying a compound heterozygote genotype (p.L444P/ p.G202R) and primary fibroblasts from a patient diagnosed with TS, obtained from the Coriell Cell Repository (#GM00527; p.W420C/ IVS11+1G>A). Reprogramming factors delivery was by nucleofection of a linear DNA fragment containing a polycistron expressing the pluripotency factors (Oct4, Sox2, Klf4, c-Myc) and GFP as reporter, all linked by 2A self-cleaving peptides and under the control of CAG promoter. The ex-

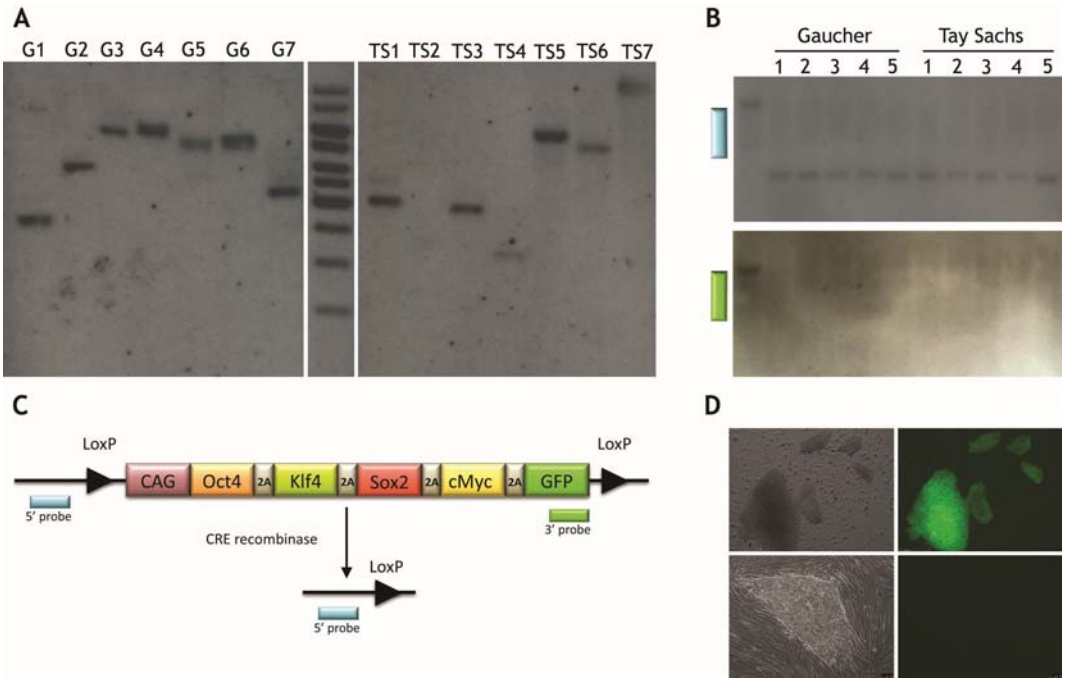

Fig 9. Reprogramming cassette delivery and elimination: A) Southern blot analysis of GD and TS iPSc lines (G1-G7 and TS1-TS7) with 5´probe. B) Southern blot analysis of GD and TS iPSC before and after delivery of CRE recombinase with either 3´probe or 5´probe. C) Schematic representation of reprogramming construct and reprogramming cassette elimination strategy. D) 10x magnification photos of GFP fluorescence iPSC. Upper panel, before delivery of CRE recombinase and lower panel after delivery of CRE recombinase.

pression cassette was flanked by LoxP sites, allowing its removal by Cre recombinase delivery once reprogramming was complete (Fig9).

WT and TS GFP positive colonies with ESC-like morphology appeared around 4 weeks after nucleofection. GD colonies suffered a noticeable delay and appeared after 5 to 6 weeks. Seven GD and seven TS colonies were isolated and expanded. Some iPSC lines silenced the reprogramming cassette spontaneously after 8 – 12 passages as judged by

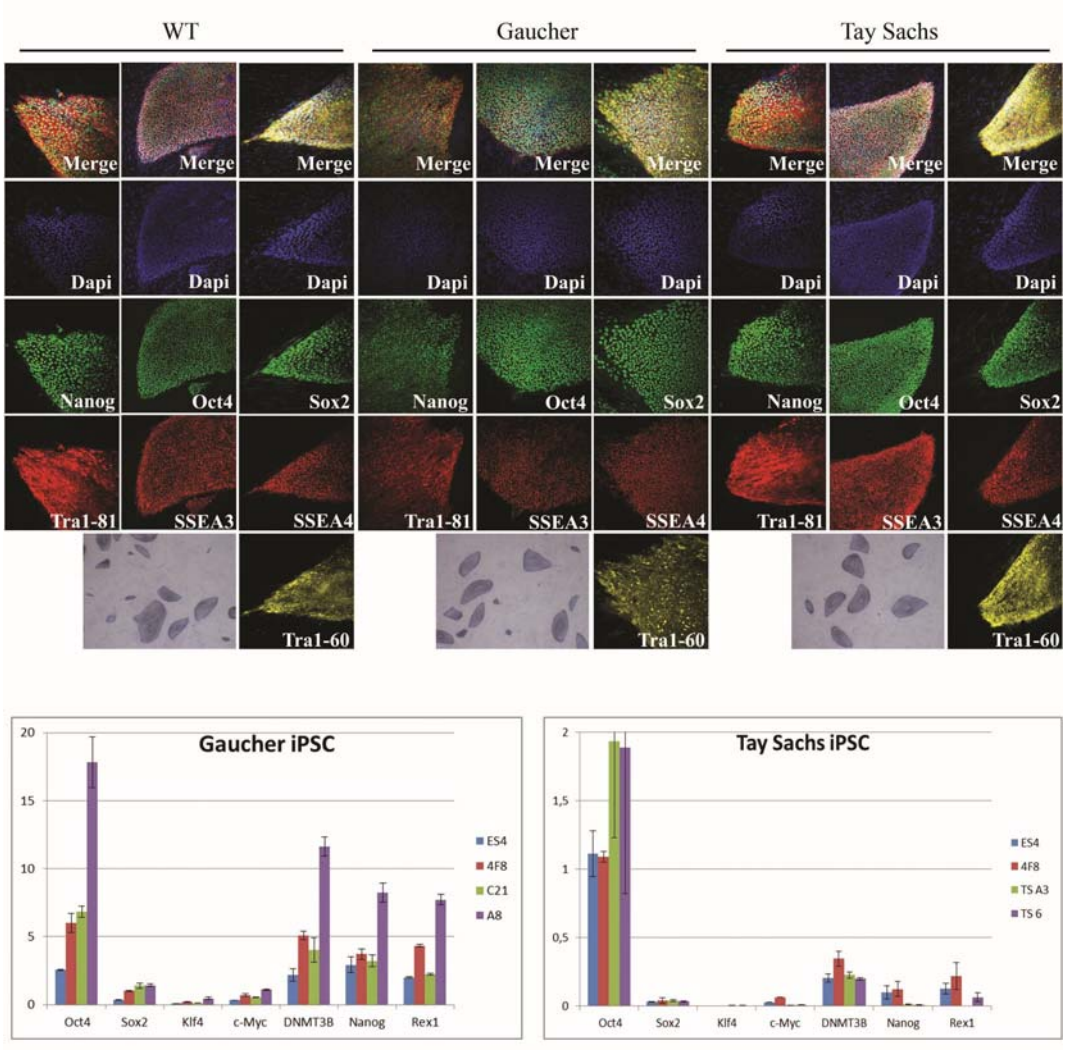

Fig10. iPSC pluripotency characterization: Upper panel, Immunostaining with different pluripotency markers (20x). Morphology of the resulting colonies and AP staining (10x). Lower panel: qPCR for expression of pluripotency factors.

GFP expression, while others remained GFP positive, indicating persistence of transgene expression. In order to remove the reprogramming cassette, iPSC lines showing GFP expression were transduced with a non-integrative lentiviral vector expressing Cre recombinase and cherry fluorescent protein as a reporter and plated over an irHFF feeder layer. After three days, cherry positive pluripotent cells were isolated by FACS, replated and expanded, leading to the establishment of subclones which showed no GFP expression (suggesting loss of the transgene) and no Cherry expression (suggesting no integration of the lentiviral vector used to deliver CRE recombinase). Southern blot analysis confirmed that loss of GFP expression was due to the excision of the reprogramming cassette (Fig9).

In order to establish that the iPSC lines isolated were truly pluripotent, an exhaustive characterization was performed. GD and TS iPSC lines showed similar morphology to hESC ES4 cell line and maintained their characteristics over long-term culture. Pluripotency of the iPSC derived cell lines was confirmed by alkaline phosphatase activity, immunodetection of specific pluripotency markers (Oct4, Sox2, Nanog, Tra1-60, Tra1-81, SSEA3 and SSEA4) and by real-time qPCR expression analysis of pluripotency associated genes (Oct4, Sox2, Klf4, c-Myc, DNMT3B, Nanog and Rex1) (Fig10). In order to check that the delay in the reprogramming of GD did not affect its pluripotent condition, GD iPSC pluripotency was further analyzed by FACS and by microarray gene expression (Fig11 and Fig12).

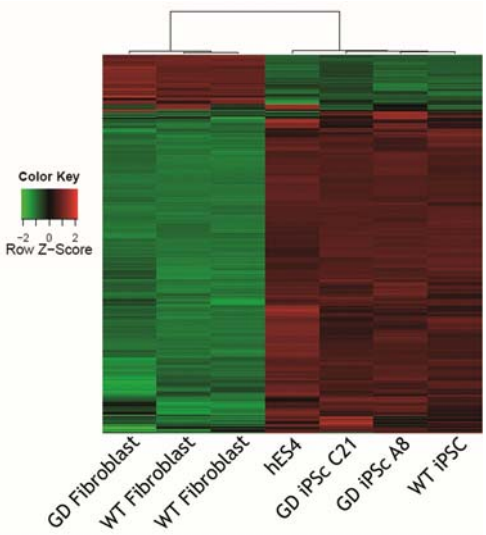

Fig11. Trascriptional profiling by microarray analysis. GD fibroblasts from a patient, two WT fibroblast populations, hESC 4, GD iPSC lines (iPSC-GD-C21 and iPSC-GD-A8) and a WT iPSC line.

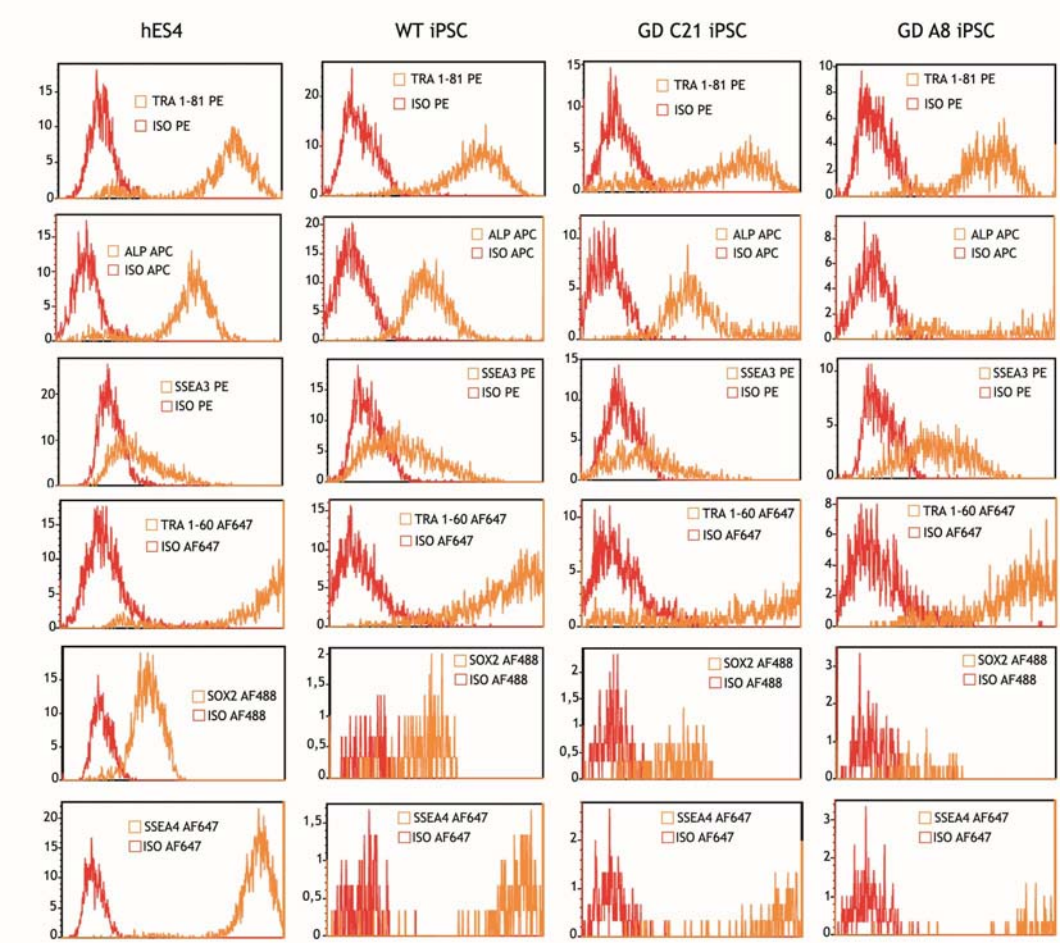

Fig12. Cytometry analysis of pluripotency in hESC 4, WT iPSC and GD iPSC C21 and A8.

Pluripotency is the capability of a cell to differentiate into any cell type of the organism. Pluripotency can be demonstrated by *in vitro* or *in vivo* differentiation (teratoma formation). Typically, this involves detection of at least two markers from each germ layer (ectoderm, mesoderm and endoderm). Increasingly stronger levels of proof are afforded by chimera formation, germline transmission and tetraploid complementation, which demonstrate the potential of an iPSC line to develop into a complete organism. For ethical reasons, in the human system, demonstration of pluripotency is necessarily limited to *in vitro* differentiation and teratoma formation. GD and TS iPSC showed full differentiation capacity when they were induced to differentiate *in vitro* to the three

germ layers, expressing typical markers of endoderm (FOXA2, AFP), mesoderm (ASMA and ASA), and ectoderm (Tuj1 and GFAP). GD and TS iPSC were also injected into SCID-beige mice and formed teratomas, which presented *in vivo* differentiation detected by immunohistochemistry with the same markers already described for the *in vitro* differentiation to the three germ layers (Fig13).

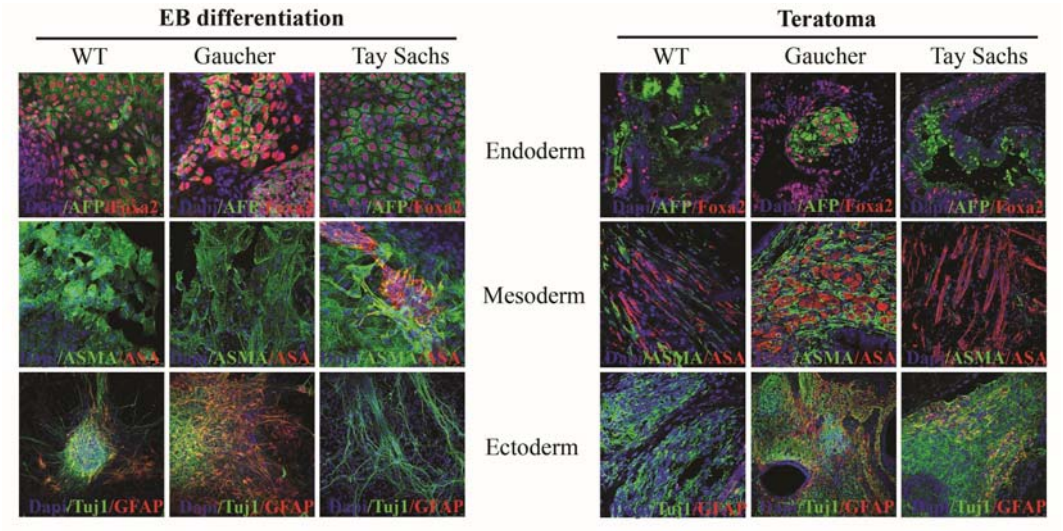

Fig13. *In vitro* differentiation (ectoderm 20x, mesoderm 40xTS WT 20xGD, endoderm 40x) and teratoma formation (ectoderm 40xTS WT 20xGD, mesoderm 40x, endoderm 40x) analyzed by immunohistochemistry.

A karyotype analysis was performed to evaluate genomic integrity after reprogramming. TS iPSC lines presented a normal karyotype; GD iPSC lines presented an inversion in the 12th chromosome. In addition, verification that the TS and GD iPSC lines were indeed derived from the original TS and GD fibroblasts was performed by STR genotyping (Fig14)

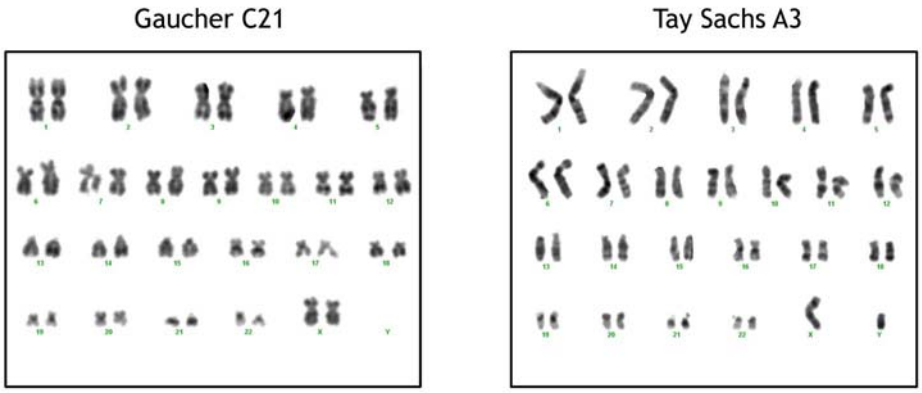

	TH01		D21S11		D5S818		D113S317		D7S820		D16S539		CSF1PO		AMEL	vWA		TPOX	
Fibros TS	6	7	29		11		11		7	11	9	11	12	13	XY	16	18	8	11
iPSC TS	6	7	29		11		11		7	11	9	11	12	13	XY	16	18	8	11
Fibros GD	6	7	28	32,2	11	12	11		9	10	8	11	12	13	XX	16	17	9	11
iPSC GD	6	7	28	32,2	11	12	11		9	10	8	11	12	13	XX	16	17	9	11

Fig14. Authentication and karyotype: Upper panel: karyotype analysis of GD C21 and TS A3 iPSC. Lower panel: Results of cell authentication analysis, TS fibroblasts and TS iPSC in one hand and GD fibroblasts and GD iPSC in the other, match perfectly, indicating that the derived iPSC lines come from the analyzed fibroblasts.

II. Disease phenotype characterization

Disease models, by definition, must recapitulate disease phenotype at the molecular and cellular levels if they are to be useful for basic mechanistic studies or therapy development. Therefore, the characterization of the disease phenotype in the obtained iPSC and differentiated disease relevant cell types was needed.

Gaucher phenotype

First, it was confirmed that the GD iPSC derived contained the same GD mutations (c.721 G>A and c.1448 T>C) reported in the original fibroblasts they were derived from

(Fig15). Second, enzymatic activity assays for GBA were performed in WT or GD cells for both the initial fibroblasts and the iPSC derived from them (Fig15). GBA activity was clearly reduced in GD fibroblasts compared to WT fibroblasts (GD fibroblasts had only 1,91% of the GBA activity found in WT fibroblasts). In both WT and GD iPSC, GBA activity was reduced compared to that found in the corresponding fibroblasts, but GBA activity was still lower in GD iPSC in comparison to WT iPSC (GD iPSC showed only 14,55% of the activity expressed by WT iPSC). In order to determine whether the lower GBA activity in GD cells could be partially due to lower GBA protein levels, western blot analysis was performed

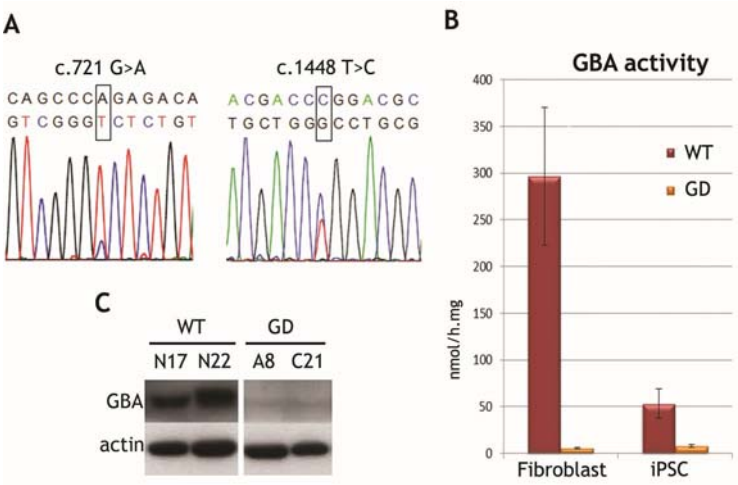

Fig15. A) Mutation detection in GD-iPSC C21 B) Acid-b-glucosidase activity in wt vs. GD cells in fibroblasts (P=0,0024) and iPSC (P=0,0074). C) Western blot analysis of WT iPSC N17 and N22, GD iPSC A8 and C21.

which indeed showed lower steady state levels of GBA protein in GD cells (Fig15).

In order to check that possible differences in genetic background between WT and GD iPSC could affect the results, congenic GD iPSC lines rescued for GBA expression were established by transducing them with a lentiviral vector expressing WT GBA1 gene and isolating subclones. This strategy led to the establishment of four

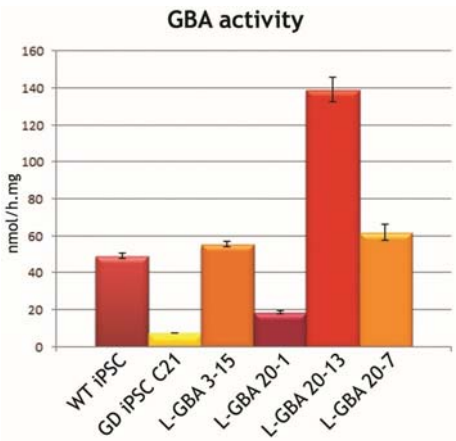

Fig16. Genetic rescue of GD iPSC C21 with lentiviral vector expressing GBA1. Acid-b-glucosidase enzymatic activity levels in WT, GD and 4 rescued lines

corrected subclones, three of which had similar or higher levels of GBA activity than those found in WT iPSC (Fig16).

Having established that GD iPSC show lower GBA protein levels and activity, the basic biochemical feature of GD, the next step was to differentiate GD iPSC to the main cell types typically affected by the disease. In all types of GD, one of the affected cell types are macrophages which, due to glucocerebroside accumulation, are transformed in Gaucher cells, accumulating in different tissues and being responsible for many of the systemic aspects of the disease. Our GD iPSC were derived from a patient diagnosed with the acute neuronopathic form of the disease, in which neurons are also damaged by glucocerebroside accumulation, impairing their function and leading to neuron degeneration. Because of it, GD iPSC were differentiated to macrophages and neurons.

Macrophages

For the differentiation to macrophages two cell lines were used: the GD C21 and the corrected GD iPSC L-GBA 3-15, which had GBA activity levels similar to that of WT iPSC. The protocol used was a combination of the differentiation protocols used by Raya et al (Raya et al. 2009) for obtaining HSC from human iPSC and that used by Choi et al (Choi et al. 2011) for mature myeloid cells derivation from human pluripotent stem cells with some modifications. Briefly, iPSC were cultured as EBs, differentiated to the hematopoietic lineage by co-culture on OP9 stromal cells and growth factor treatment for 14–17 days, and subjected to two successive macrophage inducing cytokine cocktail regimes for 2 and 10 days, respectively, as described in Materials and Methods section.

The resulting population derived from GD C21 iPSC was analyzed by FACS and showed expression of typical markers from the monocyte-macrophage lineage: CD11b (18.3%), CD14 (35.6%), CD33 (35.5%) and CD163 (13.6%) (Fig17). The analysis also concluded that there were populations expressing more than one marker from the monocyte-

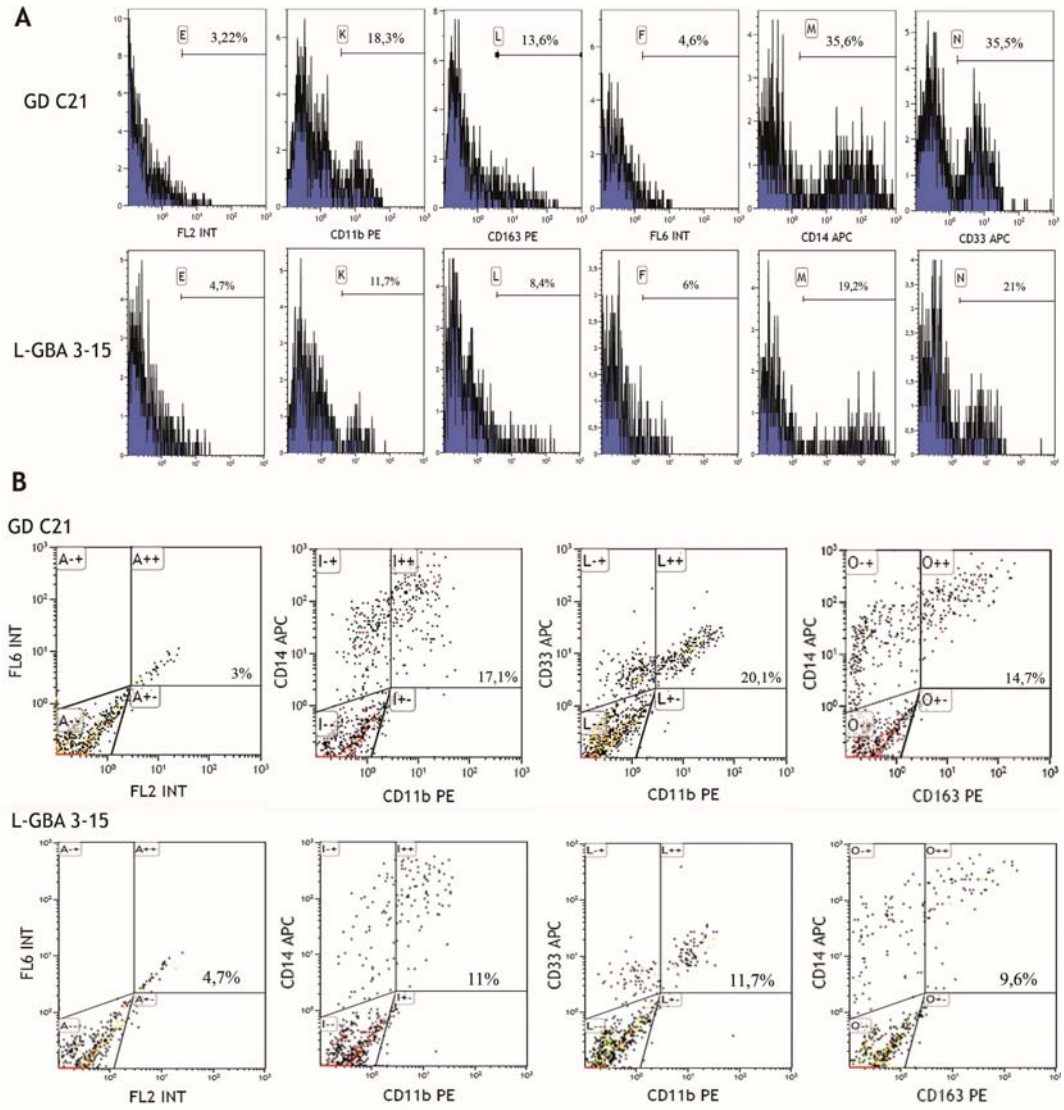

Fig17. Characterization of macrophages derived from GD iPSC C21 and recued L-GBA 3-15. A) Histograms showing % of cells positive for monocyte-macrophage lineage markers CD11b, CD163, Cd14 and CD33 B) Scatter plots showing % of double positive cells for monocyte-macrophage lineage markers CD14/CD11b, CD33/CD11b and CD14/CD163.

macrophage lineage: CD14 plus CD11b (17.1%), CD33 plus CD11b (20.1%) and CD14 plus CD163 (14.7%) (Fig17). Macrophages produced with the above protocol were proved to be functional macrophages as ascertained by phagocytosis of fluorescent

opsonized beads (Fig18). The resulting population derived from the corrected sub-clone L-GBA 3 – 15 showed an overall similar pattern of marker expression: CD11b (11.7%), CD14 (19.2%), CD33 (21%), CD163 (8.4%); CD14 plus CD11b (11%), CD33 plus CD11b (12%), and 9.6% of the cells expressing CD14 plus CD163 (9.6%) (Fig17).

GBA activity of the macrophages obtained from GD C21 and L-GBA 3-15 iPSC was analyzed by FACS together with CD14 marker. As expected, GD C21 iPSC derived macrophages showed 3 to 6 times less GBA than L-GBA 3-15, in accordance with the GBA activity observed, which was higher in the corrected macrophages than in the GD.

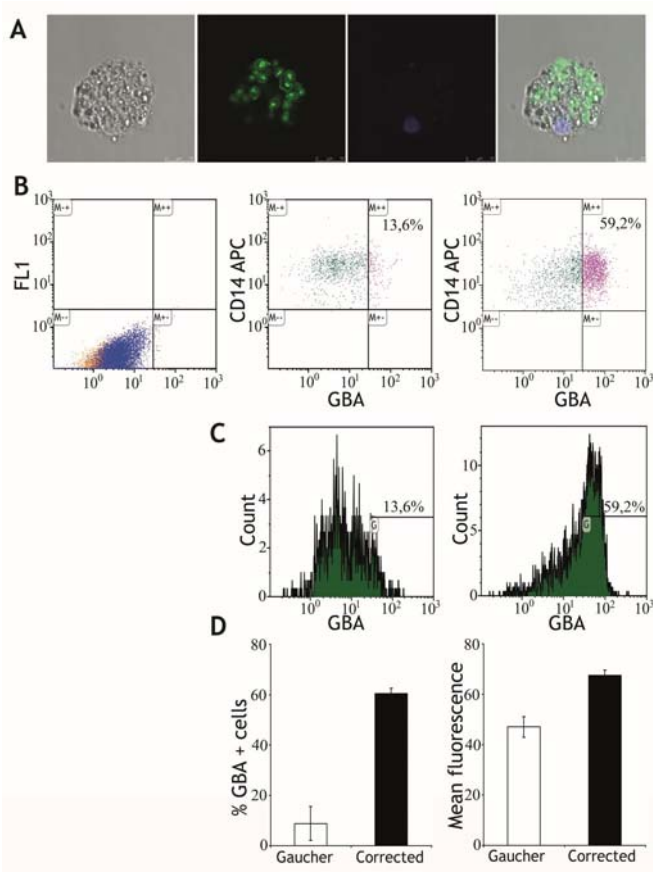

Fig18. Comparison of macrophages derived from GD iPSc vs. genetically rescued GD iPSC. A) Phagocytosis assay: micrographs showing morphology, fluorescent beads, DAPI stain and merge of iPSC derived macrophages after internalization of fluorescent beads (40x).B) Scatter plots showing % of high expressing GBA1 cells and GBA activity C) Histograms showing % of high expressing GBA1 cells and GBA activity D) Bar chart showing quantification of % of high expressing GBA1 cells and mean fluorescence (n=2).

In conclusion, functional macrophages were obtained, concluding that diminished GBA expression and activity levels do not affect macrophage differentiation in vitro.

Dopaminergic neurons

As GD type II has a strong neuronopathic component, differentiation to neuronal types is crucial to the usefulness of the model. A previously described protocol for derivation of dopaminergic neurons from ESC (Cho et al. 2008a) was chosen for the analysis of the phenotype in the iPSC derived neurons. This protocol has been shown to produce a high percentage of mature dopaminergic neurons capable of electrophysiological activity (Cho et al. 2008b) and consists in the formation of spherical neural masses (SNMs) that can be expanded and subsequently differentiated to dopaminergic neurons using a combination of N2, B27, ascorbic acid and the mid-brain patterning factors FGF8 and SHH (Fig. 19)

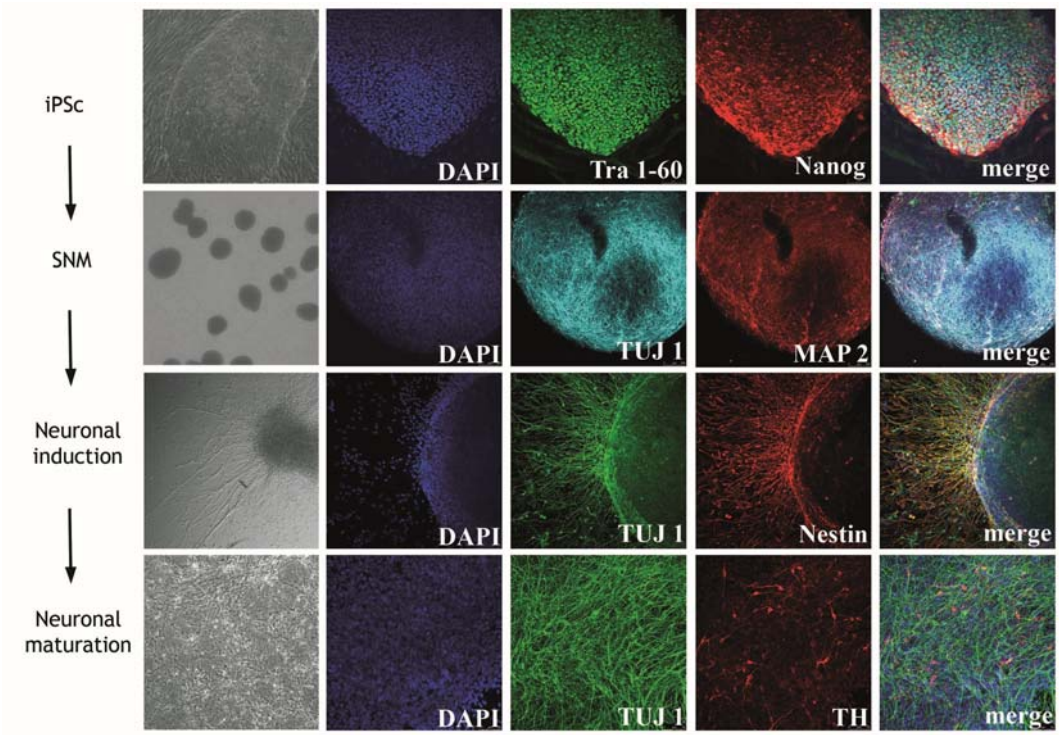

Fig19. Dopaminergic neuron derivation from iPSC GD, TS and WT. Pictures are representative for all lines. Rows from top to bottom: iPSC, SNM, differentiating SNM (20x) and mature dopaminergic neurons (40x). Markers indicated in each panel.

Wild type, GD C21 and L-GBA 3-15 iPSC were differentiated with this protocol. SNMs obtained from the cell lines were analyzed by immunofluorescence, showing expression of neural lineage (Tuj1) and neural precursor markers (Pax6, Map2). At the end of the protocol, slides were analyzed by immunofluorescence, resulting in heterogeneous cultures with neuronal morphology expressing Tuj1 marker. A significant percentage of TUJ1+ neurons were also positive for tyrosine hydroxylase (TH), a marker of dopaminergic neurons. In addition, clusters of mature neurons positive for neurofilament, synapsin and NeuN were found (Fig23). Nevertheless, Map2 marker was also found in the majority of neurons, indicating heterogeneity of different developmental stages in the resulting population.

No significant differences in differentiation ability between the three lines were observed, suggesting that GBA expression levels have little effect on the differentiation process; yield and proportion of mature neurons. While the differentiation protocol was generally reproducible, yields were variable from experiment to experiment for all three lines used, presumably due to stochastic events and subtle variation in culture parameters.

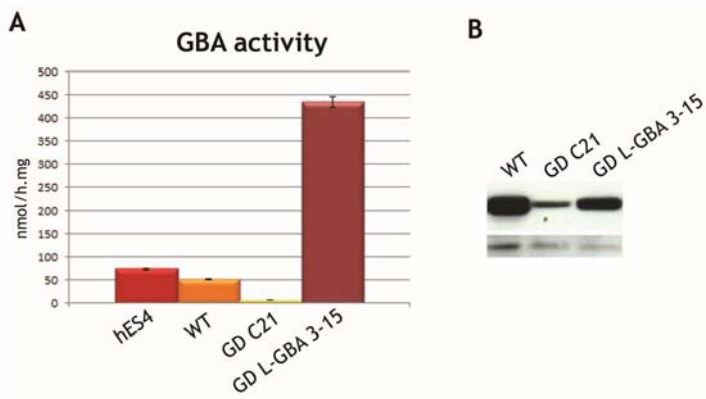

Fig20. GBA characterization in differentiated neurons derived from iPSC and hES A) GBA activity B) Western blot detection for GBA

The iPSC derived neurons were further analyzed in order to check the recapitulation of the GD phenotype. Neurons were subjected to western blot analysis and for GBA activity assays as described in the material and methods chapter. Neurons derived from GD C21

iPSC showed less GBA activity than those derived from WT iPSC and this result was coherent with the GBA protein levels as seen in the western blot results (Fig20)

Tay Sachs phenotype

The TS fibroblast line utilized to derive iPSC has a compound heterozygote genotype consisting of one allele with a mutation in exon 11 (c.1260 G>C) which leads to an aminoacid substitution (Trp420Cys), and the second allele carrying the intronic mutation IVS11+1 G>A, which leads to a splice site mutation, altering normal RNA processing (Miranda et al. 1994). The presence of both mutations was confirmed by sequencing in both fibroblasts and iPSC (Fig21). An enzymatic activity assay was performed in the initial fibroblasts and in the derived iPSC. HexA activity was clearly reduced in both TS fibroblast and iPSC compared to WT (Fig21).

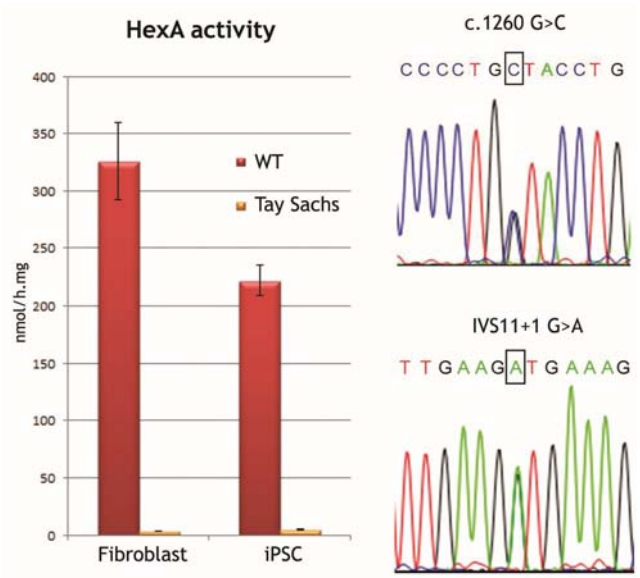

Fig21. iPSC TS characterization. Left panel: b-Hexosaminidase A activity in WT vs. TS cells in fibroblasts and iPSC. Right panel: Mutation detection in TS-iPSC A3

TS disease phenotypes in TS iPSC were analyzed and compared to both WT iPSC and with TS iPSC that had been rescued by transduction with a lentiviral vector expressing the WT HEXA gene. As in the case of GD, this allowed for the development of an isogenic cell line pair allowing comparison of the WT and mutated TS alleles in an otherwise identical genetic background. TS iPSC were transduced with a lentiviral vector ex-

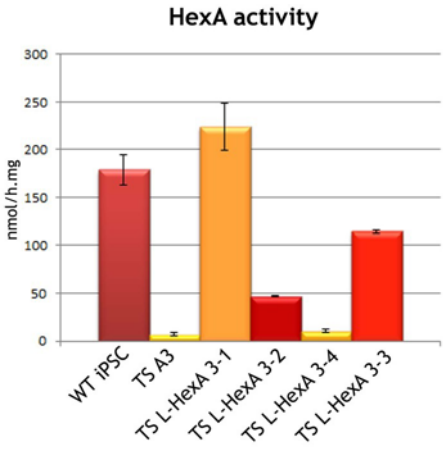

Fig22. Genetic rescue of TS iPSC A3 with lentiviral vector expressing HexA. b-Hexosaminidase enzymatic activity levels in WT, TS and 4 rescued lines

pressing the wild type form of the HexA gene, providing full enzymatic activity to the HexA enzyme heterodimer. This correction led to the establishment of four corrected subclones, two of which had similar or higher levels than WT iPSC (TS L-HexA 3-1 and TS L-HexA 3-3) (Fig22).

Clinical manifestations in TS are almost exclusively neurologic and the pathology is restricted to the nervous system. G_{M2} is mainly found on the gray matter of the brain, forming part of the plasma membranes of the neurons. For G_{M2} degradation, the plasma membrane containing glycosphingolipids is endocytosed, passing through the endosomal compartments which finally lead to lysosomes. In the lack of HexA enzyme, G_{M2} cannot be degraded and it accumulates on the lysosome, impairing cell function and leading to brain damage (Gravel et al. 2001). Because of this, differentiation to neuronal cells is fundamental in the phenotype characterization of TS disease. As TS hallmarks (enlarged lysosomes and multillamelar bodies in the cytoplasm) are found in all neuronal types and differentiation to dopaminergic neurons protocol was already set up, TS iPSC were derived to neuronal lineage using the same protocol that was used with the GD iPSC for dopaminergic neuron derivation.

Wild type, TS A3 and TS L-HexA 3-1 were differentiated to the neuronal lineage with the Cho protocol and, as in the case of GD, SNMs obtained from the cell lines were analyzed by immunofluorescence, showing expression of neural lineage (Tuj1) and neural precursor markers (Pax6, Map2). Final slides were analyzed by immunofluorescence, showing the same characteristics as in the GD case: heterogeneous cultures with neuronal morphology expressing Tuj1 marker, in which a significant percentage was posi-

tive for dopaminergic marker TH. Also, heterogeneous development stages were found as indicated by the presence of Map2 marker as well as neurofilament, synapsin and NeuN (Fig23).

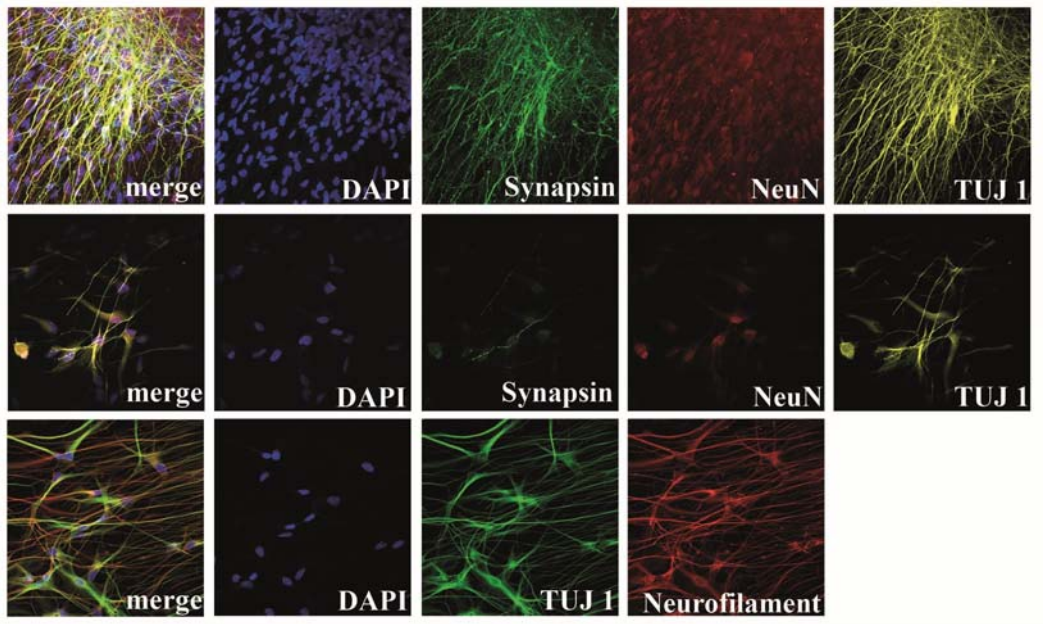

Fig23. Analysis of mature neurons derived from GD, TS and WT iPSC. Pictures are representative for all lines (40x). Markers indicated in each panel.

Wild type, TS A3 and TS L-HexA 3-1 showed similar differentiation ability, suggesting that HexA activity is not crucial for the neuronal development and that G_{M2} accumulation does not impair it. However, as in GD, differentiation results were reproducible but variable from experiment to experiment for all three lines, without a noticeable bias for any of the cell lines, underlying the heterogeneity present on the differentiation protocols.

One typical characteristic in TS is the accumulation of G_{M2} and cholesterol in the secondary lysosomes of the neurons of both central nervous system and peripheral nervous system. This is easily observable by immunostaining of G_{M2} ganglioside and the

lysosomal marker Lamp2. Thus, for TS phenotype characterization, wild type, TS A3 and TS L-HexA 3-1 derived neurons were analyzed by immunofluorescence of neuronal marker Tuj1 together with Lamp2 and ganglioside G_{M2}, revealing an enlargement and increasing the number of the lysosomes in the TS A3 derived neurons, comparing to wild type and the corrected TS L-HexA 3-1 (Fig24). Also it is observable an increase in the GM2 ganglioside in the TS A3 derived neurons compared to wild type and corrected. TEM on patients' brains reveals that the neuronal cytoplasm is full with multillame-

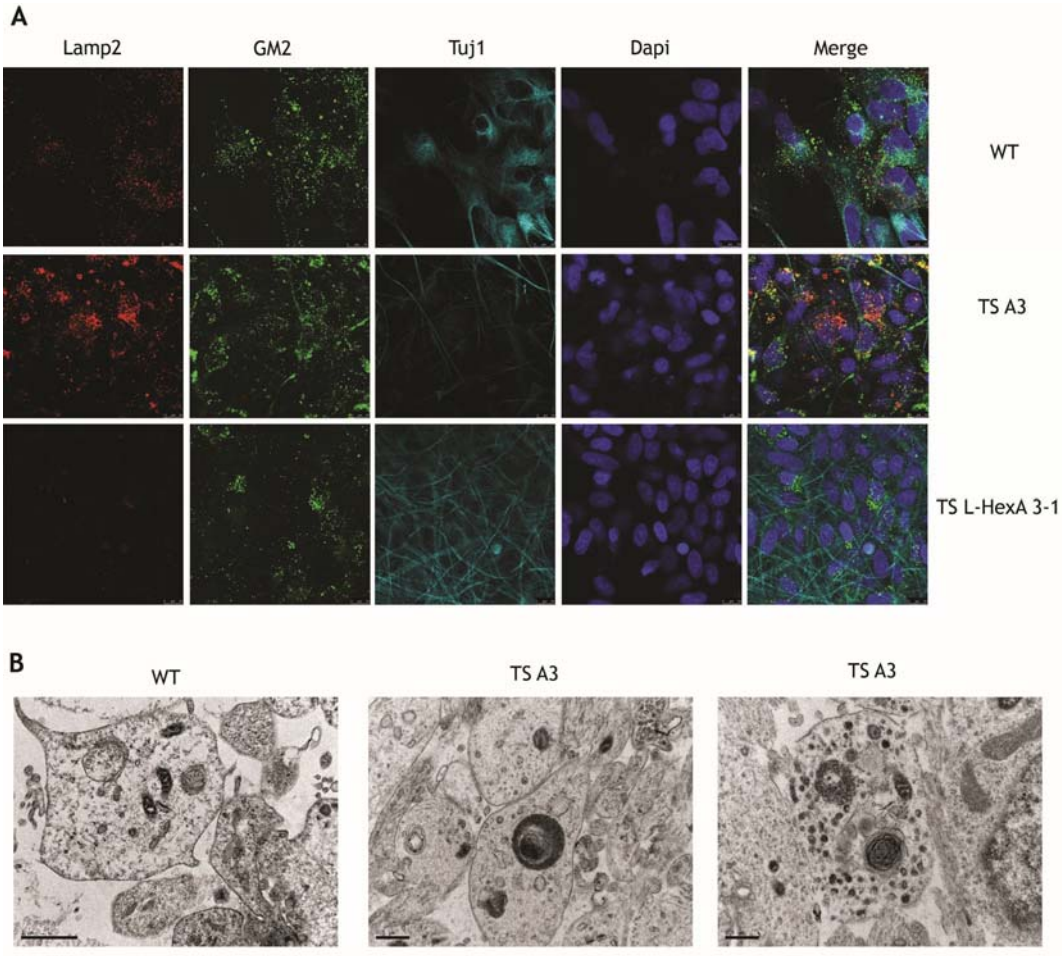

Fig24. Phenotype characterization of derived neurons from TS iPSC A3. A) Fluorescence microscopy images (40x) showing Lamp2 (lysosome marker) GM2 and Tuj1. B) Transmission electron microscopy on WT and iPSC neurons. Arrows mark lysosome ultrastructures.

lar membranous bodies (MCBs) which correspond to the secondary lysosomes containing accumulation of G_{M2} (Terry et al. 1963). TEM analysis on the wild type and TS A3 derived neurons recapitulates the ultrastructure observed on patients' brains, showing MCBs in the cytoplasm of TS A3 neurons and not in the WT (Fig24).

III. Using GD and TS iPSC derived neurons for small compound testing

Gaucher Disease and chemical chaperones.

GD can be treated with splenectomy, blood transfusions and analgesics, but these are directed to the alleviation of the symptoms rather than to eliminate the cause of the disease. Systemic aspects of the disease could be addressed by bone marrow transplantation, in which the find of a compatible donor is the limiting factor; or by gene therapy, delivering the GBA1 gene to hematopoietic stem cells, but because of its associated risk, it is not currently a method used in the clinic. The most used GD treatments involve ERT, SRT and recently it has been added the use of pharmacological chaperones. ERT consists in a regular intravenous infusion of a modified GBA with N-acetylglucosamine and mannose residues so it can be incorporated into the patient's macrophages (Barton et al. 1991; Beutler 2004; Aviezer et al. 2009). SRT is directed to reduce the GBA substrate, the glucosylceramide, by inhibiting the glucosyltransferase with the use of imino sugars as the N-butyldeoxynojirimycin (NB-DNJ) (Platt et al. 1994; Cox et al. 2000; Butters et al. 2005; Aerts et al. 2006; Elstein et al. 2009). Both strategies have demonstrated to be effective treating the systemic aspect of the disease (Schiffmann et al. 1997; Grabowski et al. 1998; Platt et al. 2001; Weinreb et al. 2002), but none is able to cross the blood brain barrier with enough efficiency to have any

impact on the neuronal aspects of the disease (Prows et al. 1997; Aerts et al. 2006; Benito et al. 2011).

Pharmacological chaperones are based in GBA inhibitors which use at sub-inhibitory concentrations leads to the stabilization of the GBA structure, protecting it from premature degradation and facilitating its trafficking through the ER to the lysosome. On the lysosome, the glucosylceramide concentration displaces the complex enzyme-inhibitor to enzyme-substrate, recovering the GBA activity (Yu et al. 2007; Parenti 2009; Benito et al. 2011). In this respect, the use of imino sugar-based scaffolds as N-(n-nonyl) deoxynojirimycin (NN-DNJ), increased the GBA activity in mutant forms p.N370S and p.G202R (Sawkar et al. 2002; Sawkar et al. 2005), but also resulted in an inhibitor of both α and β glucosidases, which could lead to secondary effects (Suzuki et al. 2007). Recently, bicyclic nojirimycin analogues with sp2 imino sugar structure were found to be highly selective competitive inhibitors of GBA but no other glucosidases (Luan et al. 2009). Their chaperoning effects were characterized in GD fibroblasts, but not in GD neurons, offering the perfect framework to validate the iPSC-GD model as a drug testing platform by analyzing the effect of the bicyclic nojirimycin analogues in the derived neurons from the iPSC-GD lines.

Initially, five bicyclic nojirimycin analogues were chosen and tested on WT and GD fibroblasts. Compounds were added to the culture media for 4 days, using different concentrations from 0 to 100 μM and then GBA activity was analyzed. Three of the compounds (6S-NOI-GJ, 6S-NOI-NJ and 6N-NOI-NJ) were able to increase the GBA activity on the GD fibroblasts, but inhibited its activity in WT fibroblasts (Fig25). The other two compounds (NOI-NJ and 6S-ADBI-NJ) performed an increase on GBA activity on GD fibroblasts of 2-4 fold change comparing to untreated GD fibroblasts without having a negative effect on the WT fibroblasts (Fig25). Because of this, the effect of the com-

pounds on the GBA activity of the derived neurons was focused on these two compounds: NOI-NJ and 6S-ADBI-NJ.

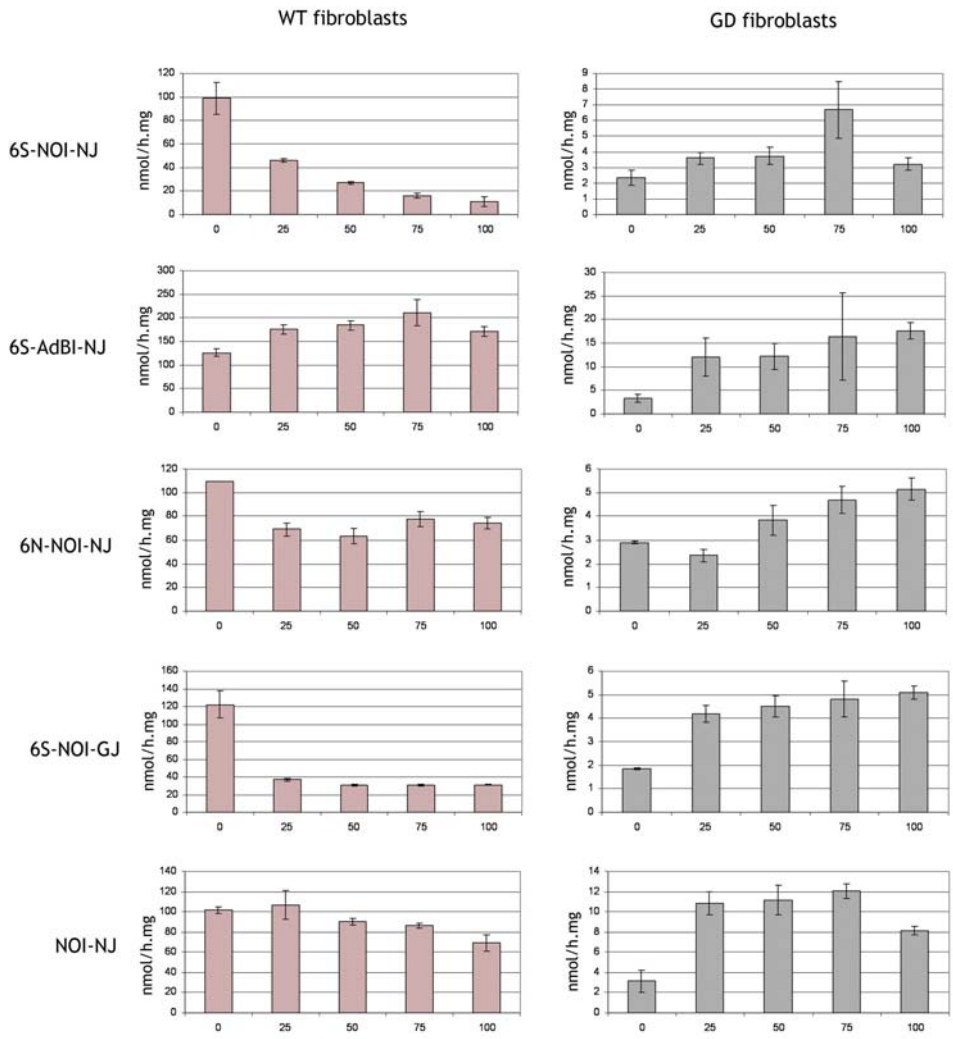

Fig25. Acid-b-glucosidase enzymatic activity levels in WT and GD fibroblasts treated with the different bicyclic nojirimycin analogues

For testing the NOI-NJ and 6S-ADBI-NJ compounds in GD derived neurons, different iPSC lines (WT, iPSC GD C21 and GD L-GBA 3-15) were differentiated to dopaminergic neurons following the protocol used before (Cho et al. 2008a). On the last four days of

differentiation, 30µM of either NOI-NJ or 6S-ADBI-NJ were added to the media. The addition of the compounds did not affect the efficiency or yield of differentiation result. Protein extracts from treated and untreated iPSC derived neurons from both WT, GD iPSC and corrected GD L-GBA 3-15 were analyzed for GBA protein levels and activity. NOI-NJ and 6S-ADBI-NJ treated GD neurons show increased GBA activity by 3-4 fold compared to untreated GD neurons (Fig26). An increase of activity was also noticeable in both treated WT and corrected L-GBA 3-15 neurons. These results are consistent with the increase of protein levels observed in the treated WT, GD and corrected neurons in the western blot analysis (Fig26), suggesting that the increase of GBA activity is due to an increase of the protein levels. Together, these results suggest that both compounds were able to increase the GBA stability and improve its trafficking to the lysosomes.

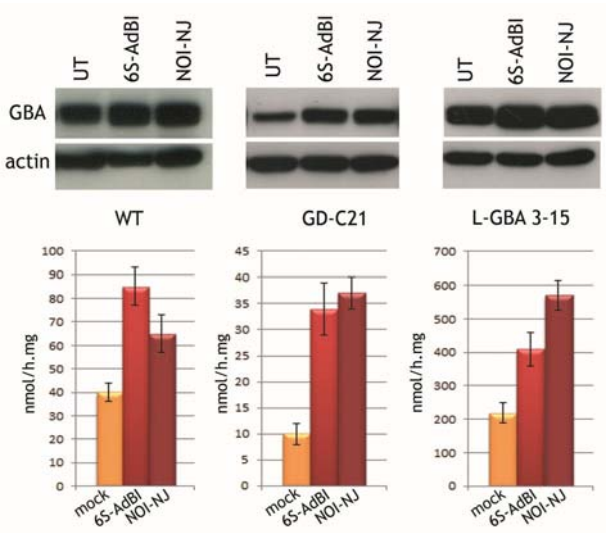

Fig26. Acid-b-glucosidase protein and enzymatic activity levels in differentiated dopaminergic neuronal cultures derived from WT, GD, and L-GBA corrected GD iPSC subjected to 30uM of 6S-ADBI-NJ and NOI-NJ

Tay Sachs and the exocytosis strategy

There have been studies for Tay Sachs therapy which involve ERT; unfortunately they have not been successful mainly due to the difficulty of the enzyme to cross the BBB and target neuronal cells (Johnson et al. 1973; von Specht et al. 1979). Miglustat (N-butyldeoxynojirimycin or NB-DNJ) has been studied as a possible agent for SRT in TS, but despite its promising results in mice models (Platt et al. 1997; Baek et al. 2008),

results have not been reproduced in human patients (Maegawa et al. 2009; Shapiro et al. 2009). Also, design and treatment with pharmacological chaperones is ongoing (Rountree et al. 2009; Clarke et al. 2011; Osher et al. 2011) for structural mutants in which the heterodimer HexA cannot be transported to the lysosome, not being useful for activity mutants in which the HexA heterodimer is formed, able to be transported to the lysosome but that cannot degrade the G_{M2}, so pharmacological chaperones may have an effect on determinate mutants but are not applicable to all TS patients.

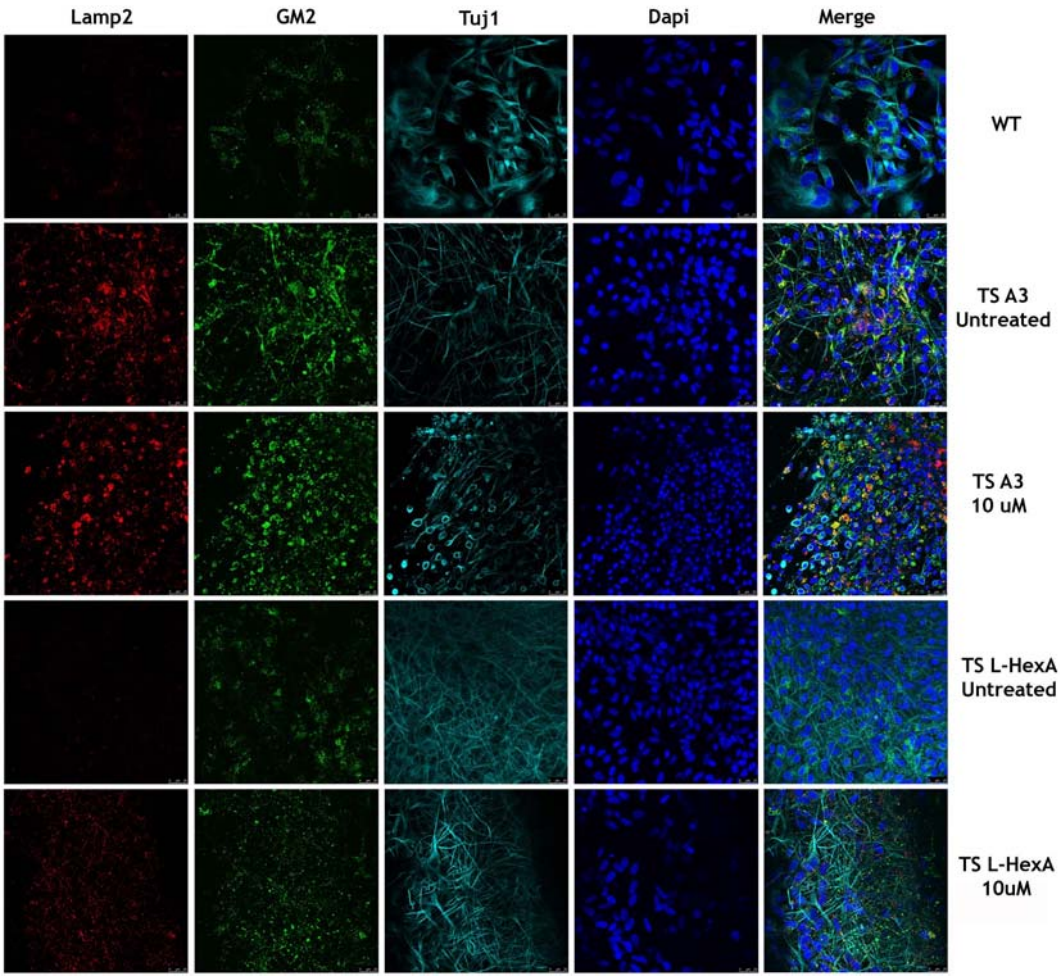

Fig27. Neurons derived from WT, TS A3 and TS L-HexA 3-1 treated with 10uM of NCGC00250218-01

A new approach for lysosomal storage diseases is the promotion of the exocytosis of the lysosomes and its content, reducing the negative effect of the lipid accumulation on the cell machinery (Klein et al. 2005; Medina et al. 2011). Particularly, δ-tocopherol has probed to reduce lysosomal cholesterol accumulation and decrease the lysosome volume by promoting exocytosis in Niemann-Pick type C and Wolman disease (Xu et al. 2012). In the same work, δ-tocopherol was also tested in fibroblasts of other six lysosomal storage diseases including TS. Access to relevant human cell types in TS for drug testing is difficult, but the iPSC-TS model presented in this defense offer a platform for obtaining human neuronal cells in which δ-tocopherol and its analogue can be tested.

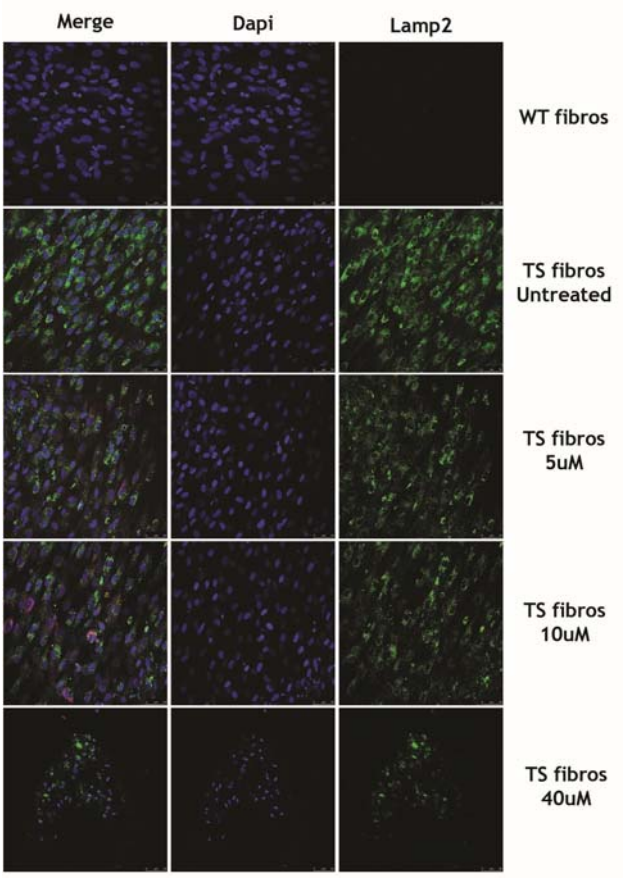

Fig28. Fibroblasts treated with different concentrations of NCGC00250218-01

Two compounds were tested one is δ-tocopherol (NCGC00160622-03) and the other is a metabolically stable δ-tocopherol analogue (NCGC00250218-01). Neurons were derived from WT, TS A3 and TS L-HexA 3-1 iPSC following the protocol described above. Both compounds were added to the differentiation media on the last four days of the differentiation protocol. Final concentrations used were 40µM for NCGC00160622-03 and 10µM for NCGC00250218-01 which were the IC50 tested in fibroblasts. All WT derived neurons treated with the compounds presented cytotoxicity, detached from

the plate and died before the treatment was complete. TS and TS L-HexA derived neurons also presented cytotoxicity and died with 40µM of NCGC00160622-03 and were clearly damaged at 10 µM of NCGC00250218-01. Neuron slides which survived the treatment were fixed with PFA and immunostained with Lamp2 and G_{M2}, showing that the treatment with NCGC00250218-01 not only did not reduce the lysosome number and size, but increased it (Fig27). In order to confirm the fibroblast results achieved by our collaborators, an analysis with variable concentrations from 5 µM to 40 µM revealed that the compounds used were also producing cytotoxicity without lysosome size or number reduction. This negative results might be due to an error while synthetizing the compounds, because the lysosome reduction effect in fibroblasts have been reproduced and observed in different laboratories.

Discussion

Discussion

This PhD dissertation describes the development of iPSC based disease models for Gaucher disease and Tay Sachs disease. The method of choice was the nucleofection of a reprogramming construct into dermal fibroblasts of GD and TS patients. The derived WT, GD and TS iPSC satisfy the standard quality requirements in the field: they show ESC like morphology, express pluripotency markers (confirmed by both immunostaining and qPCR), and are able to differentiate to all three germ layers both *in vitro* and by teratoma formation *in vivo*. The TS iPSC have a normal karyotype, while the GD iPSC present an inversion on the chromosome 12, which did not affect the phenotype for the purposes of the research as the results show. GD and TS iPSC were genotyped by sequencing to confirm the presence of the original mutations observed in the fibroblasts, c.721 G>A and c.1448 T>C in GD and c.1260 G>C and IVS11+1 G>A in TS. Moreover, cell line origin verification was performed by STR analysis to confirm GD and TS fibroblasts as the original donor cells of the resulting GD and TS derived iPSC. GD and TS iPSC were differentiated to the main cell types involved in each disease: macrophages and neurons in GD and neurons in TS. In both cases, the differentiated cells reproduce the disease hallmarks. In GD, reduced acid-b-glucosidase deficiency in both protein levels and enzymatic activity were observed in both neurons and macrophages. In TS, an increase in the size and number of lysosomes was observed in TS iPSC derived neurons by TEM and immunostaining. Furthermore, the differentiated cells were used to evaluate candidate drugs for the treatment of both diseases, providing a novel human based *in vitro* preclinical model.

The classic method of reprogramming involves using retroviral vectors expressing a small number of ESC related transcription factors, most frequently Oct4, Sox2, Klf4 and c-Myc, either cloned individually or as a polycistron (Gonzalez et al. 2009). In this work a linearized DNA fragment was used which included a CAG promoter driven

polycistronic cassette constituted by Oct4, Sox2, Klf4, c-Myc and GFP linked by 2A self-cleaving peptides. The cassette was flanked by LoxP sites, allowing the excision and elimination of the cassette from the host genome by transient CRE recombinase expression once the reprogramming was complete. In this way, genomic insertions are minimized and if the reprogramming cassette does not silence spontaneously, it can be removed with CRE recombinase. When analyzing the insertions, 90% of the iPSC clones had only one transgene insertion. Some of the clones were able to silence the transgene expression after 8-12 passages, but the rest did not and transgene excision was performed, eliminating problems derived from incomplete silencing or possible reactivation of the transgene during differentiation.

One factor to consider when deriving iPSC from patient fibroblasts are possible deleterious effects of the mutation on the viability and physiology of the fibroblasts to be reprogrammed. Previous reports have demonstrated the need for ectopic expression of the WT gene in mutated cells as a necessary prerequisite for successful reprogramming (Raya et al. 2009; Huang et al. 2011). There was no need to express wild type GBA and HEXA to reprogram GD and TS patient fibroblasts. TS fibroblasts gave rise to iPSC colonies in the same time frame as WT fibroblasts (4 weeks). However, in the case of GD, iPSC colonies took longer to develop (5-6 weeks), an observation which has not been previously reported in published works on GD fibroblast reprogramming (Park et al. 2008; Panicker et al. 2012), suggesting that the diminished reprogramming ability could be due to a slower rate of fibroblast cell division observed in GD fibroblasts. Genetic rescue was not needed in this case and we did not test whether the presence of WT GBA improved reprogramming efficiency or time-course of colony appearance. Regardless of the slower reprogramming process, GD iPSC were similar to WT iPSC by morphology, growth rate and expression of pluripotency markers as confirmed by immunofluorescence, microarray profiling and flow cytometry analysis.

Discussion

Several publications have reported the development of iPSC disease based models, establishing a convenient source of human disease specific cell types for dissecting mechanisms of pathogenesis and providing an intermediate level of testing of pharmacological compounds between animal models and clinical trials (reviewed in Tiscornia et al. 2011; Onder et al. 2012). There are several advantages of iPSC disease models in contrast with other types of disease models such as primary tissue from patients or animal disease models. Primary cells from patients are hard to procure and are often not the specific cell type involved in the pathology. Animal models, while having the advantage of studying the disease at the organismal level, suffer the disadvantage of species specific differences and partial reproduction of the human disease presentation. IPSC based models provide an ample source of the specific human cell type involved in the disease. GD iPSC were differentiated to macrophages, the main cell type involved in the systemic effect of the disease, and neurons, damaged in type II and III forms of the disease. Meanwhile, as TS is mainly neurodegenerative, TS iPSC were differentiated only to neurons.

GD iPSC macrophage differentiation proved challenging, but succeeded in differentiating both WT and GD iPSC to macrophages by using a combination of the differentiation protocols used by Raya (Raya et al. 2009) and Choi (Choi et al. 2011). The resulting macrophages showed expression of typical markers from the monocyte-macrophage lineage and proved to be functional by phagocytosis of fluorescent opsonized beads. GBA activity was reduced in GD C21 macrophages compared to L-GBA 3-15 macrophages as assessed by cytometry analysis.

The neuronal subtypes affected in GD are still unclear, although the fact that neurodegeneration takes in a number of regions and structures of the brain (Enquist et al. 2007) suggests that more than one neuronal type is affected. One neuronal cell type known to be affected are the pyramidal neurons of the hippocampus. As differentiation

to this particular cell type is not well worked out, differentiation of the GD iPSC to dopaminergic neurons was chosen, for which robust and well characterized differentiation protocols exist. Since in TS all neuronal types present membranous cytoplasmic bodies characteristic of the disease, differentiation them to the dopaminergic fate was also chosen.

WT, GD, GD L-GBA, TS and TS L-HexA neurons derived from the corresponding iPSC using the dopaminergic differentiation protocol, resulted in heterogeneous populations with high percentage of Tuj1+ neurons. Mature neuron markers as neurofilament, synapsin and NeuN were expressed in cell clusters. Neuronal precursor marker Map2+ was found in the majority of the neurons of the culture, indicating also heterogeneity on the developmental stage. All the cell lines produced TH+ dopaminergic neurons, experiencing variability between lines and between experiments which did not correlate with the presence or absence of GBA or HexA in the cells. GD derived neurons showed less GBA expression and, in consequence, the GBA activity was lower than in WT and GD L-GBA derived neurons. TS derived neurons also recapitulated the TS phenotype; more lysosomes were found on the TS derived neurons by immunofluorescence and by TEM, multillamelar membranous cytoplasmic bodies were detected in TS but not in WT.

Given the high cost of developing pharmacological compounds for disease, being able to test potential candidates early during the process on the relevant type of human cell is of great value. Human iPSC provide a platform able to differentiate to affected cell types and test the potential candidates before starting further preclinical studies and for showing it, GD and TS differentiated neurons have been used for testing novel pharmacological compounds.

Available treatments in GD are directed to alleviate the systemic symptoms of the disease, with no clinical benefit for patients suffering from the neuronopathic symptoms of the disease. In this study, 2 new bicyclic nojirimycin analogues (Luan et al. 2009),

with high specificity for â-glucosidases, have been tested in the differentiated neurons. With sub-inhibitory concentrations (30 µM), both compounds can increase protein and enzymatic activities several fold in differentiated neuronal cultures derived from GD type II iPSC; furthermore, this effect is also observed in WT cells, indicating that the effect is not specific to the mutated form of the enzyme. The compound NOI-NJ has demonstrated to have good pharmacokinetics, can cross the cell membrane by diffusion (Luan et al. 2010) and has the ability to enhance acid-b-glucosidase activity in mouse tissues, including brain, as well as the lack of acute toxicity at high doses in normal mice (Luan et al. 2009), supporting their development as therapeutic candidates.

While the manuscript describing the development of the GD iPSC model was being reviewed for publication an article was published describing the derivation of iPSC from different patients fibroblasts with three different genotypes of the disease (Panicker et al. 2012). In this work, iPSC were derived, characterized and differentiated to neurons and macrophages. Furthermore the pharmacological chaperone Isofagomine and recombinant GBA were tested on the derived macrophages which showed partial or total recovery of the WT phenotype respectively. These results were consistent with the already known efficacies of both treatments in the clinic, underscoring the usefulness of a human cellular model for testing potential pharmacological candidates. Nevertheless, they did not present data of either treatment on neurons, even when Isofagomine has showed increased GBA protein and activity in the brain of mice models of GD disease (Sun et al. 2011; Sun et al. 2012). Two previous publications in which GD iPSC were generated (Park et al. 2008) and differentiated to dopaminergic neurons (Mazzulli et al. 2011) did not use the system to evaluate therapeutic compounds. The present study is the first to test chaperone candidates on GD type II derived neurons from its correspondent iPSC, being complementary to the studies presented above.

Tay Sachs therapy is focused on supportive care and neither ERT nor SRT have reported benefits in the clinic (Johnson et al. 1973; Maegawa et al. 2009; Shapiro et al. 2009). Along with the design and testing of pharmacological chaperones for the á-subunit of the HexA enzyme, studies on the promotion of exocytosis for treating lysosomal storage diseases have been made. It has been demonstrated that ä-tocopherol mediated exocytosis normalize the lysosome size in Niemann-Pick and Wolman diseases. Also, ä-tocopherol shows a reducing effect on the lysosome size of TS fibroblasts (Xu et al. 2012). In this study, ä-tocopherol and its analogue NCGC00250218-01 have been further tested in neurons derived from TS iPSC. None of them was able to normalize the TS phenotype, moreover, differentiated neurons showed high cytotoxicity at low concentrations of the compounds. In contrast with published reports and results obtained in other laboratories, cytotoxicity was observed in both iPSC derived neurons as well as fibroblasts for both TS and WT cells. Furthermore, no clear reduction of the size of the lysosome was noticeable in surviving cells. As cytotoxicity was occurring in both TS and WT and there was no reported evidence of cytotoxicity on fibroblasts at high concentrations of ä-tocopherol, we hypothesize that an undetected problem occurred during the synthesis of the particular batch of small molecules used. Further studies are required in order to confirm or reject the preliminary data on neurons and fibroblasts obtained in this study.

G_{M2} degradation pathways differ in human and mouse, complicating the study of the pathology of the disease in mouse models. In humans there are 3 diseases caused by the malfunction of this pathway: Tay Sachs disease, in which the á-subunit of the HexA (áâ) enzyme is defective; Sandhoff disease, caused by mutations in the HEXB gene (â-subunit), affecting both HexA (áâ) and HexB (ââ) enzymes; G_{M2} activator deficiency affects all the hexosaminidase enzymes. G_{M2} in humans can only be degraded by HexA; meanwhile, in mice, G_{M2} can be also degraded by sialidase, producing G_{A2} which will be further degraded by HexA and HexB (Gravel et al. 2001). Thus, mice models for TS can-

not reproduce the observed phenotype of the disease in humans and for studying the effect of the G_{M2} accumulation the Sandhoff mouse model is usually used. Recently an article has published the iPSC derivation from a mouse model of Sandhoff disease (Ogawa et al. 2013). They found impairment on the neuronal differentiation of the Sandhoff iPSC which was rescued when â-subunit was restored, connecting the differentiation impairment to the G_{M2} accumulation. In contrast, in the present study it was not detected any effect of the TS mutation on the differentiation capability of human TS iPSC to neurons, highlighting the lack of reliable models for the study of not only TS, but also the effects that the G_{M2} accumulation has on the G_{M2} gangliosidoses.

In this study, it has been demonstrated the utility of iPSC for disease modeling as a complementary approach to mouse modeling to advance the understanding of GD and TS diseases. Both models have been derived and characterized, probing that the principal hallmarks of the diseases are present. Also, it has been demonstrated their utility to test and develop novel drugs for treatment. The present models will be able to be used for the study of the mechanisms of the disease, including metabolomics and transcriptomics in order to uncover pathways affected by the diseases. It would be of great value the development of iPSC panels covering the most common genotypes of the diseases, in order to evaluate the effect and possible treatment for each mutation.

Conclusions

Conclusions

1. iPSC technology can be used for modeling monogenic diseases.
2. Despite their genetic defect, Gaucher and Tay Sachs diseases can be reprogrammed, giving rise to full pluripotent iPSC.
3. Gaucher iPSC can be differentiated to typical affected cell types by the disease such as dopaminergic neurons and macrophages and those recapitulate the reduction of GBA protein and lack of GBA activity typical of the mutations p.L444P and p.G202R of the GBA1 gene.
4. GD iPSC can be used as a platform for producing differentiated neurons for testing potential drugs in preclinical studies.
5. The bicyclic nojirimycin analogues NOI-NJ and 6S-ADBI-NJ increase GBA protein levels and enzymatic activity in neurons derived from GD type II iPSC, offering a possible treatment for the neuronopathic forms of the disease.
6. Tay Sachs iPSC can be differentiated to dopaminergic neurons, recapitulating typical hallmarks of the disease as enlarged size of the lysosomes and the lamellar ultrastructures observed at TEM.
7. TS iPCS can be used as a platform for producing differentiated neurons for testing potential drugs in preclinical studies.
8. Although promising results have been published, further studies need to be developed with δ-tocopherol analogues to prove their effectiveness in reducing the size of the lysosomes in TS neurons without causing cytotoxicity.

Summary – Resumen

Summary - Resumen

Para comprender los múltiples fenómenos observados en los seres vivos se han utilizado animales modelo como la mosca de la fruta, nemátodos, bacterias, levaduras, pez cebra, ratones e incluso mamíferos de mayor tamaño como cerdos, ovejas y primates. Estos modelos son representaciones simplificadas del fenómeno en estudio, especialmente útiles cuando el modelo real no puede ser estudiado directamente por razones técnicas o éticas como es el caso de los estudios de enfermedades humanas.

Los ratones han sido usados para la mayoría de estudios biomédicos. Las ventajas de este modelo son amplias: pequeño, con una alta capacidad reproductiva, relativamente barato y fácil de mantener. Además, la ingeniería genética desarrollada en las últimas décadas del siglo 20 ha permitido las modificaciones genéticas necesarias para reproducir el genotipo de enfermedades humanas en el ratón. El uso de animales modelo permite un estudio a nivel de organismo, procurando un ambiente fisiológico en el que los diferentes tipos celulares y órganos interactúan. Sin embargo, hay diferencias entre humanos y ratones que limitan la fidelidad del ratón a la hora de reproducir, ya no sólo los fenotipos clínicos de las enfermedades observados en los humanos, sino también los efectos de los fármacos ensayados pueden tener diferentes resultados (Wilson 1996; Odom et al. 2007; Perel et al. 2007). Para paliar esto, se han usado modelos celulares humanos con la ventaja de ofrecer acceso al ambiente real en el que se encuentra el defecto, pero perdiendo las ventajas que da el estudio in vivo. El cultivo primario de células ha procurado información sobre la etiología de las enfermedades, estudios del efecto de fármacos así como estudios sobre su toxicidad. El problema es obtener la cantidad suficiente de células para los estudios, además de que el acceso a los tejidos realmente afectados es complicado en casos de determinadas enfermedades como por ejemplo las neurodegenerativas.

Recientemente se han establecido líneas pluripotentes como las líneas de ESC derivadas de embriones preimplantacionales diagnosticados genéticamente (Pickering et al. 2005; Mateizel et al. 2006) o con la derivación de iPSC de células primarias de pacientes (Tiscornia et al. 2011). Ambos modelos tienen un alto potencial de crecimiento celular, ofreciendo una gran cantidad de material, además de poder ser diferenciados a los tipos celulares más afectados en cada enfermedad. Las iPSC también son fáciles de derivar, tomando como población inicial células procedentes de biopsias de pacientes optando a la posibilidad de obtener un panel de iPSC de diferentes genotipos de una misma enfermedad derivadas de distintos pacientes para poder estudiar los aspectos específicos de cada mutación.

No hay un modelo perfecto, de manera que los conocimientos adquiridos de uno y de otro pueden ser complementados. Los modelos basados en células humanas pueden ser usados para estudiar los mecanismos de las enfermedades y como plataforma para probar fármacos y ayudar en su desarrollo. Por otro lado, los modelos animales pueden ser usados para obtener información sobre los aspectos sistémicos de la enfermedad y la farmacocinética de los fármacos validados previamente en los modelos celulares, siempre teniendo en cuenta que la fisiología entre el modelo animal y el humano es distinta.

Así, en esta memoria se describe el desarrollo de modelos celulares de iPSC para dos enfermedades de almacenamiento lisosomal: la enfermedad de Gaucher y la enfermedad de Tay Sachs.

Enfermedad de Gaucher

La enfermedad de Gaucher es una enfermedad autosómica recesiva incluida en el grupo de enfermedades de almacenamiento lisosomal. Afecta a uno de cada 40000-

60000 nacidos vivos en la población general y uno de cada 400-600 en la población judía ashkenazi. Gaucher está causada por mutaciones en el gen GBA1, localizado en Chr1q21, que codifica para la enzima glucocerebrosidasa (GBA). La GBA es la encargada de catabolizar el sustrato glucosilceramida en ceramida y glucosa y su mal funcionamiento provoca la acumulación del sustrato en los lisosomas de macrófagos y neuronas principalmente.

Tiene tres presentaciones clínicas atendiendo a la edad de presentación de los síntomas y a la presencia de afectación neurológica (Knudson et al. 1962):

Tipo I: Forma no neuronopática (OMIM #230800). Es la presentación más suave de la enfermedad en la que no hay síntomas neurológicos, pero sí de carácter sistémico. La aparición de los síntomas se puede dar a cualquier edad, pero lo más habitual es su aparición en la edad adulta.

Tipo II: Neuronopática aguda (OMIM #230900). Es la forma menos frecuente de presentación de enfermedad (uno en cada 150000 nacidos vivos), pero también la más severa. La aparición de los síntomas neurológicos se da antes del sexto mes de vida y la progresión es rápida, derivando en la muerte del paciente antes de cumplir los tres años.

Tipo III: Neuronopática crónica (OMIM #2310000). Es una forma intermediaria entre el tipo I y el II. Los síntomas aparecen en la infancia o adolescencia con una afectación neurológica menos grave y con una progresión más lenta que la del tipo II, pero con una afectación visceral idéntica al tipo I.

La sintomatología de la enfermedad de Gaucher se trata mediante el uso de analgésicos, transfusiones de sangre y extirpación del bazo y parte del hígado. Por otro lado, la causa de la enfermedad, la acumulación de glucosilceramida, se trata mediante terapia de sustitución enzimática, terapia de reducción de sustrato o mediante

chaperonas farmacológicas. En la sustitución enzimática, se administra la enzima GBA al paciente, que es reconocida e incorporada por los macrófagos, sustituyendo al GBA endógeno mutado y elevando los niveles de actividad de la GBA dentro de la célula (Beutler 2004). En la terapia de reducción de sustrato lo que se busca es reducir el sustrato de la GBA, la glucosilceramida, a través de la inhibición de la glucosiltransferasa por imino-azúcares como el N-butyldeoxynojirimycin (NB-DNJ) (Aerts et al. 2006). Ninguno de estos dos tipos de terapia ha mostrado efectividad en la sintomatología neurológica, de forma que sólo se usan con éxito en pacientes del tipo I o III. Por otro lado, las chaperonas farmacológicas son inhibidores de la GBA que al unirse de forma reversible con la enzima, estabilizan su estructura, evitando su degradación y promoviendo su transporte al lisosoma, donde el inhibidor se separa del enzima, dejándolo libre para que ejerza su función. Las chaperonas son análogos de los imino-azúcares usados en la terapia de reducción enzimática y algunos de ellos, capaces de cruzar la barrera hematoencefálica, ofreciendo la posibilidad de tratar las formas neuronopáticas (Benito et al. 2011).

Los modelos en ratón desarrollados para el estudio de la enfermedad no resultaron ser del todo satisfactorios ya que, a pesar de que presentaban una baja actividad GBA y acumulación de glucosilceramida en hígado y cerebro, los ratones morían 48 horas después de nacer (Tybulewicz et al. 1992; Liu et al. 1998). El único modelo de ratón creado capaz de recapitular la sintomatología neurológica (Enquist et al. 2007) lo hace por eliminación de GBA, no mimetizando las mutaciones encontradas en humanos, siendo útil para el estudio de los efectos patológicos de la enfermedad en los distintos tejidos, pero no para ensayos de fármacos.

Enfermedad de Tay Sachs

Tay Sachs es una enfermedad autosómica recesiva incluida en el grupo de enfermedades de almacenamiento lisosomales y más concretamente en el grupo de las gangliosidosis tipo G_{M2}. Está causada por mutaciones en el gen HEXA, localizado en Chr15q23 y que codifica para la subunidad α de la enzima heterodimérica β-hexosaminidasa (HexA) que cataliza la degradación del ganglióside G_{M2}. Fallos en HexA provocan la acumulación de G_{M2} en los lisosomas de células neuronales, interfiriendo con la actividad celular y causando degeneración neuronal.

La enfermedad de Tay Sachs afecta a uno de cada 360000 nacidos en la población general y uno cada 2500-3600 en la población judía ashkenazi. La enfermedad tiene tres formas de presentación de acuerdo a la edad en la que se presenta y la gravedad de los síntomas. En la forma infantil aguda, los síntomas (falta de respuesta antes estímulos externos, debilidad y pérdida de habilidades mentales y motoras) aparecen entre los 3 y 5 meses de vida y empeoran rápidamente, causando la muerte antes de los 4 años de edad. En la forma subaguda tardía que comienza con ataxia entre los 2 y los 10 años de edad, con un deterioro psicomotor progresivo. Los pacientes fallecen entre los 15 y los 20 años de edad. La forma crónica tardía puede aparecer en cualquier punto presentando gran variabilidad en las manifestaciones y su progresión, llegando a encontrar pacientes de avanzada edad (Gravel et al. 2001).

Actualmente el tratamiento para la enfermedad de Tay Sachs se centra en cuidados paliativos. Se estudia la posibilidad de usar la terapia de sustitución enzimática, reducción de sustrato y chaperonas farmacológicas, sin embargo, a pesar de los esfuerzos, hasta el momento ninguna ha resultado efectiva (von Specht et al. 1979; Maegawa et al. 2009; Shapiro et al. 2009; Clarke et al. 2011; Osher et al. 2011). Una nueva línea de investigación en el tratamiento de la enfermedad es la estimulación de

la exocitosis de los lisosomas, con lo que se restaura el tamaño normal del lisosoma y se reduce la acumulación de G_{M2} (Klein et al. 2005; Medina et al. 2011; Xu et al. 2012)

El metabolismo del G_{M2} es diferente en ratones y en humanos. En humanos, el G_{M2} sólo puede ser degradado por la enzima HexA, sin embargo en ratones puede serlo por la HexA y por la acción de la sialidasa, haciendo que los ratones KO para HEXA no desarrollen el fenotipo descrito en humanos. Para los estudios del efecto de la acumulación del G_{M2} en el tejido neuronal se usan ratones deficientes en HEXB (enfermedad de Sandhoff), que sí acumulan G_{M2} en neuronas, pero por el contrario, no pueden ser utilizados para probar fármacos específicos para Tay Sachs.

Resultados

En este trabajo se presenta la derivación de células madre pluripotentes inducidas (iPSC) a partir de fibroblastos de pacientes tanto de Gaucher como de Tay Sachs. Las iPSC se generaron introduciendo un fragmento lineal de ADN que contenía los factores de reprogramación Oct4, Sox2, Klf4 y c-Myc junto con GFP como marcador, todos unidos por secuencias p2A y bajo el control del promotor CAG. Este casete de expresión está flanqueado por secuencias LoxP, permitiendo su escisión por expresión de la recombinasa CRE una vez completada la reprogramación.

Las iPSC de Gaucher y Tay Sachs presentan una morfología característica de células madre embrionarias, junto con la expresión de marcadores de pluripotencia analizados por inmunofluorescencia y PCR cuantitativa. Además, las iPSC generadas son capaces de diferenciarse *in vivo* e *in vitro* a las tres capas germinales del embrión: endodermo, ectodermo y mesodermo, cumpliendo así con los estándares de calidad exigidos. El análisis del cariotipo es normal en las iPSC de Tay Sachs, pero revela una inversión en el

cromosoma 12 en las iPSC de Gaucher que no afecta en la diferenciación ni en el fenotipo de la enfermedad mostrado.

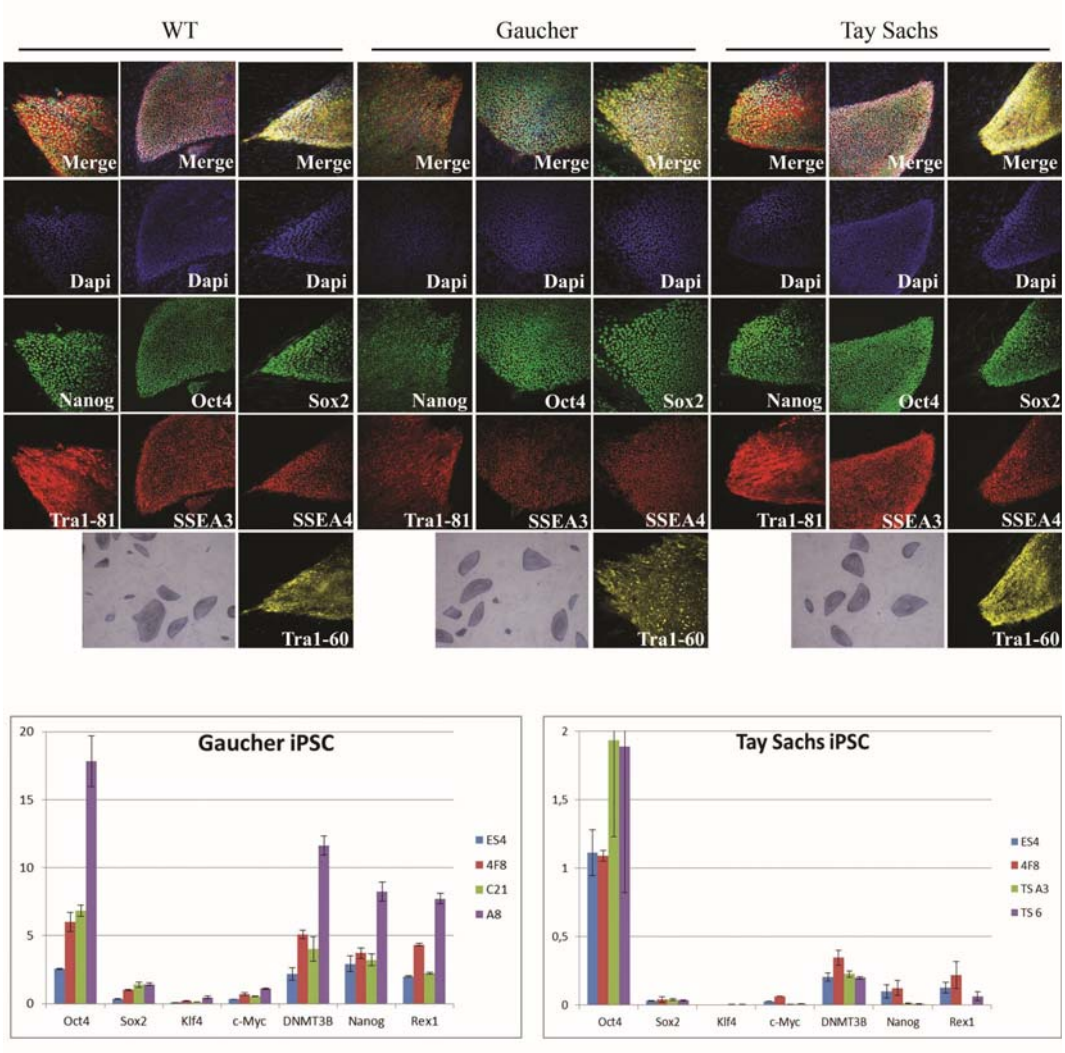

FigR-1. Análisis de pluripotencia de las iPSC derivadas de fibroblastos WT y de pacientes de TS y GD

El fenotipo de la enfermedad de Gaucher fue comprobado en fibroblastos y iPSC de Gaucher con ensayos enzimáticos que probaban que tanto los fibroblastos como las iPSC derivadas de ellos tenían una actividad de GBA menor a la de las correspondientes

WT; además, el western blot reveló que la cantidad de enzima GBA en las iPSC de Gaucher era menor que en las WT.

Las GD iPSC fueron diferenciadas a los tipos celulares más afectados por la enfermedad: macrófagos y neuronas. Se obtuvieron macrófagos (CD11b+, CD14+, CD33+ y CD163+) funcionales capaces de fagocitar micro partículas fluorescentes opsonizadas. También se midieron sus niveles de GBA y su actividad por citometría de flujo, demostrando que los macrófagos recapitulaban el fenotipo de la enfermedad. Por otro lado, las iPSC fueron diferenciadas a neuronas dopaminérgicas (TH) que expresaban marcadores neuronales típicos (Tuj1) junto con marcadores de diferentes estadíos de maduración (Map2, neurofilament, synapsin y NeuN). Estas neuronas mostraron menor cantidad de enzima GBA en los western blots, además de una menor actividad enzimática de GBA, de acuerdo con el fenotipo de la enfermedad.

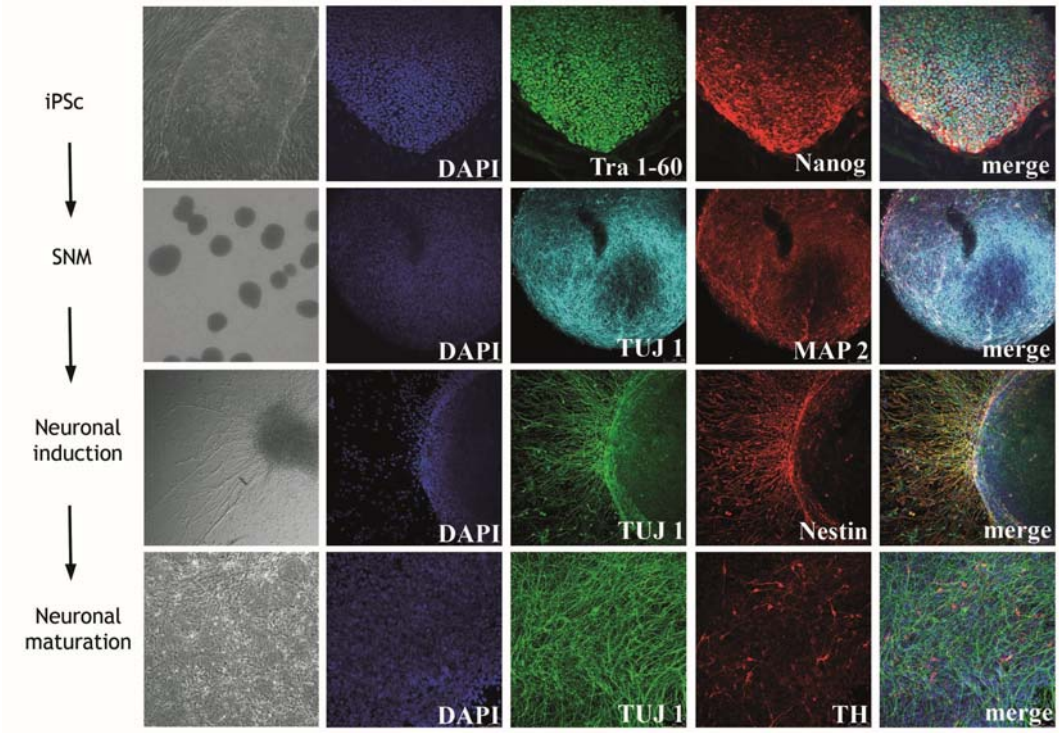

FigR-2. Panel de los diferentes estadíos de la diferenciación a neuronas dopaminérgicas

Ninguno de los tratamientos usados hasta ahora para la enfermedad de Gaucher ha mostrado tener efecto en el sistema nervioso. Sin embargo, recientemente se ha visto que unas chaperonas farmacológicas análogas a la nojirimicina bicíclica con alta especificidad por la GBA, pueden cruzar la barrera hematoencefálica, llegando al cerebro (Luan et al. 2009). Así, las neuronas derivadas de GD C21 iPSC fueron usadas para probar estos análogos. Se probaron dos compuestos, NOI-NJ y 6S-ADBI-NJ, que ofrecían un aumento en la actividad enzimática de la GBA en fibroblastos de Gaucher sin causar un efecto negativo en los fibroblastos control. Ambos compuestos fueron añadidos al medio de cultivo en los 4 últimos días de diferenciación neuronal. Las neuronas obtenidas se lisaron y se hicieron mediciones de la actividad enzimática del GBA, mostrando una mayor actividad (3-4 veces mayor) aquellas neuronas de Gaucher que habían sido tratadas con los compuestos respecto de las no tratadas. El western blot también mostró una mayor cantidad de proteína GBA en los extractos de neuronas que habían sido tratadas con los compuestos respecto de las que no lo habían sido. Estos resultados sugieren que los análogos de la nojirimicina bicíclica incrementan la cantidad de proteína GBA y por tanto, elevan la actividad enzimática.

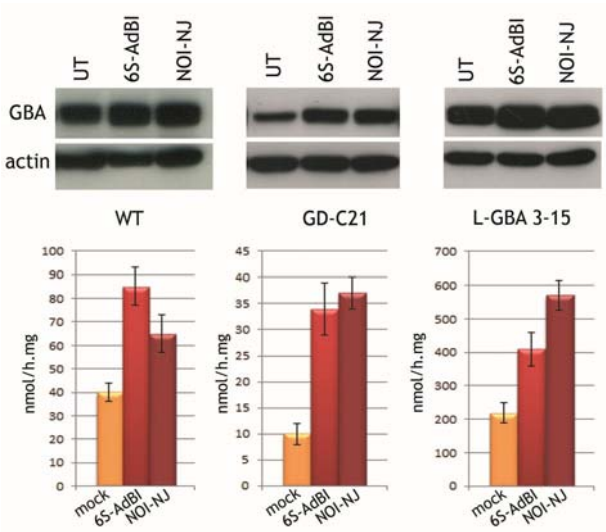

FigR-3. Neuronas derivadas de iPSC WT, GD y GD rescatadas y tratadas con NOI-NJ y 6S-ADBI-NJ

Para caracterizar el fenotipo de las TS iPSC se analizó la actividad de la HexA, mostrando una clara reducción de la actividad de HexA en los fibroblastos y en las iPSC de Tay Sachs respecto de los fibroblastos e iPSC WT. Las iPSC se diferenciaron a

neuronas, ya que la patología de TS se da casi exclusivamente en el sistema nervioso. Se utilizó el mismo protocolo que con las GD iPSC, obteniendo neuronas que presentaban características típicas de neuronas de pacientes de TS tales como el agrandamiento y aumento de número de lisosomas, observable por inmunofluorescencia (Lamp2, GM2); y la aparición de cuerpos laminares en el citoplasma de las neuronas, analizado con el microscopio electrónico de transmisión.

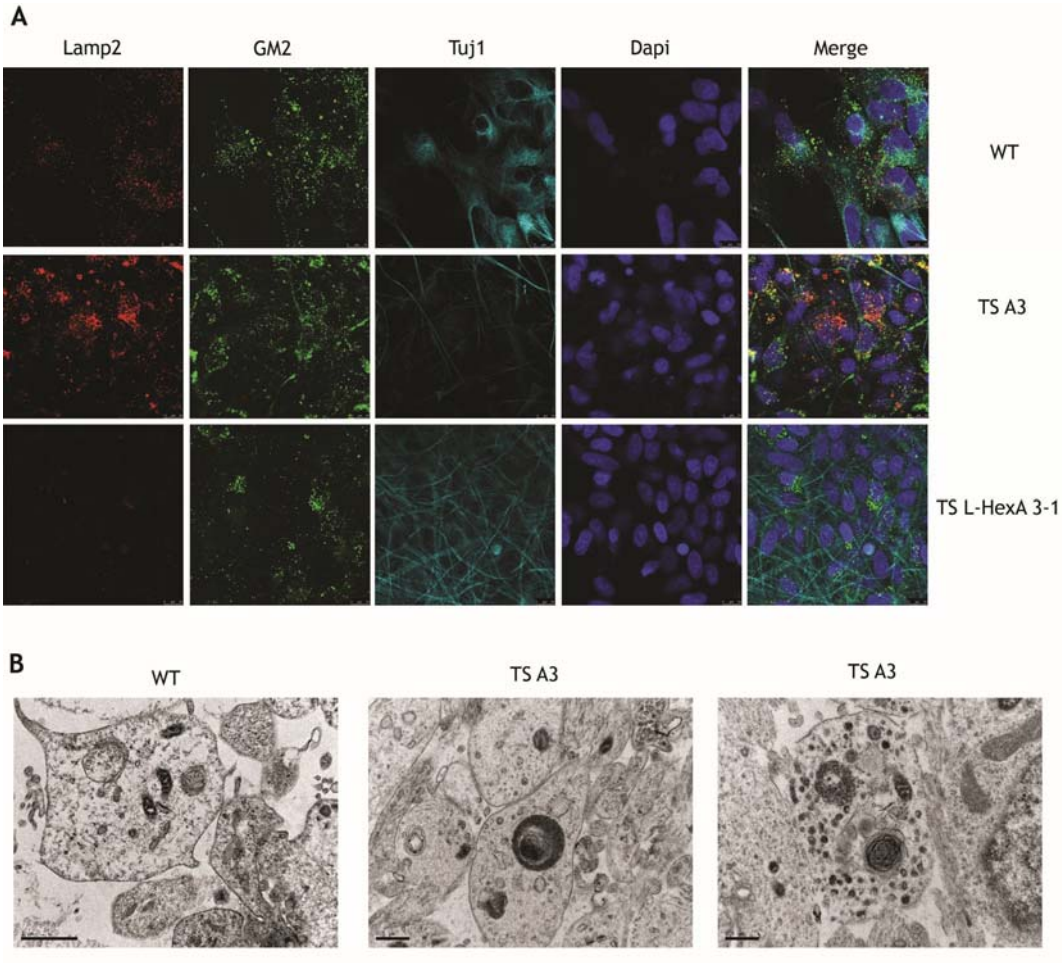

FigR-4. Neuronas WT, TS Y TS corregidas observadas al microscopio confocal (A) y con el microscopio electrónico de transmisión (B). En ambas se puede apreciar un aumento del tamaño y cantidad de los lisosomas en TS respecto de WT

Al no haber encontrado en estrategias de tratamiento tales como la sustitución enzimática o la reducción de sustrato un tratamiento eficaz frente a los síntomas de Tay Sachs, otras estrategias están siendo estudiadas. Se ha publicado un estudio en el que el δ-tocoferol favorece la exocitosis de lisosomas en las enfermedades de Niemann Pick y Wolman, normalizando en ellas la cantidad y el tamaño de los lisosomas. El δ-tocoferol puede ser utilizado en las enfermedades de almacenamiento lisosomal incluyendo TS. Así, las neuronas derivadas de TS iPSC se usaron como plataforma para

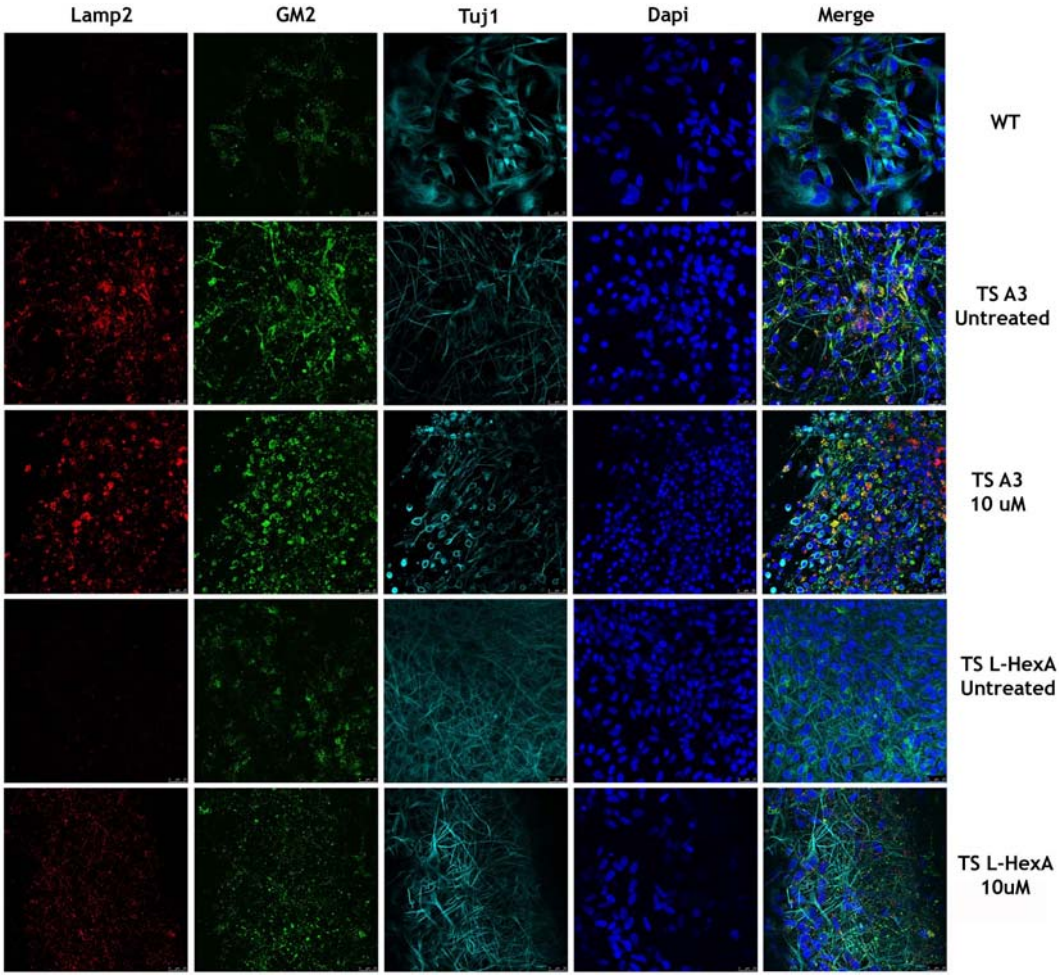

FigR-5. Neuronas derivadas de WT, TS y TS corregidas tratadas con 10uM de NCGC00250218-01

probar el efecto del δ-tocoferol y un análogo. Ambos compuestos se añadieron al medio de diferenciación en los últimos 4 días del protocolo. A pesar de los resultados obtenidos anteriormente, ambos compuestos mostraron citotoxicidad en neuronas tanto WT como TS, sin observar una normalización en el tamaño del lisosoma en las células supervivientes. Esta citotoxicidad también fue observada en fibroblastos WT y TS. Estos resultados contrastan con los resultados publicados, pudiendo deberse a una síntesis incorrecta de los compuestos. Más experimentos han de llevarse a cabo para poder constatar los efectos, positivos o negativos, de los compuestos probados.

En esta memoria se ha descrito la derivación de iPSC para "modelar" las enfermedades de Gaucher y Tay Sachs. Las iPSC se consiguieron mediante la nucleofección de un vector de reprogramación en fibroblastos procedentes de pacientes de GD y TS. Estas iPSC cumplen los requisitos de calidad típicos (morfología de ESC, expresión de marcadores de pluripotencia y habilidad de diferenciarse *in vivo* e *in vitro*). Mientras el cariotipo es normal en las iPSC de TS, presenta una inversión en el cromosoma 12 en las iPSC de Gaucher que no interfiere con la diferenciación ni con el fenotipo típico mostrado en la enfermedad. Las iPSC generadas fueron diferenciadas a los tipos celulares más afectados por las enfermedades, neuronas en TS y neuronas y macrófagos en GD. Las células diferenciadas reproducen características típicas de las respectivas enfermedades. En el caso de la enfermedad de Gaucher, tanto en neuronas como en macrófagos se pudo observar una disminución en la cantidad de enzima GBA así como una deficiencia en los niveles de actividad del enzima. En Tay Sachs, las neuronas mostraban un aumento en el tamaño y la cantidad de lisosomas que se pudo analizar por inmunofluorescencia, marcando Lamp2 (marcador de lisosomas) y G_{M2}, y por microscopía electrónica de transmisión. Las neuronas diferenciadas tanto en Gaucher como en Tay Sachs fueron utilizadas para evaluar posibles fármacos para el tratamiento de las enfermedades, pudiendo ser usadas como un modelo para hacer estudios preclínicos *in vitro*.

Summary - Resumen

Bibliography

Bibliography

1. Abrahamov, A, Elstein, D, et al. Gaucher's disease variant characterised by progressive calcification of heart valves and unique genotype. *Lancet* **346**: (8981) 1000-3 (1995)

2. Aerts, JM, Hollak, CE, et al. Substrate reduction therapy of glycosphingolipid storage disorders. *J Inherit Metab Dis* **29**: (2-3) 449-56 (2006)

3. Aguilar-Moncayo, M, Garcia-Moreno, MI, et al. Bicyclic (galacto)nojirimycin analogues as glycosidase inhibitors: effect of structural modifications in their pharmacological chaperone potential towards beta-glucocerebrosidase. *Org Biomol Chem* **9**: (10) 3698-713 (2011)

4. Akeboshi, H, Chiba, Y, et al. Production of recombinant beta-hexosaminidase A, a potential enzyme for replacement therapy for Tay-Sachs and Sandhoff diseases, in the methylotrophic yeast Ogataea minuta. *Appl Environ Microbiol* **73**: (15) 4805-12 (2007)

5. Akeboshi, H, Kasahara, Y, et al. Production of human beta-hexosaminidase A with highly phosphorylated N-glycans by the overexpression of the Ogataea minuta MNN4 gene. *Glycobiology* **19**: (9) 1002-9 (2009)

6. Alfonso, P, Rodriguez-Rey, JC, et al. Expression and functional characterization of mutated glucocerebrosidase alleles causing Gaucher disease in Spanish patients. *Blood Cells Mol Dis* **32**: (1) 218-25 (2004)

7. Ando, S. Gangliosides in the nervous system. *Neurochem Int* **5**: (5) 507-37 (1983)

8. Arpaia, E, Dumbrille-Ross, A, et al. Identification of an altered splice site in Ashkenazi Tay-Sachs disease. *Nature* **333**: (6168) 85-6 (1988)

9. Aviezer, D, Brill-Almon, E, et al. A plant-derived recombinant human glucocerebrosidase enzyme--a preclinical and phase I investigation. *PLoS One* **4**: (3) e4792 (2009)

10. Baek, RC, Kasperzyk, JL, et al. N-butyldeoxygalactonojirimycin reduces brain ganglioside and GM2 content in neonatal Sandhoff disease mice. *Neurochem Int* **52**: (6) 1125-33 (2008)

11. Barneveld, RA, Keijzer, W, et al. Assignment of the gene coding for human beta-glucocerebrosidase to the region q21-q31 of chromosome 1 using monoclonal antibodies. *Hum Genet* **64**: (3) 227-31 (1983)

12. Barton, NW, Brady, RO, et al. Replacement therapy for inherited enzyme deficiency--macrophage-targeted glucocerebrosidase for Gaucher's disease. *N Engl J Med* **324**: (21) 1464-70 (1991)

13. Bembi, B, Agosti, E, et al. Aminohydroxypropylidene-biphosphonate in the treatment of bone lesions in a case of Gaucher's disease type 3. *Acta Paediatr* **83**: (1) 122-4 (1994)

14. Bengtsson, H, Simpson, K, et al. aroma.affymetrix: A generic framework in R for analyzing small to very large Affymetrix data sets in bounded memory. (2008)

15. Benito, JM, Garcia Fernandez, JM, et al. Pharmacological chaperone therapy for Gaucher disease: a patent review. *Expert Opin Ther Pat* **21**: (6) 885-903 (2011)

16. Berg, JM, Tymoczko, JL, et al. Biochemistry. (2007)

17. Beutler, E and Kuhl, W. Detection of the defect of Gaucher's disease and its carrier state in peripheral-blood leucocytes. *Lancet* **1**: (7647) 612-3 (1970a)

18. Beutler, E, Kuhl, W, et al. Detection of Gaucher's disease and its carrier state from fibroblast cultures. *Lancet* **2**: (7668) 369 (1970b)

19. Beutler, E, Kuhl, W, et al. Beta-glucosidase activity in fibroblasts from homozygotes and heterozygotes for Gaucher's disease. *Am J Hum Genet* **23**: (1) 62-6 (1971)

20. Beutler, E and Gelbart, T. Gaucher disease mutations in non-Jewish patients. *Br J Haematol* **85**: (2) 401-5 (1993)

21. Beutler, E. Enzyme replacement in Gaucher disease. *PLoS Med* **1**: (2) e21 (2004)

22. Boles, DJ and Proia, RL. The molecular basis of HEXA mRNA deficiency caused by the most common Tay-Sachs disease mutation. *Am J Hum Genet* **56**: (3) 716-24 (1995)

23. Boulting, GL, Kiskinis, E, et al. A functionally characterized test set of human induced pluripotent stem cells. *Nat Biotechnol* **29**: (3) 279-86 (2011)

24. Brady, RO, Kanfer, J, et al. The Metabolism of Glucocerebrosides. I. Purification and Properties of a Glucocerebroside-Cleaving Enzyme from Spleen Tissue. *J Biol Chem* **240**: 39-43 (1965)

25. Butters, TD, Dwek, RA, et al. Imino sugar inhibitors for treating the lysosomal glycosphingolipidoses. *Glycobiology* **15**: (10) 43R-52R (2005)

26. Cachon-Gonzalez, MB, Wang, SZ, et al. Effective gene therapy in an authentic model of Tay-Sachs-related diseases. *Proc Natl Acad Sci U S A* **103**: (27) 10373-8 (2006)

27. Callahan, JW, Archibald, A, et al. First trimester prenatal diagnosis of Tay-Sachs disease using the sulfated synthetic substrate for hexosaminidase A. *Clin Biochem* **23**: (6) 533-6 (1990)

28. Clarke, JT, Mahuran, DJ, et al. An open-label Phase I/II clinical trial of pyrimethamine for the treatment of patients affected with chronic GM2 gangliosidosis (Tay-Sachs or Sandhoff variants). *Mol Genet Metab* **102**: (1) 6-12 (2011)

29. Cohen-Tannoudji, M, Marchand, P, et al. Disruption of murine Hexa gene leads to enzymatic deficiency and to neuronal lysosomal storage, similar to that observed in Tay-Sachs disease. *Mamm Genome* **6**: (12) 844-9 (1995)

30. Cormand, B, Grinberg, D, et al. Two new mild homozygous mutations in Gaucher disease patients: clinical signs and biochemical analyses. *Am J Med Genet* **70**: (4) 437-43 (1997)

31. Cowan, CA, Atienza, J, et al. Nuclear reprogramming of somatic cells after fusion with human embryonic stem cells. *Science* **309**: (5739) 1369-73 (2005)

32. Cox, T, Lachmann, R, et al. Novel oral treatment of Gaucher's disease with N-butyldeoxynojirimycin (OGT 918) to decrease substrate biosynthesis. *Lancet* **355**: (9214) 1481-5 (2000)

33. Chabas, A, Cormand, B, et al. Unusual expression of Gaucher's disease: cardiovascular calcifications in three sibs homozygous for the D409H mutation. *J Med Genet* **32**: (9) 740-2 (1995)

34. Chamoles, NA, Blanco, M, et al. Gaucher and Niemann-Pick diseases--enzymatic diagnosis in dried blood spots on filter paper: retrospective diagnoses in newborn-screening cards. *Clin Chim Acta* **317**: (1-2) 191-7 (2002)

35. Cho, MS, Hwang, DY, et al. Efficient derivation of functional dopaminergic neurons from human embryonic stem cells on a large scale. *Nat Protoc* **3**: (12) 1888-94 (2008a)

36. Cho, MS, Lee, YE, et al. Highly efficient and large-scale generation of functional dopamine neurons from human embryonic stem cells. *Proc Natl Acad Sci U S A* **105**: (9) 3392-7 (2008b)

37. Choi, KD, Vodyanik, M, et al. Hematopoietic differentiation and production of mature myeloid cells from human pluripotent stem cells. *Nat Protoc* **6**: (3) 296-313 (2011)

38. Choy, FY, Wei, C, et al. Gaucher disease: functional expression of the normal glucocerebrosidase and Gaucher T1366G and G1604A alleles in Baculovirus-transfected Spodoptera frugiperda cells. *Am J Med Genet* **65**: (3) 184-9 (1996)

39. d'Azzo, A, Proia, RL, et al. Faulty association of alpha- and beta-subunits in some forms of beta-hexosaminidase A deficiency. *J Biol Chem* **259**: (17) 11070-4 (1984)

40. Dekker, N, van Dussen, L, et al. Elevated plasma glucosylsphingosine in Gaucher disease: relation to phenotype, storage cell markers, and therapeutic response. *Blood* **118**: (16) e118-27 (2011)

41. Devost, NC and Choy, FY. Mutation analysis of Gaucher disease using dot-blood samples on FTA filter paper. *Am J Med Genet* **94**: (5) 417-20 (2000)

42. Dimos, JT, Rodolfa, KT, et al. Induced pluripotent stem cells generated from patients with ALS can be differentiated into motor neurons. *Science* **321**: (5893) 1218-21 (2008)

43. Elstein, D and Zimran, A. Review of the safety and efficacy of imiglucerase treatment of Gaucher disease. *Biologics* **3**: 407-17 (2009)

44. Enquist, IB, Nilsson, E, et al. Effective cell and gene therapy in a murine model of Gaucher disease. *Proc Natl Acad Sci U S A* **103**: (37) 13819-24 (2006)

45. Enquist, IB, Lo Bianco, C, et al. Murine models of acute neuronopathic Gaucher disease. *Proc Natl Acad Sci U S A* **104**: (44) 17483-8 (2007)

46. Enquist, IB, Nilsson, E, et al. Successful low-risk hematopoietic cell therapy in a mouse model of type 1 Gaucher disease. *Stem Cells* **27**: (3) 744-52 (2009)

47. Feng, B, Jiang, J, et al. Reprogramming of fibroblasts into induced pluripotent stem cells with orphan nuclear receptor Esrrb. *Nat Cell Biol* **11**: (2) 197-203 (2009)

48. Fernandes, M, Kaplan, F, et al. A new Tay-Sachs disease B1 allele in exon 7 in two compound heterozygotes each with a second novel mutation. *Hum Mol Genet* **1**: (9) 759-61 (1992)

49. Furst, W and Sandhoff, K. Activator proteins and topology of lysosomal sphingolipid catabolism. *Biochim Biophys Acta* **1126**: (1) 1-16 (1992)

50. Ginns, EI, Choudary, PV, et al. Gene mapping and leader polypeptide sequence of human glucocerebrosidase: implications for Gaucher disease. *Proc Natl Acad Sci U S A* **82**: (20) 7101-5 (1985)

51. Gonzalez, F, Barragan Monasterio, M, et al. Generation of mouse-induced pluripotent stem cells by transient expression of a single nonviral polycistronic vector. *Proc Natl Acad Sci U S A* **106**: (22) 8918-22 (2009)

52. Gonzalez, F, Boue, S, et al. Methods for making induced pluripotent stem cells: reprogramming a la carte. *Nat Rev Genet* **12**: (4) 231-42 (2011)

53. Grabowski, GA, Kruse, JR, et al. First-trimester prenatal diagnosis of Tay-Sachs disease. *Am J Hum Genet* **36**: (6) 1369-78 (1984)

54. Grabowski, GA, White, WR, et al. Expression of functional human acid beta-glucosidase in COS-1 and Spodoptera frugiperda cells. *Enzyme* **41**: (3) 131-42 (1989)

55. Grabowski, GA. Gaucher disease. Enzymology, genetics, and treatment. *Adv Hum Genet* **21**: 377-441 (1993)

56. Grabowski, GA, Leslie, N, et al. Enzyme therapy for Gaucher disease: the first 5 years. *Blood Rev* **12**: (2) 115-33 (1998)

57. Grace, ME, Graves, PN, et al. Analyses of catalytic activity and inhibitor binding of human acid beta-glucosidase by site-directed mutagenesis. Identification of residues critical to catalysis and evidence for causality of two Ashkenazi Jewish Gaucher disease type 1 mutations. *J Biol Chem* **265**: (12) 6827-35 (1990)

58. Grace, ME, Ashton-Prolla, P, et al. Non-pseudogene-derived complex acid beta-glucosidase mutations causing mild type 1 and severe type 2 gaucher disease. *J Clin Invest* **103**: (6) 817-23 (1999)

59. Gravel, RA, Kaback, MM, et al. The GM2 gangliosidoses. (2001)

60. Guenther, MG, Frampton, GM, et al. Chromatin structure and gene expression programs of human embryonic and induced pluripotent stem cells. *Cell Stem Cell* **7**: (2) 249-57 (2010)

61. Gurdon, JB. The developmental capacity of nuclei taken from intestinal epithelium cells of feedind tadpoles. *Journal of Embryology & Experimental Morphology* **10**: 622-640 (1962)

62. Hansson, HA, Holmgren, J, et al. Ultrastructural localization of cell membrane GM1 ganglioside by cholera toxin. *Proc Natl Acad Sci U S A* **74**: (9) 3782-6 (1977)

63. Hechtman, P and Kaplan, F. Tay-Sachs disease screening and diagnosis: evolving technologies. *DNA Cell Biol* **12**: (8) 651-65 (1993)

64. Heng, JC, Feng, B, et al. The nuclear receptor Nr5a2 can replace Oct4 in the reprogramming of murine somatic cells to pluripotent cells. *Cell Stem Cell* **6**: (2) 167-74 (2010)

65. Hodanova, K, Melkova, Z, et al. Transient expression of wild-type and mutant glucocerebrosidases in hybrid vaccinia expression system. *Eur J Hum Genet* **11**: (5) 369-74 (2003)

66. Hoogerbrugge, PM, Brouwer, OF, et al. Allogeneic bone marrow transplantation for lysosomal storage diseases. The European Group for Bone Marrow Transplantation. *Lancet* **345**: (8962) 1398-402 (1995)

67. Horowitz, M, Wilder, S, et al. The human glucocerebrosidase gene and pseudogene: structure and evolution. *Genomics* **4**: (1) 87-96 (1989)

68. Horowitz, M, Tzuri, G, et al. Prevalence of nine mutations among Jewish and non-Jewish Gaucher disease patients. *Am J Hum Genet* **53**: (4) 921-30 (1993)

69. Huang, HP, Chen, PH, et al. Human Pompe disease-induced pluripotent stem cells for pathogenesis modeling, drug testing and disease marker identification. *Hum Mol Genet* **20**: (24) 4851-64 (2011)

70. Huangfu, D, Osafune, K, et al. Induction of pluripotent stem cells from primary human fibroblasts with only Oct4 and Sox2. *Nat Biotechnol* **26**: (11) 1269-75 (2008)

71. Irizarry, RA, Bolstad, BM, et al. Summaries of Affymetrix GeneChip probe level data. *Nucleic Acids Res* **31**: (4) e15 (2003)

72. Jmoudiak, M and Futerman, AH. Gaucher disease: pathological mechanisms and modern management. *Br J Haematol* **129**: (2) 178-88 (2005)

73. Johnson, WG, Desnick, RJ, et al. Intravenous injection of purified hexosaminidase A into a patient with Tay-Sachs disease. *Birth Defects Orig Artic Ser* **9**: (2) 120-4 (1973)

74. Kaback, MM, Bailin, G, et al. Automated thermal fractionation of serum hexosaminidase: effects of alteration in reaction variables and implications for Tay-Sachs disease heterozygote screening. *Prog Clin Biol Res* **18**: 197-212 (1977)

75. Kaback, MM. Population-based genetic screening for reproductive counseling: the Tay-Sachs disease model. *Eur J Pediatr* **159 Suppl 3**: S192-5 (2000)

76. Kim, JB, Greber, B, et al. Direct reprogramming of human neural stem cells by OCT4. *Nature* **461**: (7264) 649-3 (2009)

77. Klein, D, Bussow, H, et al. Exocytosis of storage material in a lysosomal disorder. *Biochem Biophys Res Commun* **327**: (3) 663-7 (2005)

78. Knudson, A and Kaplan, W. Genetics of the sphingolipidoses. (1962)

79. Koprivica, V, Stone, DL, et al. Analysis and classification of 304 mutant alleles in patients with type 1 and type 3 Gaucher disease. *Am J Hum Genet* **66**: (6) 1777-86 (2000)

80. Lacorazza, HD, Flax, JD, et al. Expression of human beta-hexosaminidase alpha-subunit gene (the gene defect of Tay-Sachs disease) in mouse brains upon engraftment of transduced progenitor cells. *Nat Med* **2**: (4) 424-9 (1996)

81. Liu, Y, Suzuki, K, et al. Mice with type 2 and 3 Gaucher disease point mutations generated by a single insertion mutagenesis procedure. *Proc Natl Acad Sci U S A* **95**: (5) 2503-8 (1998)

82. Luan, Z, Higaki, K, et al. Chaperone activity of bicyclic nojirimycin analogues for Gaucher mutations in comparison with N-(n-nonyl)deoxynojirimycin. *Chembiochem* **10**: (17) 2780-92 (2009)

83. Luan, Z, Higaki, K, et al. A Fluorescent sp2-iminosugar with pharmacological chaperone activity for gaucher disease: synthesis and intracellular distribution studies. *Chembiochem* **11**: (17) 2453-64 (2010)

84. Lukacs, Z, Nieves Cobos, P, et al. Dried blood spots in the diagnosis of lysosomal storage disorders--possibilities for newborn screening and high-risk population screening. *Clin Biochem* **44**: (7) 476 (2011)

85. Maegawa, GH, Banwell, BL, et al. Substrate reduction therapy in juvenile GM2 gangliosidosis. *Mol Genet Metab* **98**: (1-2) 215-24 (2009)

86. Maherali, N, Sridharan, R, et al. Directly reprogrammed fibroblasts show global epigenetic remodeling and widespread tissue contribution. *Cell Stem Cell* **1**: (1) 55-70 (2007)

87. Marti, M, Mulero, L, et al. Characterization of pluripotent stem cells. *Nat Protoc* **8**: (2) 223-53 (2013)

88. Martino, S, Marconi, P, et al. A direct gene transfer strategy via brain internal capsule reverses the biochemical defect in Tay-Sachs disease. *Hum Mol Genet* **14**: (15) 2113-23 (2005)

89. Martino, S, di Girolamo, I, et al. Neural precursor cell cultures from GM2 gangliosidosis animal models recapitulate the biochemical and molecular hallmarks of the brain pathology. *J Neurochem* **109**: (1) 135-47 (2009)

90. Masip, M, Veiga, A, et al. Reprogramming with defined factors: from induced pluripotency to induced transdifferentiation. *Mol Hum Reprod* **16**: (11) 856-68 (2010)

91. Mateizel, I, De Temmerman, N, et al. Derivation of human embryonic stem cell lines from embryos obtained after IVF and after PGD for monogenic disorders. *Hum Reprod* **21**: (2) 503-11 (2006)

92. Mazzulli, JR, Xu, YH, et al. Gaucher disease glucocerebrosidase and alpha-synuclein form a bidirectional pathogenic loop in synucleinopathies. *Cell* **146**: (1) 37-52 (2011)

93. McEachern, KA, Nietupski, JB, et al. AAV8-mediated expression of glucocerebrosidase ameliorates the storage pathology in the visceral organs of a mouse model of Gaucher disease. *J Gene Med* **8**: (6) 719-29 (2006)

94. Medina, DL, Fraldi, A, et al. Transcriptional activation of lysosomal exocytosis promotes cellular clearance. *Dev Cell* **21**: (3) 421-30 (2011)

95. Mikkelsen, TS, Hanna, J, et al. Dissecting direct reprogramming through integrative genomic analysis. *Nature* **454**: (7200) 49-55 (2008)

96. Miranda, SRP, Gwon, S, et al. A G {r_arrow} A transition at position IVS-11 +1 of the HEX A {alpha}-chain gene in a non-Ashkenazic Mexican Tay-Sachs infant. *Journal Name: American Journal of Human Genetics; Journal Volume: 55; Journal Issue: Suppl.3; Conference: 44. annual meeting of the American Society of Human Genetics, Montreal (Canada), 18-22 Oct 1994; Other Information: PBD: Sep 1994* Medium: X; Size: pp. A362.2124 (1994)

97. Mizukami, H, Mi, Y, et al. Systemic inflammation in glucocerebrosidase-deficient mice with minimal glucosylceramide storage. *J Clin Invest* **109**: (9) 1215-21 (2002)

98. Myerowitz, R. Splice junction mutation in some Ashkenazi Jews with Tay-Sachs disease: evidence against a single defect within this ethnic group. *Proc Natl Acad Sci U S A* **85**: (11) 3955-9 (1988)

99. Myerowitz, R and Costigan, FC. The major defect in Ashkenazi Jews with Tay-Sachs disease is an insertion in the gene for the alpha-chain of beta-hexosaminidase. *J Biol Chem* **263**: (35) 18587-9 (1988)

100. Nakagawa, M, Koyanagi, M, et al. Generation of induced pluripotent stem cells without Myc from mouse and human fibroblasts. *Nat Biotechnol* **26**: (1) 101-6 (2008)

101. Nakano, T, Muscillo, M, et al. A point mutation in the coding sequence of the beta-hexosaminidase alpha gene results in defective processing of the enzyme protein in an unusual GM2-gangliosidosis variant. *J Neurochem* **51**: (3) 984-7 (1988)

102. Neuwelt, EA, Johnson, WG, et al. Characterization of a new model of GM2-gangliosidosis (Sandhoff's disease) in Korat cats. *J Clin Invest* **76**: (2) 482-90 (1985)

103. Nilsson, O and Svennerholm, L. Accumulation of glucosylceramide and glucosylsphingosine (psychosine) in cerebrum and cerebellum in infantile and juvenile Gaucher disease. *J Neurochem* **39**: (3) 709-18 (1982)

104. Odom, DT, Dowell, RD, et al. Tissue-specific transcriptional regulation has diverged significantly between human and mouse. *Nat Genet* **39**: (6) 730-2 (2007)

105. Ogawa, Y, Tanaka, M, et al. Impaired neural differentiation of induced pluripotent stem cells generated from a mouse model of Sandhoff disease. *PLoS One* **8**: (1) e55856 (2013)

106. Ohashi, T, Hong, CM, et al. Characterization of human glucocerebrosidase from different mutant alleles. *J Biol Chem* **266**: (6) 3661-7 (1991)

107. Ohno, K and Suzuki, K. A splicing defect due to an exon-intron junctional mutation results in abnormal beta-hexosaminidase alpha chain mRNAs in Ashkenazi Jewish patients with Tay-Sachs disease. *Biochem Biophys Res Commun* **153**: (1) 463-9 (1988)

108. Okada, S, Veath, ML, et al. Ganglioside GM2 storage diseases: hexosaminidase deficiencies in cultured fibroblasts. *Am J Hum Genet* **23**: (1) 55-61 (1971)

109. Okita, K, Ichisaka, T, et al. Generation of germline-competent induced pluripotent stem cells. *Nature* **448**: (7151) 313-7 (2007)

110. Onder, TT and Daley, GQ. New lessons learned from disease modeling with induced pluripotent stem cells. *Curr Opin Genet Dev* **22**: (5) 500-8 (2012)

111. Osher, E, Fattal-Valevski, A, et al. Pyrimethamine increases beta-hexosaminidase A activity in patients with Late Onset Tay Sachs. *Mol Genet Metab* **102**: (3) 356-63 (2011)

112. Panicker, LM, Miller, D, et al. Induced pluripotent stem cell model recapitulates pathologic hallmarks of Gaucher disease. *Proc Natl Acad Sci U S A* **109**: (44) 18054-9 (2012)

113. Parenti, G. Treating lysosomal storage diseases with pharmacological chaperones: from concept to clinics. *EMBO Mol Med* **1**: (5) 268-79 (2009)

114. Park, IH, Arora, N, et al. Disease-specific induced pluripotent stem cells. *Cell* **134**: (5) 877-86 (2008)

115. Paw, BH, Kaback, MM, et al. Molecular basis of adult-onset and chronic GM2 gangliosidoses in patients of Ashkenazi Jewish origin: substitution of serine for glycine at

position 269 of the alpha-subunit of beta-hexosaminidase. *Proc Natl Acad Sci U S A* **86**: (7) 2413-7 (1989)

116. Paw, BH, Moskowitz, SM, et al. Juvenile GM2 gangliosidosis caused by substitution of histidine for arginine at position 499 or 504 of the alpha-subunit of beta-hexosaminidase. *J Biol Chem* **265**: (16) 9452-7 (1990)

117. Paw, BH, Wood, LC, et al. A third mutation at the CpG dinucleotide of codon 504 and a silent mutation at codon 506 of the HEX A gene. *Am J Hum Genet* **48**: (6) 1139-46 (1991)

118. Perel, P, Roberts, I, et al. Comparison of treatment effects between animal experiments and clinical trials: systematic review. *BMJ* **334**: (7586) 197 (2007)

119. Phaneuf, D, Wakamatsu, N, et al. Dramatically different phenotypes in mouse models of human Tay-Sachs and Sandhoff diseases. *Hum Mol Genet* **5**: (1) 1-14 (1996)

120. Pickering, SJ, Minger, SL, et al. Generation of a human embryonic stem cell line encoding the cystic fibrosis mutation deltaF508, using preimplantation genetic diagnosis. *Reprod Biomed Online* **10**: (3) 390-7 (2005)

121. Pierce, KR, Kosanke, SD, et al. Animal model of human disease: GM2 gangliosidosis. *Am J Pathol* **83**: (2) 419-22 (1976)

122. Platt, FM, Neises, GR, et al. N-butyldeoxynojirimycin is a novel inhibitor of glycolipid biosynthesis. *J Biol Chem* **269**: (11) 8362-5 (1994)

123. Platt, FM, Neises, GR, et al. Prevention of lysosomal storage in Tay-Sachs mice treated with N-butyldeoxynojirimycin. *Science* **276**: (5311) 428-31 (1997)

124. Platt, FM, Jeyakumar, M, et al. Inhibition of substrate synthesis as a strategy for glycolipid lysosomal storage disease therapy. *J Inherit Metab Dis* **24**: (2) 275-90 (2001)

125. Proia, RL and Soravia, E. Organization of the gene encoding the human beta-hexosaminidase alpha-chain. *J Biol Chem* **262**: (12) 5677-81 (1987)

126. Prows, CA, Sanchez, N, et al. Gaucher disease: enzyme therapy in the acute neuronopathic variant. *Am J Med Genet* **71**: (1) 16-21 (1997)

127. Rahmann, H, Rosner, H, et al. A functional model of sialo-glyco-macromolecules in synaptic transmission and memory formation. *J Theor Biol* **57**: (1) 231-7 (1976)

128. Raya, A, Rodriguez-Piza, I, et al. Disease-corrected haematopoietic progenitors from Fanconi anaemia induced pluripotent stem cells. *Nature* **460**: (7251) 53-9 (2009)

129. Ringden, O, Groth, CG, et al. Ten years' experience of bone marrow transplantation for Gaucher disease. *Transplantation* **59**: (6) 864-70 (1995)

130. Ron, I and Horowitz, M. ER retention and degradation as the molecular basis underlying Gaucher disease heterogeneity. *Hum Mol Genet* **14**: (16) 2387-98 (2005)

131. Rountree, JS, Butters, TD, et al. Design, synthesis, and biological evaluation of enantiomeric beta-N-acetylhexosaminidase inhibitors LABNAc and DABNAc as potential agents against Tay-Sachs and Sandhoff disease. *ChemMedChem* **4**: (3) 378-92 (2009)

132. Rudensky, B, Paz, E, et al. Fluorescent flow cytometric assay: a new diagnostic tool for measuring beta-glucocerebrosidase activity in Gaucher disease. *Blood Cells Mol Dis* **30**: (1) 97-9 (2003)

133. Samavarchi-Tehrani, P, Golipour, A, et al. Functional genomics reveals a BMP-driven mesenchymal-to-epithelial transition in the initiation of somatic cell reprogramming. *Cell Stem Cell* **7**: (1) 64-77 (2010)

134. Sanders, DN, Zeng, R, et al. GM2 gangliosidosis associated with a HEXA missense mutation in Japanese Chin dogs: a potential model for Tay Sachs disease. *Mol Genet Metab* **108**: (1) 70-5 (2013)

135. Sandhoff, K and Klein, A. Intracellular trafficking of glycosphingolipids: role of sphingolipid activator proteins in the topology of endocytosis and lysosomal digestion. *FEBS Lett* **346**: (1) 103 -7 (1994)

136. Sawkar, AR, Cheng, WC, et al. Chemical chaperones increase the cellular activity of N370S beta -glucosidase: a therapeutic strategy for Gaucher disease. *Proc Natl Acad Sci U S A* **99**: (24) 15428-33 (2002)

137. Sawkar, AR, Adamski-Werner, SL, et al. Gaucher disease-associated glucocerebrosidases show mutation-dependent chemical chaperoning profiles. *Chem Biol* **12**: (11) 1235-44 (2005)

138. Schiffmann, R, Heyes, MP, et al. Prospective study of neurological responses to treatment with macrophage-targeted glucocerebrosidase in patients with type 3 Gaucher's disease. *Ann Neurol* **42**: (4) 613-21 (1997)

139. Shapiro, BE, Pastores, GM, et al. Miglustat in late-onset Tay-Sachs disease: a 12-month, randomized, controlled clinical study with 24 months of extended treatment. *Genet Med* **11**: (6) 425-33 (2009)

140. Sidransky, E. Gaucher disease: complexity in a "simple" disorder. *Mol Genet Metab* **83**: (1-2) 6-15 (2004)

141. Sorge, J, Gross, E, et al. High level transcription of the glucocerebrosidase pseudogene in normal subjects and patients with Gaucher disease. *J Clin Invest* **86**: (4) 1137-41 (1990)

142. Stone, DL, Tayebi, N, et al. Glucocerebrosidase gene mutations in patients with type 2 Gaucher disease. *Hum Mutat* **15**: (2) 181-8 (2000)

143. Sun, Y, Ran, H, et al. Isofagomine in vivo effects in a neuronopathic Gaucher disease mouse. *PLoS One* **6**: (4) e19037 (2011)

144. Sun, Y, Liou, B, et al. Ex vivo and in vivo effects of isofagomine on acid beta-glucosidase variants and substrate levels in Gaucher disease. *J Biol Chem* **287**: (6) 4275-87 (2012)

145. Suzuki, Y, Berman, PH, et al. Detection of Tay-Sachs disease heterozygotes by assay of hexosaminidase A in serum and leukocytes. *J Pediatr* **78**: (4) 643-7 (1971)

146. Suzuki, Y, Tsuji, K, et al. Iminosugars: From Synthesis to Therapeutic Applictions. (2007)

147. Tada, M, Tada, T, et al. Embryonic germ cells induce epigenetic reprogramming of somatic nucleus in hybrid cells. *EMBO J* **16**: (21) 6510-20 (1997)

148. Tada, M, Takahama, Y, et al. Nuclear reprogramming of somatic cells by in vitro hybridization with ES cells. *Curr Biol* **11**: (19) 1553-8 (2001)

149. Takahashi, K and Yamanaka, S. Induction of pluripotent stem cells from mouse embryonic and adult fibroblast cultures by defined factors. *Cell* **126**: (4) 663-76 (2006)

150. Takeda, K, Nakai, H, et al. Fine assignment of beta-hexosaminidase A alpha-subunit on 15q23-q24 by high resolution in situ hybridization. *Tohoku J Exp Med* **160**: (3) 203-11 (1990)

151. Tanaka, A, Ohno, K, et al. GM2-gangliosidosis B1 variant: analysis of beta-hexosaminidase alpha gene abnormalities in seven patients. *Am J Hum Genet* **46**: (2) 329-39 (1990)

152. Taranger, CK, Noer, A, et al. Induction of dedifferentiation, genomewide transcriptional programming, and epigenetic reprogramming by extracts of carcinoma and embryonic stem cells. *Mol Biol Cell* **16**: (12) 5719-35 (2005)

153. Tayebi, N, Stubblefield, BK, et al. Reciprocal and nonreciprocal recombination at the glucocerebrosidase gene region: implications for complexity in Gaucher disease. *Am J Hum Genet* **72**: (3) 519-34 (2003)

154. Terry, RD and Weiss, M. Studies in Tay-Sachs disease. II. Ultrastructure of the cerebrum. *J Neuropathol Exp Neurol* **22**: 18-55 (1963)

155. Thompson, TE and Tillack, TW. Organization of glycosphingolipids in bilayers and plasma membranes of mammalian cells. *Annu Rev Biophys Biophys Chem* **14**: 361-86 (1985)

156. Tiscornia, G, Singer, O, et al. Production and purification of lentiviral vectors. *Nat Protoc* **1**: (1) 241-5 (2006)

157. Tiscornia, G, Vivas, EL, et al. Diseases in a dish: modeling human genetic disorders using induced pluripotent cells. *Nat Med* **17**: (12) 1570-6 (2011)

158. Tiscornia, G, Vivas, EL, et al. Neuronopathic Gaucher's disease: induced pluripotent stem cells for disease modelling and testing chaperone activity of small compounds. *Hum Mol Genet* **22**: (4) 633-45 (2013)

159. Torres, PA, Zeng, BJ, et al. Tay-Sachs disease in Jacob sheep. *Mol Genet Metab* **101**: (4) 357 -63 (2010)

160. Triggs-Raine, BL, Akerman, BR, et al. Sequence of DNA flanking the exons of the HEXA gene, and identification of mutations in Tay-Sachs disease. *Am J Hum Genet* **49**: (5) 1041-54 (1991)

161. Trop, I, Kaplan, F, et al. A glycine250--> aspartate substitution in the alpha-subunit of hexosaminidase A causes juvenile-onset Tay-Sachs disease in a Lebanese-Canadian family. *Hum Mutat* **1**: (1) 35-9 (1992)

162. Tropak, MB and Mahuran, D. Lending a helping hand, screening chemical libraries for compounds that enhance beta-hexosaminidase A activity in GM2 gangliosidosis cells. *FEBS J* **274**: (19) 4951-61 (2007)

163. Tsuji, D, Akeboshi, H, et al. Highly phosphomannosylated enzyme replacement therapy for GM2 gangliosidosis. *Ann Neurol* **69**: (4) 691-701 (2011)

164. Tybulewicz, VL, Tremblay, ML, et al. Animal model of Gaucher's disease from targeted disruption of the mouse glucocerebrosidase gene. *Nature* **357**: (6377) 407-10 (1992)

165. Urbach, A, Bar-Nur, O, et al. Differential modeling of fragile X syndrome by human embryonic stem cells and induced pluripotent stem cells. *Cell Stem Cell* **6**: (5) 407-11 (2010)

166. van Es, HH, Veldwijk, M, et al. A flow cytometric assay for lysosomal glucocerebrosidase. *Anal Biochem* **247**: (2) 268-71 (1997)

167. von Specht, BU, Geiger, B, et al. Enzyme replacement in Tay-Sachs disease. *Neurology* **29**: (6) 848-54 (1979)

168. Watanabe, Y, Takahashi, T, et al. The analysis of the functions of human B and T cells in humanized NOD/shi-scid/gammac(null) (NOG) mice (hu-HSC NOG mice). *Int Immunol* **21**: (7) 843 -58 (2009)

169. Weinreb, NJ, Charrow, J, et al. Effectiveness of enzyme replacement therapy in 1028 patients with type 1 Gaucher disease after 2 to 5 years of treatment: a report from the Gaucher Registry. *Am J Med* **113**: (2) 112-9 (2002)

170. Wernig, M, Meissner, A, et al. In vitro reprogramming of fibroblasts into a pluripotent ES-cell-like state. *Nature* **448**: (7151) 318-24 (2007)

171. Wilson, JM. Animal models of human disease for gene therapy. *J Clin Invest* **97**: (5) 1138-41 (1996)

172. Williams, SM, Haines, JL, et al. The use of animal models in the study of complex disease: all else is never equal or why do so many human studies fail to replicate animal findings? *Bioessays* **26**: (2) 170-9 (2004)

173. Xu, M, Liu, K, et al. delta-Tocopherol reduces lipid accumulation in Niemann-Pick type C1 and Wolman cholesterol storage disorders. *J Biol Chem* **287**: (47) 39349-60 (2012)

174. Xu, YH, Quinn, B, et al. Viable mouse models of acid beta-glucosidase deficiency: the defect in Gaucher disease. *Am J Pathol* **163**: (5) 2093-101 (2003)

175. Yamanaka, S, Johnson, MD, et al. Targeted disruption of the Hexa gene results in mice with biochemical and pathologic features of Tay-Sachs disease. *Proc Natl Acad Sci U S A* **91**: (21) 9975 -9 (1994)

176. Yu, J, Vodyanik, MA, et al. Induced pluripotent stem cell lines derived from human somatic cells. *Science* **318**: (5858) 1917-20 (2007a)

177. Yu, Z, Sawkar, AR, et al. Pharmacologic chaperoning as a strategy to treat Gaucher disease. *FEBS J* **274**: (19) 4944-50 (2007b)

178. Zeng, BJ, Torres, PA, et al. Spontaneous appearance of Tay-Sachs disease in an animal model. *Mol Genet Metab* **95**: (1-2) 59-65 (2008)

179. Zimran, A, Sorge, J, et al. Prediction of severity of Gaucher's disease by identification of mutations at DNA level. *Lancet* **2**: (8659) 349-52 (1989)

180. Zimran, A, Sorge, J, et al. A glucocerebrosidase fusion gene in Gaucher disease. Implications for the molecular anatomy, pathogenesis, and diagnosis of this disorder. *J Clin Invest* **85**: (1) 219 -22 (1990)

Acknowledgements
Agradecimientos

A Juan Carlos Izpisúa-Belmonte y Miquel Gómez Clares por permitirme formar parte del CMRB.

A Gustavo Tiscornia, por ser mi mentor, mi padre científico, mi guía espiritual, por enseñarme lo que sé, por soltarme de la mano y dejar que volara sola, por las noches en blanco con experimentos o manuscritos.

A los integrantes pasados y presentes del CMRB. Demasiados para nombraros a todos… Por los encuentros en los pasillos a altas horas de la noche/fines de semana/fiestas de guardar, por los no me sale, por los yupi salió!!! Ah, no, que eso era el control positivo… Porque me habéis apoyado, porque me habéis visto crecer… Por las cervezas compartidas, por los viernes en el Bitácora, por el voley!

A los becarios! No habría sido lo mismo sin vosotros! Ignasi, Eduard, Adriana, Cristina, Raquel, Álex, los últimos en abandonar el barco, Lorena, Borja (viva los becarios de barrios chungos!) y los no oficiales, sobre todo Josu, Noelia y Leire.

A mis lunch girls! Por los pica-picas porque sí, por las comadres, por los días de la claridad!

A Montse, por cuidar de mí, por sacar tiempo de debajo de las piedras para poder echarme una mano, porque vales mucho ☺

A Marianna, mi igual-diferente. Por estar ahí, por las charlas científicas y personales, por empujarme a saltar, porque contigo soy más grande, porque nunca pensé que de un kebab fuera a surgir nada así.

A Jorge, Ángel, Lorena P, Carlos, Lorena G, Eva. Porque sois de lo mejor que me llevo, porque las cenas, risas y frikadas siempre alegraban un día gris.

A mis happy chicas, por vuestra alegría, por vuestro apoyo, por mostrarme otras formas de ver la vida.

A Blanca, por ser un sol.

A Vane, por su alegría, por sus collejas (y por las que yo te di)

A tu, Barcelona, perquè m'has permès passetjar pels teus carrers i gaudir-te, a l'alba i al capvespre, per les teves nits i els teus dies, les teves platjes, pel teu dolç hivern, per acollir-me durant aquests gairebé sis anys a la teva falda...Gràcies!

A mis amigos de siempre, Belén, Alfredo, José, porque tras tanto tiempo separados siempre encontramos un hueco para vernos.

A mis biólogos y bioquímicos de la UAM: Helena, Ana Q, David R, Elena, Andrés, Dani, Guille… Y tantos que no tengo espacio para nombrar!

A David L, por las largas charlas, por estar ahí.

A Susana Pulido, porque siempre eres un ejemplo de fortaleza para mí.

A Guille, por arriesgar y perseverar.

A todos los profesores que han ido pasando por mi vida, desde parvulitos hasta el día de hoy. En especial a Margarita Serna, que me volcó su pasión por la biología y Jorge Barrio, con quien siempre es un placer discutir sobre biología, física, política y filosofías de vida.

Pero sobre todo, a mi familia, por entender y respetar que mis caminos son distintos.